



HAL
open science

Identification and control of low-cost robot manipulators

Zilong Shao

► **To cite this version:**

Zilong Shao. Identification and control of low-cost robot manipulators. Automatic Control Engineering. Ecole Centrale de Lille, 2016. English. NNT : 2016ECLI0001 . tel-01484288

HAL Id: tel-01484288

<https://theses.hal.science/tel-01484288>

Submitted on 7 Mar 2017

HAL is a multi-disciplinary open access archive for the deposit and dissemination of scientific research documents, whether they are published or not. The documents may come from teaching and research institutions in France or abroad, or from public or private research centers.

L'archive ouverte pluridisciplinaire **HAL**, est destinée au dépôt et à la diffusion de documents scientifiques de niveau recherche, publiés ou non, émanant des établissements d'enseignement et de recherche français ou étrangers, des laboratoires publics ou privés.

N° d'ordre : 2 9 0

CENTRALE LILLE

THESE

Présentée en vue
d'obtenir le grade de

DOCTEUR

En

Spécialité : Automatique, Génie Informatique, Traitement du Signal et Images

Par

Zilong SHAO

DOCTORAT DELIVRE PAR CENTRALE LILLE

Titre de la thèse :

Identification et commande des robots manipulateurs à bas prix

Identification and control of low-cost robot manipulators

Soutenue le 24 mars 2016 devant le jury d'examen :

Président	<i>François Pierrot, Research Director, CNRS, LIRMM</i>
Rapporteur	<i>Christine Chevallerau, Research Director, CNRS, IRCCyN</i>
Rapporteur	<i>Olivier Stasse, Research Director, CNRS, LAAS</i>
Membre	<i>Isabelle Fantoni, Research Director, CNRS, Heudiasyc</i>
Membre	<i>Christian Duriez, Research Director, INRIA-Lille</i>
Directeur de thèse	<i>Wilfrid Perruquetti, Professor, Ecole Centrale de Lille</i>
Co-directeur de thèse	<i>Gang Zheng, Research Scientist, INRIA-Lille</i>
Co-directeur de thèse	<i>Denis Efimov, Research Scientist, INRIA-Lille</i>
Invité	<i>Jean-Pierre Richard, Professor, Ecole Centrale de Lille</i>

Thèse préparée dans le Centre de Recherche en Informatique, Signal et Automatique de Lille
Ecole Doctorale SPI 072 (Lille I, Lille III, Artois, ULCO, UVHC, Centrale Lille)

Acknowledgements

My PhD work presented in this thesis has mainly been done in Non-A Team in Inria Lille, from March 2013 to February 2016. This work is partly financially supported by China Scholarship Council (CSC). I would like to express my most sincere gratitude and appreciation to my supervisors Prof Wilfrid Perruquetti, and my two co-supervisors Denis Efimov and Gang Zheng, for their valuable guidance, continuing support and endless patience throughout my thesis. Their remarkable knowledge and admirable qualities have always inspired me, and always remind me of what a researcher should be.

I would like to express my sincere gratitude to the members of my PhD Committee, Mr. François Pierrot, Mme. Christine Chevallerau, Mr. Olivier Stasse, Mme. Isabelle Fantoni and Mr. Christian Duriez, Mr. Jean-Pierre Richard, for their attention paid to my thesis manuscript and the presentation.

I would like to thank strongly my director Mr. Wilfrid Perruquetti, and my co-directors Mr Gang Zheng and Mr Denis Efimov for their continuing support, endless patience and valuable guidance and encouragement. During the past three years, they have been always very supportive to me, not only on my academical work, but also on my family life. Their remarkable mind and admirable qualities have always inspired me, and always remind me of how a great professor should be. It has been an honour for me to work with them and they set good examples for scientific researchers.

I also would like to express my sincere gratitude to all the members in the "Non- Asymptotic Estimation for Online Systems" (NON-A) team, it has been a privilege for me to work together with these intelligent and friendly colleagues. I would especially like to mention the colleagues and friends in my office, Matteo Guerra, Hafiz Ahmed, Maxime Feingesicht, and so on. Thanks to them, I have passed three agreeable years.

I also would like to thank Centre de Recherche en Informatique, Signal et Automatique de Lille (CRISAL) for their financial support, with which I was able to take course at EECI International Graduate School on Control and attended International Conference on Intelligent Robots and Systems (IROS) in Hamburg 2015.

Further thanks give to my parents and family for their incessant support. I would like to thank my dearest Hui Zhou, who is always so patient and supportive through all the tough times.

Table of contents

List of figures	v
List of tables	vii
1 Introduction	1
1.1 Background and motivation	1
1.2 Previous work	3
1.2.1 Robot Dynamics	3
1.2.2 Robot Dynamics Properties	7
1.2.3 Control of rigid manipulators	9
1.2.4 Control of flexible-joint manipulators	15
1.3 Contribution of the thesis	19
1.4 Outline of the thesis	20
2 Auxiliary controller design for low-cost rigid manipulator with built-in controller	23
2.1 Introduction	23
2.2 Problem statement and analysis	24
2.2.1 Problem statement	24
2.2.2 Problem analysis	25
2.3 Modelling and identification	26
2.3.1 Dynamics modelling	26
2.3.2 Model Identification	29
2.3.3 Derivative estimation	30
2.4 Auxiliary adaptive controller design	32
2.4.1 Adaptive controller design	32
2.4.2 Numerical implementation of the adaptive controller	34
2.5 Simulation	35

2.5.1	Model description	35
2.5.2	Constant input	37
2.5.3	Model parameter identification	38
2.5.4	Auxiliary adaptive controller	39
2.5.5	Auxiliary PID controller	40
2.6	Conclusion	40
3	Identification and control of single-link flexible-joint robots using velocity measurement	43
3.1	Introduction	43
3.2	Problem statement	45
3.3	System model	47
3.4	Parameter identification using angular velocity measurement	48
3.5	PD controller with gravity compensation	49
3.5.1	Without parameter uncertainty	49
3.5.2	With parameter uncertainty	52
3.6	Two-stage adaptive controller using inertial sensors	55
3.6.1	Motor position reference design	56
3.6.2	Adaptive input design	58
3.7	Simulation	60
3.7.1	Model specification	60
3.7.2	Identification results	60
3.7.3	Controller performance	61
3.8	Conclusion	62
4	Identification and control using measurements of higher order derivatives	65
4.1	Introduction	65
4.2	Identification and control for single-link flexible-joint robots with acceleration measurement	65
4.2.1	Identification	66
4.2.2	Two-stage adaptive controller using accelerometer	67
4.2.3	Simulations for single-link flexible-joint robots	67
4.3	Generalisation to linear system with high-order derivative measurement	68
4.3.1	Preliminaries	68
4.3.2	Problem statement	69
4.3.3	Identification	70
4.3.4	State space representation for control design	73

4.3.5	Adaptive control	74
4.3.6	Robust control	77
4.3.7	Simulations for linear system	78
4.4	Conclusion	81
5	Experiment results	83
5.1	Introduction	83
5.2	Introduction of the experiment plate-form	84
5.2.1	Description of the robot arm	84
5.2.2	All-in-one actuator	85
5.2.3	Built-in controller	85
5.2.4	Propositions and physical constraints	87
5.3	Rigid case	88
5.3.1	Built-in controller performance	88
5.3.2	Model identification	88
5.3.3	Control strategy	91
5.3.4	Performance with auxiliary controller	91
5.4	Flexible-joint case	92
5.4.1	Inertial sensors	93
5.4.2	Built-in controller performance	94
5.4.3	Model identification	95
5.4.4	Controller performance	96
5.5	Conclusion	97
	Conclusions and Perspectives	101
	References	105
	Appendix A Dynamic of a 2DOF Rigid Robot Manipulator	113
	Résumé en français	115
	List of publications	121

List of figures

1.1	ABB industrial manipulators and the control device	2
1.2	A low-cost manipulator	2
1.3	A Kuka light-weight robot	2
1.4	A rigid dynamic model with 3 DOF	4
1.5	A flexible joint dynamic model with 6 DOF	6
1.6	Principles of general model-based controller design	14
1.7	Principles of indirect adaptive control	15
1.8	Structure of the middle chapters	21
2.1	Joint plus controller system	25
2.2	Introduction of an auxiliary controller	26
2.3	Joint with motor and transmission system	27
2.4	2 DOF Manipulator	36
2.5	Performance with constant input	38
2.6	Velocity estimation	38
2.7	Acceleration estimation	38
2.8	Performance with auxiliary adaptive controller	39
2.9	Performance with auxiliary PID controller	40
3.1	DLR light weight robot III	44
3.2	A MEMS IMU	44
3.3	Actuator with built-in controller	46
3.4	Flexible-joint robot model	46
3.5	Derivative estimates for identification	61
3.6	PD controller	62
3.7	Two-stage adaptive controller	62
4.1	Velocity and position estimates by integration	68
4.2	Two-stage adaptive controller using accelerometer	69

4.3	The simulation result for adaptive controller	80
4.4	The simulation result for robust controller	81
5.1	Test manipulator	84
5.2	AX-12A all-in-one actuators	85
5.3	Built-in controller	86
5.4	P controller with saturation	87
5.5	Built-in controller performance	89
5.6	Observer performance	90
5.7	Switched control strategy	91
5.8	Auxiliary controller for Configuration 1	92
5.9	Auxiliary controller for Configuration 2	93
5.10	6 DOF IMU Digital Combo Board	94
5.11	Performance of built-in controller for single-link flexible-joint robot	95
5.12	Identification for single-link flexible-joint robot	96
5.13	Simulation of the model based on the identification result	98
5.14	Performances of PD controller and two-stage controller	99
5.1	A low-cost manipulator	116
5.2	A Kuka light-weight robot	116
5.3	Manipulateur low-cost	118
5.4	Actionneur AX-12	118
5.5	Capteur IMU	119

List of tables

1.1	Comparison between low-cost manipulator and industrial manipulator . . .	3
2.1	Parameters of 2DOF manipulator for simulation	37
3.1	Identification result with velocity measurement	61
4.1	Identification result with acceleration measurement	68
5.1	Specifications of the robot arm	85
5.2	Specifications of AX-12A actuator	86
5.3	Identification results for flexible-joint robot	97
5.1	comparaison entre manipulateur low-cost et manipulateur industriel	116

Chapter 1

Introduction

1.1 Background and motivation

Today, most of the industrial robot manipulators (Figure 1.1), are totally integrated, the mechanical structure, electronics components, actuators, sensors and operation systems are pre-integrated before the delivery. Due to high-precision actuators and components machining, these manipulators provide effective operational performance for specified tasks, but are less flexible with regard to task variations. Besides, due to their big size, high price, costly maintenance and repairing, we can only find these manipulators in factories, laboratories, for specific purposes. In addition, these machines can only be controlled by technicians who followed certain training, in case of security problem during human-machine interaction. Therefore, these manipulators are far less accessible for individuals. This is exactly the same situation for early computers before 1970s, where computers were huge, expensive and only used for military or research purposes.

It is true that “robolution” or “robotisation” is on the way, but right now is it possible for everyone to have a robot manipulator, like the generalization of personal computers? To answer this question, we should first know what properties the future “personal” manipulators should have.

In the author’s opinion, in contrast to the nowadays industrial manipulators, the future “personal” manipulators should be low-cost, small size, light-weight but with high load-to-weight ratio, user-reconfigurable, user-friendly, flexible for security during human interference, easy to maintain and repair... This kind of manipulators can be applied for research, entertainment, people assistance, medical, education..., where the industrial manipulators are not suitable, e.g., someone can be terrified in front of a feeding robot which is of an industrial manipulator.



Fig. 1.1 ABB industrial manipulators and the control device

In fact, there are already some low-cost manipulators commercialized in the market. They are of low cost, small size and light weight. A comparison between such a manipulator (PhantomX Pincher Robot Arm from Trossen Robotics© , Figure 5.1) and the latest KUKA light-weight robot (Figure 5.2) is illustrated in Table 5.1.



Fig. 1.2 A low-cost manipulator



Fig. 1.3 A Kuka light-weight robot

However, we cannot expect a manipulator designed and fabricated with a lower budget to be as powerful as one with a 20-times budget. The weaknesses of low-cost manipulators include position error in joint space, oscillation and position error in end-effector space, these drawbacks may come from hardware and/or software aspects, like controller limitation, joint and/or link elasticity, backlash, etc.

This thesis is motivated by low-cost manipulators which adopt limited “all-in-one” actuators. These actuators are integrated with DC motor, sensors, transmission system, position

Table 1.1 Comparison between low-cost manipulator and industrial manipulator

	Low-cost robot arm	Kuka light-weight robot
Price	378\$	+20 000€
Weight	550g	48kg
Max. Reach	31cm	70.7cm

control unit and network, provide high load-to-weight ratio and relieve the practitioners from designing reduction and control systems. However, for some cheap but not powerful enough actuators, due to the limitation of the the feedback information and the built-in controller design (e.g., independent joint PD or P controller), steady state errors are presented. Besides, since the material which forms the motor shaft is not stiff enough, in most cases, it's plastic, joint-flexibility are introduced, as a result, oscillation and mismatch between the link position and the feedback joint position are observed.

The objective of this thesis includes:

- to eliminate the steady state error in rigid-body case,
- to estimate and to control the link position in flexible-joint case, and to attenuate the oscillation,

for low-cost manipulators equipped with limited “all-in-one” actuators.

1.2 Previous work

This section presents a detailed survey of past and present researches related to the problem of manipulator control. The aim of this section is to lay a foundation for the remainder of the thesis by identifying what has been done, in order to propose innovative control methodologies to fill the knowledge gap identified in the published literature.

1.2.1 Robot Dynamics

Rigid Robot Dynamics

In a rigid dynamic model, the links and gearboxes are assumed to be rigid. The mass and inertia of the actuators and gearboxes are added to the corresponding link parameters. The model consists of a serial kinematic chain of n links modelled as rigid bodies as illustrated in Figure 1.4.

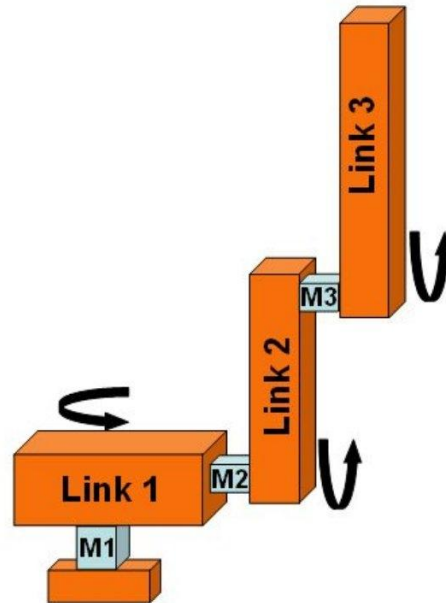


Fig. 1.4 A rigid dynamic model with 3 DOF

The model based approach to controller design systematically uses the equations describing the system dynamics. The most commonly used description is the inverse dynamic equations. These equations give the torque required to achieve a given trajectory of the robot manipulator. The most commonly used technique to derive the inverse dynamics is the Euler-Lagrange formulation based on the energy in the system.

Consider an ideal system without friction or elasticity, exerting neither forces nor moments on the environment. Then the Lagrange equations are written in the matrix form as:

$$\tau = \frac{d}{dt} \left(\frac{\partial L}{\partial \dot{q}} \right)^T - \left(\frac{\partial L}{\partial q} \right)^T, \quad (1.1)$$

where τ is the vector of generalized forces or torques, q is the state position vector, L is the Lagrangian of the manipulator defined as the difference between the kinetic energy E and the potential energy U of the system:

$$L = E - U. \quad (1.2)$$

The derivation of the Lagrange formulation leads to a compact form of the inverse dynamics:

$$\tau = M(q)\ddot{q} + C(q, \dot{q})\dot{q} + G(q), \quad (1.3)$$

where:

$M(q)$ is the inertia matrix,

$C(q, \dot{q})$ represents the Coriolis and centripetal effects,

$G(q)$ is the vector related to gravity.

In reality, a robot arm is always affected by friction and disturbances. Therefore, we shall generalize the above arm model by writing the manipulator dynamics as

$$\tau = M(q)\ddot{q} + C(q, \dot{q})\dot{q} + F(\dot{q}) + G(q) + D, \quad (1.4)$$

where $F(\dot{q})$ stands for the friction vector and D denotes the disturbance vector. The friction $F(\dot{q})$ is generally of the form:

$$F(\dot{q}) = F_v\dot{q} + F_d(\dot{q}), \quad (1.5)$$

with F_v the coefficient matrix of viscous friction, and F_d a dynamic friction term. The friction coefficients are among the parameters most difficult to determine for a given arm and, in fact, (1.5) represents only an approximate mathematical model for their influence. For more discussion, see [77].

Flexible-Joint Robot Dynamics

Consider the robot described previously with elastic gearboxes or elastic motor output-side shaft, i.e., elastic joints. This robot can be modelled by the so called flexible-joint model which is illustrated in Figure 1.5. The rigid bodies are connected by torsional spring pairs.

If the friction and inertial couplings between the motors and the rigid links are neglected we get the simplified flexible joint model. If the gear ratio is high, this is a reasonable approximation as described in, e.g., [82]. The motor mass and inertia are added to the corresponding rigid body. The total system has $2n$ DOF. The model equations of the simplified flexible joint model are expressed as:

$$\begin{cases} M(q)\ddot{q} + C(q, \dot{q})\dot{q} + G(q) = \tau_l, & (1.6a) \\ \tau_l = K(\theta - q), & (1.6b) \\ \tau_m = I\ddot{\theta} + \tau_l, & (1.6c) \end{cases}$$

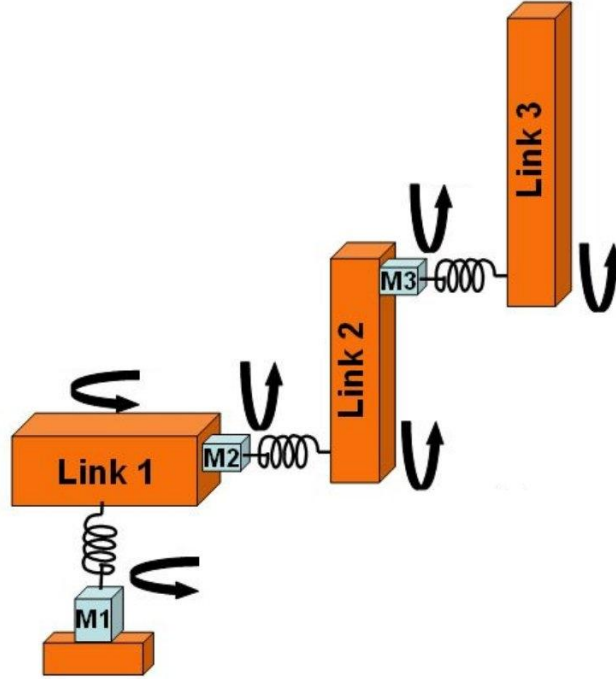


Fig. 1.5 A flexible joint dynamic model with 6 DOF

where link and motor angular positions are denoted as $q \in \mathbb{R}^n$ and $\theta \in \mathbb{R}^n$, respectively. $\tau_m \in \mathbb{R}^n$ is the motor torque and $\tau_l \in \mathbb{R}^n$ is the gearbox output torque. $K \in \mathbb{R}^{n \times n}$ is the stiffness matrix and $I \in \mathbb{R}^{n \times n}$ is the motor inertia matrix.

If the friction, the viscous damping and the couplings between the links and the motors are included we get the complete flexible joint model [22]:

$$\begin{cases} M(q)\ddot{q} + S(q)\ddot{\theta} + C_1(q, \dot{q}, \dot{\theta})\dot{q} + G(q) = \tau_l, & (1.7a) \\ \tau_l = K(\theta - q) + D(\dot{\theta} - \dot{q}), & (1.7b) \\ \tau_m = I\ddot{\theta} + S^T(q)\ddot{q} + C_2(q, \dot{q}) + f(\dot{\theta}) + \tau_l, & (1.7c) \end{cases}$$

where $S \in \mathbb{R}^{n \times n}$ is a strictly upper triangular matrix of coupled inertia between links and motors. The structure of S depends on how the motors are positioned and oriented relative to the joint axis directions.

The flexible joint models can formally be derived in the same way as the rigid model, e.g., by the Lagrange equation. The potential energy of the springs must then be added to the potential energy expressions as

$$V_s(q, \theta) = \frac{1}{2}(q - \theta)^T K(q - \theta), \quad (1.8)$$

where V_s is the elastic potential energy related to the joint elasticity, and the kinetic energy of the rotating actuators must be added as well.

1.2.2 Robot Dynamics Properties

As mentioned earlier, the equations describing the robot manipulators are highly nonlinear. However, articulated mechanics have some common inherent properties and a careful analysis, followed by a judicious use of these properties, leads to very effective controllers, as suggested by Slotine [79]. The five most commonly used properties for manipulators are: the symmetric and positive definiteness of the inertia matrix, the boundedness of the dynamical terms, the skew-symmetry, the parametrization and the passivity of the system.

Symmetric Positive Definite Inertia Matrix

The manipulator inertia matrix $M(q)$ is always symmetric and positive definite [6]. The positive definiteness implies that the quadratic form of the manipulator inertia is always a positive scalar. Physically, it means that the kinetic energy is always positive for non-zero velocity. Mathematically, this property can be expressed as:

$$E = \frac{1}{2}\dot{q}^T M(q)\dot{q} > 0, \dot{q} \neq 0, \quad (1.9)$$

where E denotes the kinetic energy.

Boundedness Property

The dynamic terms $M(q)$, $C(q, \dot{q})$, $G(q)$ and $F(\dot{q})$ in the inverse dynamics formulation vary with respect to the joint angles and their first derivatives. Since the range of variation for the joint angles is physically limited, the inertia, Coriolis/centripetal, gravitational and friction matrices are bounded with respect to q and \dot{q} . The disturbance term D which could represent inaccurately modelled dynamics, and so on, could also be assumed bounded. So we have:

$$m_1 \leq \|M(q)\| \leq m_2, \quad (1.10)$$

$$\|C(q, \dot{q})\| \leq c_b \|\dot{q}\|^2, \quad (1.11)$$

$$\| G(q) \| \leq g_b, \quad (1.12)$$

$$\| F_v \dot{q} + F_d(\dot{q}) \| \leq v \| \dot{q} \| + k, \quad (1.13)$$

$$\| D \| \leq d, \quad (1.14)$$

where:

m_1 and m_2 are positive constants,

c_b is positive constant,

g_b is positive constant,

v and k are positive constants,

d is positive constant, and,

$\| \cdots \|$ denotes the euclidean norm.

Skew-symmetry

The skew-symmetry gives the following property:

$$x^T [\dot{M}(q) - 2C(q, \dot{q})] x = 0, \quad \forall x \in R^n. \quad (1.15)$$

The derivation of this property can be referred to [52]. In fact, it is simply a statement that the forces, defined by $C(q, \dot{q})\dot{q}$, do no work on the system [69]. An important consequence of this is the following passive property.

Passive Nature of Manipulator

The passivity concept originated from electric circuits theory; a system is said to be passive if it does not create energy. A system is passive if for equal number of inputs $U(t)$ and outputs $Y(t)$, the following inequality is satisfied for some $\alpha > -\infty$:

$$\int_0^t Y(\tau)^T U(\tau) d\tau \geq \alpha, \quad \forall t > 0. \quad (1.16)$$

For a robot manipulator, considering the input as the torque vector and the output as the vector of joint velocities, the system defines a passive mapping from the input to the output. Using the Hamiltonian term H defined as the sum of the kinetic energy and the potential energy of the manipulator [69], the following holds:

$$\frac{dH}{dt} = \dot{q}\tau, \quad (1.17)$$

where:

\dot{q} is the vector of joint velocities,

τ is the input torque vector.

Then we have

$$\int_0^t \dot{q}(\tau)^T \tau(\tau) d\tau = H(t) - H(0) \geq -H(0), \quad \forall t > 0. \quad (1.18)$$

This proves the passivity property of the manipulator. This last property has been unconsciously used for some time in control engineering. By closing the loop between the joint velocity and the torque, with a passive system, the whole system remains passive. Since the new system is dissipative, it is stable. Recently the passivity property has been used considerably as a systematic design philosophy for robot controllers [68].

Linearity in Parameters

By a suitable reformulation of the dynamic equations, the constant parameters defining the dynamics of the system, e.g. link masses, moments of inertia, etc, may appear as coefficients of a general coordinate function. By defining each coefficient as a separate parameter, the dynamic equations can be written as in (1.19), which illustrates a linear relationship in parameters. Since all these constant parameters are usually subject to inaccuracies, this linear formulation of the dynamic equation is very useful for adaptive control. This reformulation that separates the unknown or partially unknown parameters from the known time functions, is used for the formulation of the adaptive update rules [52].

$$\tau = M(q)\ddot{q} + C(q, \dot{q})\dot{q} + G(q) = Y(q, \dot{q}, \ddot{q})\delta, \quad (1.19)$$

where:

$Y(q, \dot{q}, \ddot{q})$ is an $(n \times n)$ matrix of known functions, called regressor functions, and,

δ is an $(n \times 1)$ vector containing the basic constant parameters.

1.2.3 Control of rigid manipulators

In general, the problem of controlling a manipulator is to determine the time history of the generalised forces (forces or torques) to be developed by the joint actuators so as to

guarantee execution of the commanded task while satisfying given transient and steady-state requirements.

Demand for high-performance robots has led to the development of various advanced control techniques. Two general controller approaches can be distinguished for robot manipulators, the model based approaches and the non-model based approaches. The model based controllers consider some of the structures of the system in their design procedures. This group of controllers concerns mainly the computed torque controllers, which rely on cancellation of the non-linearities in the robot dynamics by inverting its dynamic equations. In contrast, non-model based controllers do not take into account the system dynamics. This kind of controllers were popular during the early days of robotics [71] since it allows a decoupled analysis of the closed-loop system using single-input/single-output (SISO) classical techniques, it is also called *independent joint control*. To deal with model uncertainties, various adaptive and robust controllers have been developed for both model based and non-model based controllers.

Computed Torque Control

The controller uses the general inverse dynamic equation of the robot manipulator as the basic design starting point. Usually the controller is composed of two parts, the feed-forward and the feedback elements. The feedforward part attempts to cancel the non-linearities in the system, while the feedback is used to stabilise the system and drives the error to zero. Considering the simplified model (1.3), given the current position and velocity of the manipulator, the computed torque control law is described as:

$$\tau = M(q)(\ddot{q}_d - K_v \dot{e} - K_p e) + C(q, \dot{q})\dot{q} + G(q), \quad (1.20)$$

where \ddot{q}_d is the desired acceleration, $e = q - q_d$, and K_v and K_p are constant gain matrices. When substituted into (1.3), the error dynamics can be written as:

$$M(q)(\ddot{e} + K_v \dot{e} + K_p e) = 0. \quad (1.21)$$

Since $M(q)$ is always positive definite, we have

$$\ddot{e} + K_v \dot{e} + K_p e = 0. \quad (1.22)$$

This is a linear differential equation which governs the error between the actual and desired trajectories. It can be proved that, if $K_v, K_p \in \mathbb{R}^{n \times n}$ are positive definite, symmetric

matrices, then the control law (1.20) applied to the system (1.3) results in exponential trajectory tracking [63].

The computed torque control law consists of two components. We can write (1.20) as

$$\tau = \underbrace{M(q)\ddot{q}_d + C(q, \dot{q})\dot{q} + G(q)}_{\tau_{ff}} + \underbrace{M(q)(-K_v\dot{e} - K_p e)}_{\tau_{fb}}, \quad (1.23)$$

where τ_{ff} is the feedforward component. It provides the amount of torque necessary to drive the system along its nominal path. The term τ_{fb} is the feedback component. It provides correction torques to reduce any errors in the trajectory of the manipulator.

However, the controller (1.20) needs the exact knowledge of $M(q)$, $C(q, \dot{q})$ and $G(q)$. The named PD-Plus-Gravity Controller [5], requires only to compute the gravity terms $G(q)$.

The PD-plus-gravity controller takes the form as

$$\tau = -K_v\dot{e} - K_p e + G(q), \quad (1.24)$$

where $K_v, K_p \in \mathbb{R}^{n \times n}$ are positive definite, symmetric matrices.

It can be proven that, the controller (1.24) is asymptotically stable for the regulation control problem [5].

In summary, the computed torque approach is based on the feedback linearisation concept. Such controllers are designed in two steps. Initially, the structure of the feedforward term that provides linearisation is established, with an estimate of the system dynamics. The second step consists of defining the feedback term such that the control objective is achieved.

Independent Joint Control

The design of computed torque method based on (1.20) is generally complicated due to the model uncertainty or computational load. A more realistic controller design strategy that can be thought of is to decompose an n -joint manipulator into n -independent systems allowing independent joint control. This control approach has been used since the early age of robotics, and is referred to as *independent joint control*. The effectiveness of SISO control is confirmed for manipulators with relatively low joint interaction reflected at the actuators. This situation is only valid for slowly moving links and highly geared transmissions. The reduction ratios in the transmissions reduce the link interactions and the variation in inertia as seen by the actuators. For manipulators with directly driven links (gear ratio = 1) or lowly geared transmissions, the interaction between links may be significant [7]. In this case, the independent joint control may not provide acceptable results and the interaction between the links has to be accommodated in the controller design via a model-based like approach.

An example of this design methodology is a proportional plus derivative (PD) control law for a robot manipulator. In its simplest form, a PD control law for each joint i can be written as:

$$\tau_i = -K_{di}\dot{e}_i - K_{pi}e_i, \quad (1.25)$$

where K_{di}, K_{pi} are positive constant.

However, with the PD controller, due to gravity or other disturbance, there is always a residual error at steady state. A common modification is to add an integral term to eliminate steady-state errors. This introduces additional complications to maintain stability and avoid integrator windup. The introduction of integral term gives rise to PID controller:

$$\tau_i = -K_{di}\dot{e}_i - K_{pi}e_i - K_{ii} \int e_i, \quad (1.26)$$

where K_{di}, K_{pi}, K_{ii} are positive constant.

For these independent joint controllers, the coupling effects between joints due to varying configurations during motion are treated as disturbance, effective rejection of these disturbances is usually achieved by either a large gain or an integral action [57].

Usually for industrial robots, independent joint control gives reasonably good results for set point regulation as well as for trajectory following. Although, the validity of the scheme can be appreciated from an engineering point of view, and the large number of applications confirm its effectiveness [12], [4], and theoretical proofs have justified the application and the stability of such schemes in robotic applications [75], [83].

Robust Controllers

Many of the previously discussed classes of controllers exist in robust versions or are intrinsically robust, e.g., PID controller. The aim of the robustness property for the controller is to render the system insensitive to parameter mismatches, i.e. uncertainty in the dynamic terms of the model-based controller; and to disturbances, e.g. joint interactions, measurement noises and noises affecting the system itself.

The control of uncertain systems is usually accomplished using either an adaptive control or a robust control philosophy. In the adaptive approach, one designs a controller that attempts to learn the uncertain parameters of the system and, if properly designed, will eventually be a “best” controller for the system in question. In the robust approach, the controller has a fixed structure that yields acceptable performance for a class of plants which includes the plant in question. In general, the adaptive approach is applicable to a wider range of uncertainties, but robust controllers are simpler to implement.

The computed torque control law (1.20) cannot usually be implemented due to its complexity or to uncertainties present in $M(q)$, $C(q, \dot{q})$, $G(q)$, and due to disturbances. Instead, one applies (1.27) below:

$$\tau = \hat{M}(q)(\ddot{q}_d + u) + \hat{C}(q, \dot{q})\dot{q} + \hat{G}(q), \quad (1.27)$$

where:

$\hat{M}(q)$, $\hat{C}(q, \dot{q})$ and $\hat{G}(q)$ are estimates of $M(q)$, $C(q, \dot{q})$ and $G(q)$,

\ddot{q}_d is the desired acceleration, and,

u is the feedback error signal, can be the P, PD or PID type.

The system uncertainties do not cause problems in terms of control as long as the estimated model is sufficiently close to the real one. The feedback loop is used to correct for the system uncertainties and to guarantee acceptable performance. As the uncertainties increase however, the system performance decays rapidly such that the system may become unstable [30], [81]. When the uncertainties are within an acceptable range, the feedback loop can be designed in such a way that the error converges to an acceptable range.

The effectiveness of the controller (1.27), is very much dependent on the accuracy of the estimated model used as the feedforward term. This dependence has motivated engineers and scientists to search for a way to render the system more insensitive to model uncertainty. As a result, various methodologies have been suggested to design the robust control scheme [1], [52]. The Lyapunov approach is one in which a candidate Lyapunov function is selected to define the robustness of the controller. The most commonly selected Lyapunov function is the pseudo-kinetic energy function [32]. It is formed using a function of the error and the inertia matrix of the manipulator. The stability and robustness of the scheme are guaranteed by establishing a strictly negative bound on the derivative of the Lyapunov function. This must be valid for any point in the operating range of the manipulator. This approach is very conservative (there is no tool to design a Lyapunov function for a generic nonlinear time-varying system), but it may nevertheless be a starting point for further refinements.

Adaptive Controllers

Adaptive control is another main approach for dealing with uncertainties. Research in adaptive control started in the early 1950's in response to the development of high performance aircraft, but research did not progress very much due to the lack of a global theory. It was abandoned until the late 1960's, when interest in adaptive controllers started again.

In many robot control problems where some form of model based control is used, some of the parameters of the plant to control are partially or totally unknown (the inertia, mass,

length, etc.). It may also happen that the process, during its normal operation, is subject to changes in parameters. The robot may be required to manipulate loads which may vary in size, weight and mass distribution. In order to give consistent responses in terms of speed and accuracy in any of these situations, the controller has to adapt itself to cope with these varying or uncertain parameters. One of the basic idea in adaptive control is to estimate the uncertain model parameters and adjust the controller parameters, this is also called *Indirect Adaptive Control*. To illustrate the difference of this idea from the general controller design ideas, we first look at the general principles of model-based controller design procedure given in Figure 1.6.

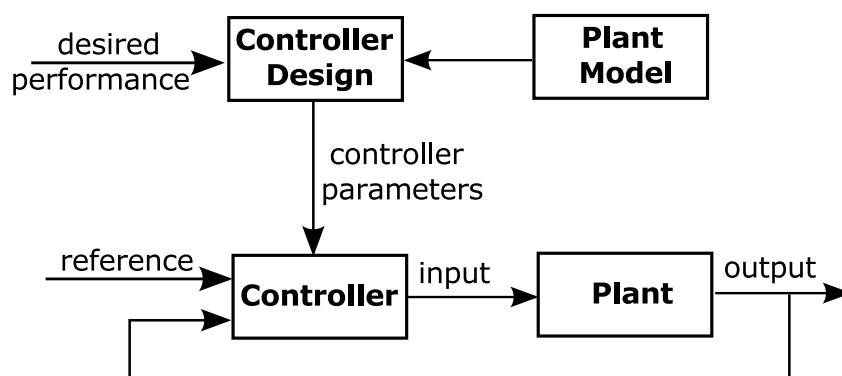


Fig. 1.6 Principles of general model-based controller design

Generally, in order to design and tune a good controller, one needs to:

- (1) Specify the desired control loop performances.
- (2) Pre-know or identify the dynamic model of the plant to be controlled.
- (3) Possess a suitable controller design method making it possible to achieve the desired performance for the corresponding plant model.

To cope with model uncertainty, the indirect adaptive control scheme (Figure 1.7) can be viewed as a real-time extension of the controller design procedure represented in Figure 1.6. The basic idea is that a suitable controller can be designed online if a model of the plant is estimated online from the available input-output measurements. The scheme is termed *indirect* because the adaptation of the controller parameters is done in two stages:

- (1) on-line estimation of the plant parameters;
- (2) on-line computation of the controller parameters based on the current estimated plant model.

Other adaptive control schemes include the *direct adaptive control* and *model-reference adaptive control*, usually referred to as MRAC [49]. In direct adaptive control, the controller parameters are calculated directly according to the plant input/output, without intermediate calculations involving plant parameter estimates. In the MRAC, a model of the plant is used

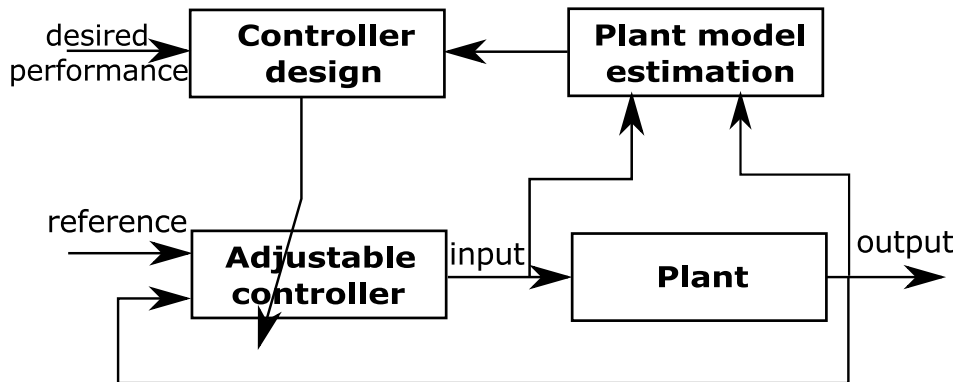


Fig. 1.7 Principles of indirect adaptive control

to generate the ideal output that the plant response must follow. The controller parameters are updated in a way that the plant achieves perfect tracking of the reference model response.

Using the linearity in parameters property, a number of adaptive controllers for robotics have been proposed [14], [39], [17], [59], [76]. A number of important refinements to this initial result are possible [81], [80], [38], [69].

1.2.4 Control of flexible-joint manipulators

Early Control Approaches

Since the first clear demonstration in 1984 that robot manipulators were exhibiting flexible effects in their joints [85], new control strategies developed specifically for this new class of robot systems started to emerge. One of the first studies on flexible-joint control was published two years later in [92], in which an adaptive controller based on an approximate linearized model of the flexible-joint dynamics was proposed. With this linear dynamics approximation, the Coriolis and Centrifugal forces were neglected. Using a similar linearized dynamics representation, a predictive controller was designed [46], but the performance was not satisfying. By this time, most of the research efforts were focused on linear control methodologies. In 1986, for the first time, a nonlinear control method was considered for a single-link flexible-joint manipulator [60]. In that paper, the authors proved that a single-link flexible-joint robotic manipulator under static nonlinear state feedback acts like a controllable linear system.

PID controller

Due to the simplicity and ease of implementation, proportional-derivative (PD) controllers have been widely used. Similar to that used for rigid robots, a simple PD regulator with

gravity compensation was proposed for flexible-joint robots [90], and simulation results for a set-point control problem are provided. An adaptive version of this simple PD regulator was derived by the same author in [89]. For the sake of simplicity, actuators dynamics and friction were neglected in the control algorithms in those two PD regulation approaches. An extension of the PD regulator for robot manipulator considering simultaneously joint flexibility, actuators dynamics as well as friction was presented in [55]. A PD controller with on-line gravity compensation was proposed for regulation tasks in [23]. One of the features of this controller is to allow more flexibility in the tuning of the proportional gains, as compared with the original controller proposed in [90].

Feedback Linearization

Feedback linearization is one of the most powerful approaches for nonlinear control system design. Essentially, the objective of this approach is to transform a nonlinear dynamic system into a fully or partly linear model, so that linear control techniques can be applied. In 1987, Spong [82] introduced the well-known linear joint stiffness dynamics model and showed that it is globally feedback linearizable, and can be reduced to that of the standard rigid-joint robots as the joint stiffness reaches infinity. This property led to the early development of several control approaches based on feedback linearization [65], [20]. Dynamic state feedback control techniques for a particular class of flexible-joint robots are suggested in [56] and [22], since conventional static state feedback approaches failed to achieve exact linearization. Experimentally, a static state feedback linearization approach was applied in [29] to a class of flexible-joint robots to guarantee global asymptotic stability. Furthermore, linearization with static and dynamic state feedbacks was also investigated in [19] for robots with mixed flexible/rigid joints.

Adaptive Control

Among the different flexible-joint control techniques available in the literature, adaptive control methods have generated the greatest interest. An adaptive control scheme which is applicable to manipulators with weak joint stiffness coefficients is proposed in [62], in the proposed scheme, a Lyapunov candidate function is defined to guarantee asymptotic stability, and bounded parameter errors. In [62], an adaptive control scheme is introduced for which asymptotic stability was ensured without restriction to low joint elasticity. Furthermore, the values of the joint stiffness coefficients were not assumed to be known. Joint position and velocity tracking errors were shown to asymptotically converge to zero. Similarly, in [98], an adaptive control law which considers uncertainties in the inertia parameters

is established. The asymptotic stability of the adaptive controller was established in the sense of Lyapunov. In [67], an adaptive trajectory tracking control law for a single-link robot with one revolute elastic joint whose parameters were assumed to be unknown is proposed. In another paper [44], the authors derived a tracking controller for an uncertain parameter robot system without using link and actuator velocity measurements. Specifically, the controller used joint stiffness matrix estimates to overcome the overparametrization problem, that is, the number of parameter estimates becomes the same as the number of unknown parameters. An adaptive output feedback controller based on a backstepping design was developed in [97]. The parameters of the system were assumed to be unknown and only link and motor position measurements were used for the synthesis of the controller. In [28], a Lyapunov-based adaptive control technique framework for flexible-joint robot with time-varying uniformly bounded disturbances is proposed, where the disturbances were characterized by a combination of unknown and known constants. [53] studied the regulation problem of flexible-joint robot with uncertain kinematics and proposed adaptive regulation scheme which considered kinematic uncertainties as well as uncertainties in actuator dynamic parameters, such as the constant joint stiffness coefficients. Simulation results were provided to confirm the effectiveness of the proposed adaptive regulator. However, the adaptive control scheme required a nonlinear observer which mat complexify the design process.

Robust Control

Besides adaptive control techniques, several robust control techniques have been proposed in the literature to cope with uncertainties, such as the robust controller derived in [91] for elastic-joint robots with uncertain kinematic and dynamic parameters and subject to unknown disturbances. Similarly, [18] presents a robust tracking controller which achieves global uniform ultimate bounded tracking despite the presence of bounded disturbances and parameter uncertainties. Similarly, a robust controller for a flexible-joint robot with both parametric and dynamic uncertainties is proposed in [37]. However, although rejection of any bounded disturbances entering the system was demonstrated, asymptotic stability could not be guaranteed. More recently, a robust controller was developed in [87] using the singular perturbation-based dynamics representation, under which the system acts on a two time-scale. In their work, a simple PD controller was used to stabilize the fast dynamics while a robust controller designed with the quantitative feedback theory was used in addition to an integral manifold corrective term to stabilize the slow dynamics. On the other hand, in [95] and [96], a robust controller containing two steps is proposed. First, a robust controller for the link dynamics is designed for the case when the link dynamics could be controlled independently of the motor dynamics. Second, a robust controller is designed recursively by

using the Lyapunov second method. The resulting robust controller was applied to a two-link flexible-joint robot. Also, the authors in [94] presented the design of a robust control scheme which comprised two parts: a model-based computed torque control part, and robust control part to maintain the tracking performance. The resulting robust controller was applied in numerical simulations for a six DOF flexible-joint robot manipulator.

Nonlinear Control

Many researchers have proposed various nonlinear control design techniques for flexible-joint robot manipulators. Some early nonlinear control techniques include a nonlinear dynamic feedback developed in [21] and a feedback linearization controller based on coordinate transformations in [43]. A nonlinear backstepping approach was proposed in [43]. However, the drawback of the backstepping control technique is that the closed-loop system becomes easily unstable if the system is subject to parametric uncertainties. To overcome this limitation, an adaptive backstepping method using tuning function was developed in [58]. In this work, the performance was assessed against a simple PD controller in tracking a $15\text{cm} \times 15\text{cm}$ square trajectory. A nonlinear regulator for flexible-joint robots which achieved constant torque disturbance rejection was derived in [2]. The design of the regulator used the nonlinear integrator backstepping technique. Lyapunov-based nonlinear controllers have also been considered in the past years. In [66], the authors investigated a nonlinear control law which guarantees global convergence either for regulation about a constant reference position or for tracking a desired trajectory. The proposed nonlinear control law was applied to a single-link robot. In addition, it was shown how the approach could be extended to cases where the robot parameters are not known. In [10], seven different schemes were experimentally implemented for a two-link planar manipulator, including a PD controller, a rigid-joint adaptive controller, a singular perturbation-based algorithm, and four nonlinear controllers derived from the nonlinear backstepping and energy-shaping design methodologies. One of the main conclusions of this study was that the complex structure of certain nonlinear controllers for flexible-joint robots (e.g. nonlinear backstepping and energy-shaping schemes) may be an obstacle to their closed-loop behaviour enhancement. The experimental results clearly showed that the inputs of such schemes chatter and result in control input magnitudes larger than the simpler controllers. Moreover, the authors did not succeed in finding feedback gains to stabilize the nonlinear backstepping controllers. According to the authors, this is due to a too-large input magnitude that hampers stabilization. This confirms the observations made in [8] and showed that a slight modification of the backstepping controller gains has a significant influence on the obtained performance. The same authors performed further experimentations on a linear but highly flexible manipulator system made of two pulleys

linked by a spring in [9]. This second experiment completed the previous one in [10] in the sense that the manipulator used in the first experiment was nonlinear but with higher joint stiffness, whereas the system in the second experiment was linear but with highly flexible joints.

1.3 Contribution of the thesis

This thesis considers the control problem of low-cost light-weight position-controlled robot arms.

First, the set-point control problem of low-cost rigid manipulators with “all-in-one” actuators is addressed in this chapter. For the derivation of the dynamics model linking the input with the state variables, the effect of the driven motor and the transmission system is considered, as a result, a second-order differential equation with constant parameters and bounded disturbance is obtained, then identification method of a nominal model is proposed, based on the identified model parameters, a model-based adaptive controller is developed. In simulation, the ability of error reduction is validated, and advantage on performance robustness with respect to model change is observed with comparison to PID controller with constant gains. Implementation on a real robot arm validates the performance of the proposed adaptive controller.

Then, the point-to-point control of single-link position-controlled robot with joint flexibility, to obtain link side information, an EMES gyroscope is used to provide link angular velocity. An identification scheme of the model parameters is presented, based on the classic model of flexible-joint robots. As a benchmark, a modified simple PD plus gravity compensation controller is considered, of which the regulation error depends on two parameter estimates. To improve the robustness with regard to parameter uncertainties, a two-stage adaptive controller is proposed, with which the final position error depends on the precision of only one parameter estimate, provided that the initial static link position can be measured. Simulation results illustrate that, the proposed two-stage controller is more robust than the PD one, with regard to parametric uncertainty. Efficacy of the proposed identification and control algorithms is also demonstrated in experiments on real robot.

Finally, the problem of model identification and output control has been studied in this work for linear time-invariant SISO system with completely unknown parameters, external disturbances, while the output is represented by high-order derivative corrupted by a bounded noise. It is shown that by introducing n recursive integrals and using a simple identification algorithm, some estimates on vector of unknown parameters and states can be obtained. Next, these information can be used in control, adaptive or robust, to provide boundedness of the

state vector of the system. Due to integration drift all results are obtained on final intervals of time. Efficacy of the proposed identification and control algorithms is demonstrated in simulations.

1.4 Outline of the thesis

The outline of the main chapters is shown in Figure 1.8. In Chapter 2, we focus on rigid-joint case, independent joint modelling, model identification, auxiliary controller design and the simulation results are presented. In Chapter 3, we study the flexible-joint case, for simplification, only single-link flexible-joint manipulator is investigated. This chapter includes dynamic modelling, model identification, state estimation and controller design using link angular velocity measurement, simulation result is also given. In Chapter 4, still for flexible-joint case, but we use link acceleration measurement for the identification, estimation and control, simulation result is also provided. This method of using second-order derivative measurement is generalized to the identification and control problem for linear system, by using high-order derivative measurement. Chapter 5 presents the experimental results of the proposed controllers (proposed in Chapter 2 and Chapter 3) implemented on a low-cost manipulator.

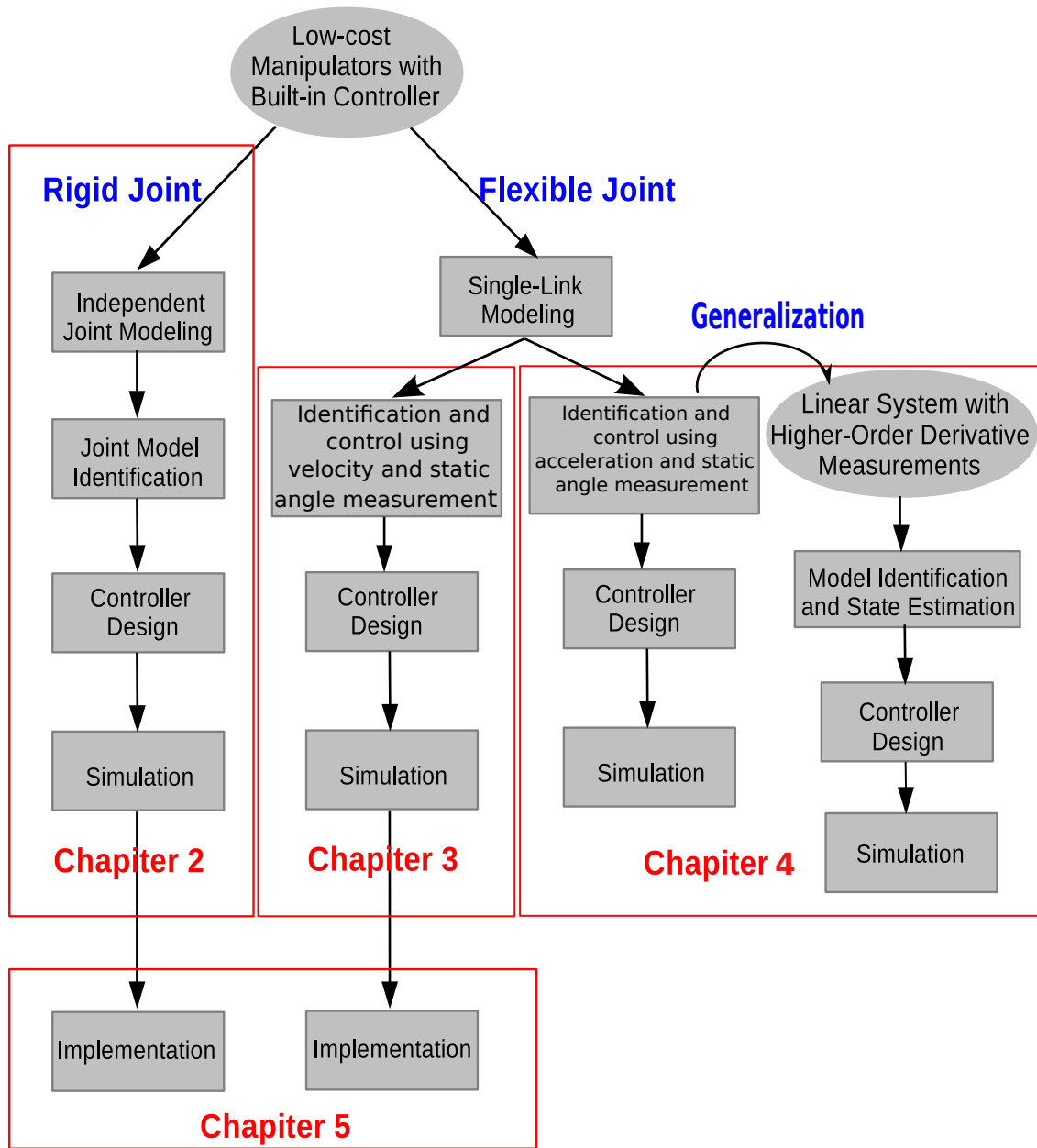


Fig. 1.8 Structure of the middle chapters

Chapter 2

Auxiliary controller design for low-cost rigid manipulator with built-in controller

2.1 Introduction

From a commercial and marketing point of view, “personal robots” must be cheap and user-friendly. A common practice for the current low-cost manipulators in the market is to adopt “all-in-one” actuators, e.g., Dynamixel AX-12A actuators from ROBOTIS. These actuators are integrated with DC motor, sensors, transmission system and position control unit, provide high load-to-weight ratio and relieve the practitioners from designing reduction system and control unit.

However, constrained by the budget, some low-cost manipulators adopt limited-performance all-in-one actuators, for which the built-in controllers are usually simple independent joint controllers, such as PID, PD or even P controller (if no velocity sensor or observer is available). Since the coupling dynamic effects between joints are ignored [13], this leads to limited performance and control precision of the manipulator [100].

The most used closed-loop controller of a servo system is PD (proportional-derivative) controller [31]. Linear analysis suggests that with high gains, precise tracking performance can be achieved. However, high gains drive easily actuators into saturation, besides, for low-cost actuators, reliable velocity feedback with high frequency is hard to obtain. That is why some commercial smart actuators (e.g., Dynamixel AX-12 and AX-18 series) use only P controller, in this case, undesirable static error cannot be avoid when a large load on the motor axis is exerted.

To improve the control performance for position controlled robot manipulators, many works have been done to provide them with torque control capability, since torque controlled

robots are preferred to achieve high performance [78]. Approach to use torque sensors, such as strain gauge [33] or optical torque sensor [34] techniques, is proposed in [35], this joint torque sensing method is adopted in [54]. However, since strain gauges are sensitive to ambient temperature variations, varying offset are often generated. For optical torque sensors, artificial flexibility inside a joint usually needs to be performed to convert the joint torque to joint deformation, while introducing joint flexibility may cause undesired performance such as vibration. In [41], a torque-position transformer for position controlled robots is introduced, with which desired joint torque is converted into instantaneous increments of joint position inputs, this approach has been implemented on the Honda ASIMO robot arm. However, this transformer is based on the total knowledge of the built-in controller, which, designed by the manufacturer of the actuators, is usually unknown or partly unknown to individual users. Besides, to calculate the desired torque, the model of the whole manipulator is indispensable, if it is not available, identification of the whole system model should be considered.

In this chapter, we consider the set-point regulation for a low-cost manipulator equipped with built-in controller. The objective is to design an auxiliary controller, without any additional sensors, to reduce the steady-state error which could not be handled by the built-in controller.

The remainder of this chapter is organized as follows: the statement and analysis of the control problem for low-cost rigid position-controlled manipulators are introduced in Section 2.2. In Section 2.3, dynamics model and model parameter identification method are given. Section 2.4 details the adaptive controller design and its implementation on discrete systems. Simulation results are presented in Section 2.5 with comparison to an auxiliary PID controller. Finally, the conclusion is given in Section 2.6.

2.2 Problem statement and analysis

2.2.1 Problem statement

Consider a n -DOF revolute robot manipulator, each joint is driven by an all-in-one actuator, each actuator is embedded with a controller.

For each joint, Figure 2.1 shows the system under the built-in controller. u is the input for the system, which could be the desired angular position. x denotes the joint position and serves as the feedback, corrupted with measurement noise. τ_m is the torque working on the motor, controlled by the built-in controller, based on the position error e , where $e = u - x$.

The following assumptions are made:

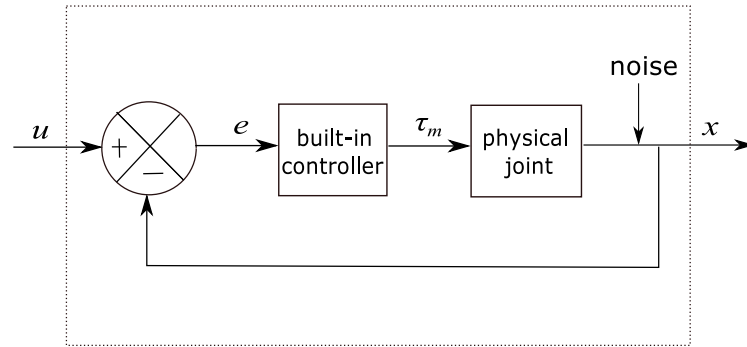


Fig. 2.1 Joint plus controller system

Assumption 2.1. *The model of the built-in controller is of an order less than 2, without integral term. More concretely, the controller can be expressed as a PD part with high gains plus bounded unmodeled error, as:*

$$\tau_m = P(u - x) - D\dot{x} + v, \quad (2.1)$$

where $P > 0$ is the proportional gain, $D \geq 0$ is the derivative gain, while v denotes the unmodeled error and is bounded.

Assumption 2.2. *The manipulator is rigid and time delay is not considered.*

Assumption 2.3. *The manipulator is of light weight and of small size.*

Assumption 2.4. *The gear ratio of the manipulator is rather small (e.g., less than 1:200).*

Assumption 2.5. *The angular velocity and acceleration of the manipulator are limited.*

Assumption 2.6. *Parameters of the dynamic model of the manipulator, e.g. joint mass, initial moments, first moments, etc, are unknown.*

Assumption 2.7. *Only joint angular position feedback is available for the user and is corrupted with noise.*

The objective is to reduce the steady-state error which could not be done by the built-in controller, without any additional sensors.

2.2.2 Problem analysis

Since the built-in controller presents steady state error with $u = x_d$, where u denotes the input for any joint, and x_d is the desired position for this joint, to reduce the position error, the way

is to design an auxiliary controller u based on x_d and position feedback x (and the derivatives of x if necessary), u will afterwards serve as the input for the previous joint plus controller system, the idea is illustrated in Figure 2.2.

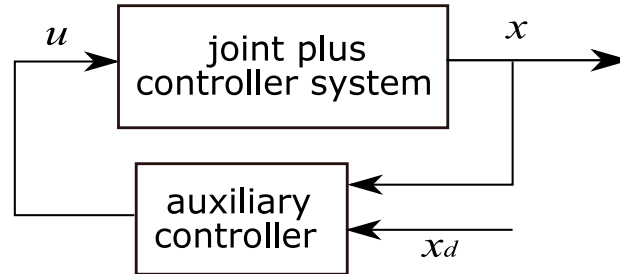


Fig. 2.2 Introduction of an auxiliary controller

Most of the model-based controller design methods are based on the centralized inverse dynamic model (1.3) of manipulators, which relates the input torque vector to the state variable vectors. However, in our case, as we have neither direct or indirect torque input (the torque to be exerted on the motor is decided by the built-in controller of which the model is unknown), nor torque measurements, centralized control seems impossible, as a result, we resort to independent joint control.

The most used independent joint controller is the PID controller. However, from a linear control theory point of view, PID controller with constant gains may not be suitable for a nonlinear and time-varying system. To seek a better performance, a model-based independent joint controller could be a better choice.

2.3 Modelling and identification

2.3.1 Dynamics modelling

Generally, the inverse dynamics model of an n -DOF robot arm with viscous friction can be denoted as:

$$\tau = M(q)\ddot{q} + C(q, \dot{q})\dot{q} + F(\dot{q}) + G(q), \quad (2.2)$$

where q is the joint variable n -vector and τ is the n -vector of the forces or torques. $M(q)$ is the inertia matrix, $C(q, \dot{q})\dot{q}$ is the Coriolis/centripetal n -vector, $F(\dot{q})$ is friction vector, and $G(q)$ is the gravity vector. One of the properties of (2.2) is that $M(q)$, $C(q, \dot{q})$, $F(\dot{q})$, $G(q)$, τ are bounded, as summarized in Section 1.2.2.

The model (2.2) is highly coupled, to get a decoupled independent joint model for joint i , we extract:

$$\tau_i = \sum_{j=1}^n M_{ij}(q)\ddot{q}_j + \sum_{j=1}^n C_{ij}(q, \dot{q})\dot{q}_j + F_i(\dot{q}) + G_i(q). \quad (2.3)$$

Most robot manipulators are driven by servo motors. The motors are connected to the manipulator links through gear trains, where the robot dynamics appear as dynamic load, as illustrated in Figure 2.3. The dynamics of a DC motor can be represented by a second-order linear differential equation. For the i th joint, the dynamics of the motor can be written as [75]:

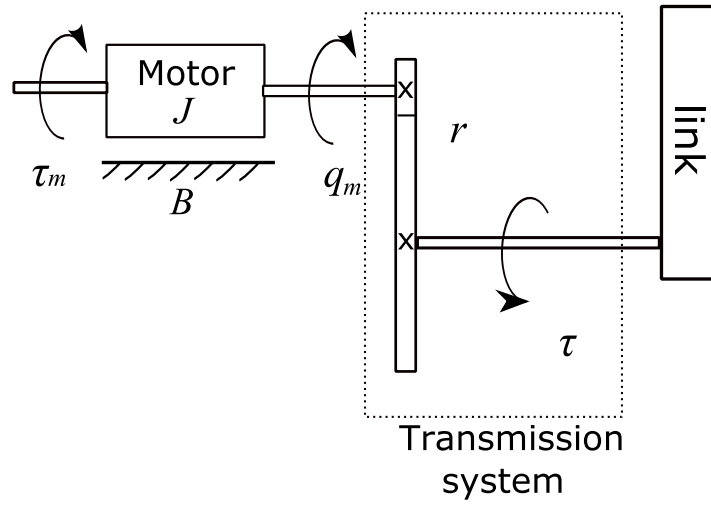


Fig. 2.3 Joint with motor and transmission system

$$J_i\ddot{q}_{mi} + B_i\dot{q}_{mi} = \tau_{mi} - r_i\tau_i, \quad (2.4)$$

where J_i is the total inertia for the motor and gear transmission system, B_i is the corresponding effective damping coefficient, \dot{q}_{mi} and \ddot{q}_{mi} are the motor-side shaft angular velocity and acceleration, r_i is the gear ratio ($r_i \leq 1$). The link is driven by the gear train with relation:

$$\dot{q}_i = r_i\dot{q}_{mi},$$

from which we derive

$$r_i = \frac{\dot{q}_i}{\dot{q}_{mi}} = \frac{\ddot{q}_i}{\ddot{q}_{mi}}. \quad (2.5)$$

Substitute (2.5) into (2.4), we obtain

$$J_i\ddot{q}_i + B_i\dot{q}_i = r_i\tau_{mi} - r_i^2\tau_i. \quad (2.6)$$

From Assumption 2.1, we have

$$\tau_{mi} = P_i(u_i - q_i) - D_i\dot{q}_i + v_i. \quad (2.7)$$

Substitute (2.7) into (2.6), it yields

$$J_i\ddot{q}_i + (B_i + r_iD_i)\dot{q}_i + r_iP_iq_i = r_iP_iu_i + r_iv_i - r_i^2\tau_i. \quad (2.8)$$

Reminder that, for most of today's robot manipulators, large gear reductions are adopted, thus r_i is rather small. From (2.8), it shows that the load torque τ_i expressed in (2.3) is largely reduced by r_i^2 and the controller unmodeled error v_i is reduced by r_i , since r_i is rather small according to Assumption 2.4. In fact, by Assumption 2.3 and Assumption 2.5, τ_i is bounded. On the other hand, since D_i and P_i are of rather high value, r_iD_i and r_iP_i can not be ignored, besides, here we consider light-weight and small-size manipulators, thus the inertial parameters of the motor and the transmission systems (J_i and B_i) are not negligible compared to the link inertial parameters. This is a very important observation since it allows us to treat afterwards τ_i and v_i as bounded disturbance and the drive system tends to dominate the dynamics [86], [50]. Then (2.8) can finally turned into:

$$\ddot{q}_i = a_i(u_i - q_i) - b_i\dot{q}_i + \lambda_i, \quad (2.9)$$

where $a_i = \frac{r_iP_i}{J_i}$, $b_i = \frac{B_i + r_iD_i}{J_i}$ and $\lambda_i = \frac{r_iv_i - r_i^2\tau_i}{J_i}$. a_i and b_i are constants and λ is bounded.

At steady state ($\dot{q} = \ddot{q} = 0$), we have $\tau_i = G_i(q)$ and $v_i = v_{ssi}$, define the steady state error $e_{si} = u_i - q_i$, then

$$e_{si} = -\frac{\lambda_i}{a_i} = \frac{r_iG_i(q) - v_{ssi}}{P_i}. \quad (2.10)$$

This result explains the existence of the steady state error ($u_i - q_i$), and according to this expression, if v_{ssi} can be neglected, then this error depends mainly on the gear ratio r_i , the proportional gain P_i and the gravity torque value $G_i(q)$, this last one depends on the mechanical structure and the configuration of the manipulator.

As a summary, for each joint, we established a second-order differential equation with constant parameters and highly bounded disturbance, this result allows us to design independent joint controllers. For simplification and generality, this model can be rewritten as:

$$\ddot{x} = -a_1x - a_2\dot{x} + ku + \lambda, \quad (2.11)$$

where $x = q_i$, $a_1 = k = \frac{r_i P_i}{J_i}$, $a_2 = \frac{B_i + r_i D_i}{J_i}$ and $\lambda = \frac{r_i v_i - r_i^2 \tau_i}{J_i}$. a_1 , a_2 and k are unknown constants and λ is bounded disturbance. (2.11) will be used for model-based controller design in the following text of this chapter.

Remark 2.1. We can get the same form of the system dynamic model as in (2.11) if the built-in controller in (2.11) is of a P element instead of PD elements, in this case, only a_2 in (2.11) changes and becomes $\frac{B_i}{J_i}$.

2.3.2 Model Identification

Considering a linear nominal model of (2.11) as follows:

$$\ddot{x} = -\bar{a}_1 x - \bar{a}_2 \dot{x} + \bar{k} u, \quad (2.12)$$

where \bar{a}_1 , \bar{a}_2 , \bar{k} are constant. Write (2.12) in the following matrix form:

$$\ddot{x} = \begin{bmatrix} x & \dot{x} & u \end{bmatrix} \begin{bmatrix} -\bar{a}_1 & -\bar{a}_2 & \bar{k} \end{bmatrix}^T. \quad (2.13)$$

Denoting

$$A = \begin{bmatrix} \ddot{x}(t_1) \\ \ddot{x}(t_2) \\ \vdots \\ \ddot{x}(t_m) \end{bmatrix}, B = \begin{bmatrix} x(t_1) & \dot{x}(t_1) & u(t_1) \\ x(t_2) & \dot{x}(t_2) & u(t_2) \\ \vdots & \vdots & \vdots \\ x(t_m) & \dot{x}(t_m) & u(t_m) \end{bmatrix}, H = \begin{bmatrix} -\bar{a}_1 \\ -\bar{a}_2 \\ \bar{k} \end{bmatrix},$$

where m is the number of samplings and t_1, t_2, \dots, t_m are the sampling instants, A and B are composed of known signals (input u , position feedback q , first-order and second-order derivatives of q estimated by differentiator). Then (2.13) is equivalent to

$$A = BH. \quad (2.14)$$

There exist many methods to solve the equation (2.14) with respect to H minimizing the disturbance influence [47]. The simplest one consists in multiplication of both sides in (2.14) by B^T ,

$$B^T H = B^T B A.$$

and sample till the instant that the matrix $B^T B$ becomes nonsingular, then by least square method, we get

$$H = (B^T B)^{-1} B^T A. \quad (2.15)$$

It is worth noting that the above method is based on the knowledge of the velocity \dot{x} and the acceleration \ddot{x} , since we have only position information x , therefore, we need to estimate \dot{x} and \ddot{x} by using observers.

If the system is sufficiently excited by a pre-designed input signal u , with observers of the first-order and second-order derivatives, then \bar{a}_1 , \bar{a}_2 , \bar{k} can be estimated.

2.3.3 Derivative estimation

Let $y(t) = x(t) + w(t)$ be a noisy observation on a finite time interval of a signal $x(t)$ where $w(t)$ represents noise, and we need to estimate the i th order derivative of $x(t)$. For this, a large amount of literatures about high-order differentiation have been published, like high-gain differentiator [15], [16], high-order sliding mode differentiator (HOSM) [51], [26], homogeneous finite-time differentiator (HOMD) [73], [74], algebraic-based differentiator (Alge) [27], [61]. The following gives a brief recall of them.

Algebraic-based differentiation

The basic idea of this approach is to approximate the noisy signal by a suitable polynomial during a small time window. Write $x(t)$ by its convergent Taylor expansion: $x(t) = \sum_{i=0}^{\infty} x^{(i)}(0) \frac{t^i}{i!}$, then consider the following truncated Taylor expansion:

$$x_N(t) = \sum_{i=0}^N x^{(i)}(0) \frac{t^i}{i!},$$

where N is the freely chosen order of the approximated polynomial. By taking Laplace transform of the above equation, it gives

$$x_N(s) = \sum_{i=0}^N \frac{x^{(i)}(0)}{s^{N+1}},$$

which is equivalent to:

$$s^{N+1} x_N(s) = s^N x(0) + s^{N-1} \dot{x}(0) + \dots + x^{(N)}(0). \quad (2.16)$$

In order to estimate the i th order derivative, which is exactly the coefficient $x^{(i)}(0)$ of the above equation, it is necessary to annihilate the remaining coefficients $x^{(j)}(0)$, $j \neq i$, by

multiplying both sides of (2.16) by the following linear differential operator:

$$\Pi_{\kappa}^{N,i} = \frac{d^{i+\kappa}}{ds^{i+\kappa}} \cdot \frac{1}{s} \cdot \frac{d^{N-i}}{ds^{N-i}}, \quad \kappa \geq 0,$$

it yields the following estimator for $x^{(i)}(0)$:

$$\frac{x^{(i)}(0)}{s^{v+i+\kappa+1}} = \frac{(-1)^{n+\kappa}}{(i+\kappa)!(N-i)!} \frac{1}{s^v} \Pi_{\kappa}^{N,i}(s^{N+1}x_N), \quad (2.17)$$

which is strictly proper if $v = N + 1 + \mu$ with $\mu > 0$. After transferring (2.17) back into the time domain and with several calculations, we can obtain the estimation of the i th order derivative of $x(t)$ (see [74] for details).

In a practical way, the first-order and second-order derivative estimates can be expressed as (refer to [61] for details):

$$\begin{cases} \hat{y}(t) = -\frac{6}{T} \int_0^1 (1-2\tau)y(t-\tau T)d\tau, \\ \hat{y}(t) = \frac{60}{T^2} \int_0^1 (6\tau^2 - 6\tau + 1)y(t-\tau T)d\tau, \end{cases} \quad (2.18)$$

where y is the corrupted signal and T is the selected window.

High-gain, HOSM and HOMD differentiators

The recursive schemes of the High-Gain, HOSM (High-order sliding mode) and HOMD (Homogeneous finite-time) differentiators are of a similar formulation, which can be described as follows:

$$\begin{aligned} \dot{z}_1 &= -k_1 \lceil z_1 - y \rceil^{\alpha} + z_2, \\ &\vdots \\ \dot{z}_i &= -k_i \lceil z_1 - y \rceil^{i\alpha - (i-1)} + z_{i+1}, \\ &\vdots \\ \dot{z}_{n-1} &= -k_{n-1} \lceil z_0 - y \rceil^{(n-1)\alpha - (n-2)} + z_n, \\ \dot{z}_n &= -k_n \lceil z_0 - y \rceil^{n\alpha - (n-1)}, \end{aligned} \quad (2.19)$$

where $\lceil a \rceil^b = |a|^b \text{sign}(a)$ and k_i is the chosen gain. Then z_i represents the estimation of the i th order derivative of y . According to [74], there are three cases:

- $\alpha = 1$, then (2.19) represents a high-gain differentiator;
- $\alpha \in (\frac{n-1}{n}, 1)$, then (2.19) represents a HOMD differentiator;

- $\alpha = \frac{n-1}{n}$, then (2.19) represents a HOSM differentiator.

2.4 Auxiliary adaptive controller design

2.4.1 Adaptive controller design

The model of the controller-plus-joint system (2.11) can be rewritten in the following form:

$$\ddot{x} = -\bar{a}_1 x - \bar{a}_2 \dot{x} + \bar{k}(u + \varphi^T \theta + d), \quad (2.20)$$

where $\bar{a}_1, \bar{a}_2, \bar{k}$ are the nominal parameters of (2.12), and

$$\varphi = \begin{bmatrix} x & \dot{x} & u \end{bmatrix}^T, \theta = \begin{bmatrix} \frac{\bar{a}_1 - a_1}{\bar{k}} & \frac{\bar{a}_2 - a_2}{\bar{k}} & \frac{k - \bar{k}}{\bar{k}} \end{bmatrix}^T,$$

where θ represents the unknown constant parameter uncertainties, and $d = \lambda/\bar{k}$ represents the disturbance as introduced in (2.11).

Take x_d as the trajectory reference, particularly, for a set-point regulation problem, $\dot{x}_d = \ddot{x}_d = 0$. We suppose $\bar{a}_1 > 0$ and $\bar{a}_2 > 0$, from [7], the **control law** is given by

$$u = \bar{k}^{-1} \bar{a}_1 x_d - \varphi^T \hat{\theta}, \quad (2.21)$$

where $\hat{\theta}$ denotes the estimate of θ and will be derived hereafter.

After substituting the control law above into (2.20), we can form the error system

$$\ddot{e} = -\bar{a}_1 e - \bar{a}_2 \dot{e} + \bar{k}(\varphi^T (\theta - \hat{\theta}) + d),$$

where $e = x - x_d$. Denote $E = \begin{bmatrix} e \\ \dot{e} \end{bmatrix}$ and $\tilde{\theta} = \theta - \hat{\theta}$, then we get

$$\dot{E} = AE + B(\varphi^T \tilde{\theta} + d), \quad (2.22)$$

with $A = \begin{bmatrix} 0 & 1 \\ -\bar{a}_1 & -\bar{a}_2 \end{bmatrix}$ and $B = \begin{bmatrix} 0 \\ \bar{k} \end{bmatrix}$.

Now select the positive-definite Lyapunov function

$$V = E^T P E + \tilde{\theta}^T \gamma^{-1} \tilde{\theta}, \quad (2.23)$$

where P is a positive-definite symmetric matrix and $\gamma > 0$. The time derivative of V equals:

$$\dot{V} = -E^T QE + 2(E^T PB\varphi^T + \gamma^{-1}\dot{\tilde{\theta}}^T)\tilde{\theta} + 2E^T PBd, \quad (2.24)$$

where Q is a positive definite matrix defined by

$$Q = -(PA + A^T P).$$

By taking

$$\dot{\tilde{\theta}} = -\gamma(\varphi B^T PE - \kappa\hat{\theta}), \quad (2.25)$$

where $\kappa > 0$, then (3.38) becomes:

$$\dot{V} = -E^T QE - \kappa\tilde{\theta}^T \tilde{\theta} + \kappa\theta^T \theta - \kappa\hat{\theta}^T \hat{\theta} + 2E^T PBd. \quad (2.26)$$

Apply Young's inequality, we have

$$\begin{aligned} 2E^T PBd &= 2\frac{1}{\sqrt{2}}E^T Q^{0.5}\sqrt{2}Q^{-0.5}PBd \\ &\leq \frac{1}{2}E^T QE + 2d^T B^T P^T Q^{-1}PBd. \end{aligned} \quad (2.27)$$

Denote $\lambda_{\min}(Q)$, $\lambda_{\max}(P)$ and δ the minimal eigenvalue of Q , the maximal eigenvalue of P and the maximal eigenvalue of $B^T P^T Q^{-1}PB$ respectively, since P and Q are positive definite, $\lambda_{\min}(Q) > 0$ and $\lambda_{\max}(P) > 0$, then we have

$$-E^T QE \leq -\lambda_{\min}(Q)|E|^2 \leq -\frac{\lambda_{\min}(Q)}{\lambda_{\max}(P)}E^T PE, \quad (2.28)$$

and

$$2d^T B^T P^T Q^{-1}PBd \leq 2\delta|d|^2 \leq 2|\delta||d|^2. \quad (2.29)$$

With (3.29), (3.30) and (3.31), we get

$$\dot{V} \leq -\frac{\lambda_{\min}(Q)}{2\lambda_{\max}(P)}E^T PE - \kappa\tilde{\theta}^T \tilde{\theta} + \kappa\theta^T \theta + 2|\delta||d|^2.$$

Since θ and d are bounded, then we can define $\beta = \sup(\kappa\theta^T \theta + 2|\delta||d|^2)$ and $\alpha = \min(\frac{\lambda_{\min}(Q)}{2\lambda_{\max}(P)}, \kappa)$, it is obvious that $\alpha > 0$ and $\beta > 0$, then we have

$$\dot{V} \leq -\alpha V + \beta. \quad (2.30)$$

As time tends to infinity, $V_{t \rightarrow \infty}$ will be bounded by $\frac{\beta}{\alpha}$, from (3.6.2), we derive

$$\lambda_{\min}(P)|E_{t \rightarrow \infty}|^2 \leq E_{t \rightarrow \infty}^T P E_{t \rightarrow \infty} \leq V_{t \rightarrow \infty} \leq \frac{\beta}{\alpha},$$

where $\lambda_{\min}(P)$ is the minimal eigenvalue of P . This gives

$$|E_{t \rightarrow \infty}| \leq \sqrt{\frac{\beta}{\alpha \lambda_{\min}(P)}}. \quad (2.31)$$

So, finally $E_{t \rightarrow \infty}$ will be bounded.

Finally, by recalling that the actual unknown parameter θ is constant, i.e., $\dot{\theta} = 0$, we obtain the **adaptive update rule** for $\hat{\theta}$ as

$$\dot{\hat{\theta}} = -\dot{\tilde{\theta}} = \gamma(\varphi B^T P E - \kappa \hat{\theta}). \quad (2.32)$$

Further more, θ depends on the precision of the parameter identification results, a better identification results give a smaller θ . From (2.32), κ is used to avoid $\hat{\theta}$ from being unstable, can be tuned by the practitioner. P can also be adjusted to increase $\alpha \lambda_{\min}(P)$.

Remark 2.2. *The input u depends on the estimate $\hat{\theta}$, while $\hat{\theta}$ depends on u from (3.40) since ϕ includes u , for the implementation on discrete system, as a common practice in digital devices, just need to take the value one step before of u to calculate the current $\hat{\theta}$ and then derive current u . In fact, a form $u = \bar{b}_1 x - \bar{b}_2 \dot{x} + \bar{b}_3 \ddot{x} + \varphi^T \theta + d$ instead of (2.20) with $\varphi = \begin{bmatrix} x & \dot{x} & \ddot{x} \end{bmatrix}^T$ can avoid this issue, but results in the estimation of the second order derivative \ddot{x} , which can hardly be reliable if x is corrupted by a noise.*

2.4.2 Numerical implementation of the adaptive controller

Write $\hat{\theta} = \begin{bmatrix} \hat{\theta}_1 & \hat{\theta}_2 & \hat{\theta}_3 \end{bmatrix}^T$, then from the control law (2.21), we have

$$u = -(x\hat{\theta}_1 + \dot{x}\hat{\theta}_2 + u\hat{\theta}_3),$$

this gives

$$u = \frac{-x\hat{\theta}_1 - \dot{x}\hat{\theta}_2}{1 + \hat{\theta}_3}, \quad \hat{\theta}_3 \neq -1. \quad (2.33)$$

According to the adaptive update rule (3.40), with $B^T P X$ a scalar, we have

$$\begin{cases} \hat{\theta}_1 &= -\gamma(B^T P X x - \kappa \hat{\theta}_1), \\ \hat{\theta}_2 &= -\gamma(B^T P X \dot{x} - \kappa \hat{\theta}_2), \\ \hat{\theta}_3 &= -\gamma(B^T P X u - \kappa \hat{\theta}_3). \end{cases} \quad (2.34)$$

However, to calculate $\hat{\theta}_3$ in the last equation of (2.34), u is not known *a priori*, thus we need an estimate \hat{u} of u . Here, we propose to let $\hat{u}(t)$ at time t be simply equal to a slightly time-delayed past value of $u(t)$ to implement the controller in discrete system [36]:

$$\hat{u}(t) = u(t - T),$$

where the small time delay T can be viewed as the measurement delay time or, simply, the sampling period of the digital controller. Clearly, the accuracy of the estimate \hat{u} improves as T decreases. Then for implementation, (2.34) is replaced by

$$\begin{cases} \hat{\theta}_{1i} &= \hat{\theta}_{1i-1} - \gamma(B^T P X_i x_i - \kappa \hat{\theta}_{1i-1}), \\ \hat{\theta}_{2i} &= \hat{\theta}_{2i-1} - \gamma(B^T P X_i \dot{x}_i - \kappa \hat{\theta}_{2i-1}), \\ \hat{\theta}_{3i} &= \hat{\theta}_{3i-1} - \gamma(B^T P X_i u_{i-1} - \kappa \hat{\theta}_{3i-1}), \end{cases}$$

where $\hat{\theta}_{1i} = \hat{\theta}_1(t_0 + iT)$ and $\hat{\theta}_{1i-1} = \hat{\theta}_1(t_0 + (i-1)T)$, same for the other variables. Then (2.33) is replaced by

$$u = \begin{cases} \frac{-x_i \hat{\theta}_{1i} - \dot{x}_i \hat{\theta}_{2i}}{1 + \hat{\theta}_{3i}}, & \text{if } |1 + \hat{\theta}_{3i}| > \varepsilon, \\ u_{i-1}, & \text{if } |1 + \hat{\theta}_{3i}| \leq \varepsilon, \end{cases} \quad (2.35)$$

where $\varepsilon > 0$ is a tolerance constant, which has to be selected close to zero.

2.5 Simulation

2.5.1 Model description

A 2DOF light-weight small-size robot manipulator is considered, which is driven by all-in-one actuators with geared transmission. The manipulator is illustrated in Figure 2.4.

For the i -th link, q_i is the associated joint position variable, m_i is the link mass, I_i is link inertia, about an axis through the center of mass (CoM) and perpendicular to the $x - y$ plan, L_i is the length of the link, d_i is the distance between joint i and the CoM of the link i , F_{vi} is the viscous friction coefficient, τ_i is the torque on joint i . Denote also g the gravitational

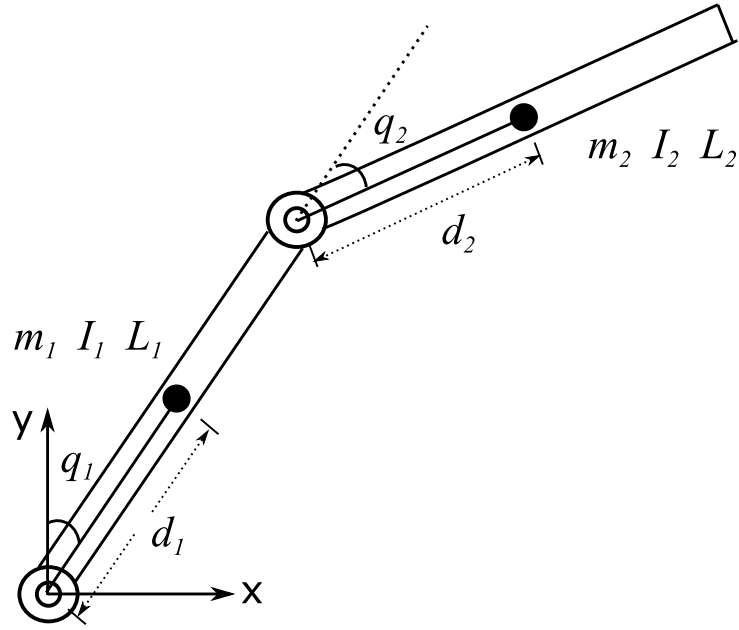


Fig. 2.4 2 DOF Manipulator

acceleration along -y axis. Then the dynamics relating τ and the joint variables q can be expressed as (See Appendix A for the derivation):

$$\left\{ \begin{array}{l} \tau_1 = (m_1 d_1^2 + m_2 L_1^2 + m_2 d_2^2 + 2m_2 L_1 d_2 \cos q_2 + I_1 + I_2) \ddot{q}_1 \\ \quad + (m_2 d_2^2 + m_2 L_1 d_2 \cos q_2 + I_2) \ddot{q}_2 \\ \quad - m_2 L_1 d_2 (2\dot{q}_1 + \dot{q}_2) \dot{q}_2 \sin q_2 + F v_1 \dot{q}_1 \\ \quad - (m_1 d_1 + m_2 L_1) g \sin q_1 - m_2 d_2 g \sin(q_1 + q_2), \\ \tau_2 = (m_2 d_2^2 + m_2 L_1 d_2 \cos q_2 + I_2) \ddot{q}_1 + (m_2 d_2^2 + I_2) \ddot{q}_2 \\ \quad + m_2 L_1 d_2 \dot{q}_1^2 \sin q_2 + F v_2 \dot{q}_2 \\ \quad - m_2 d_2 g \sin(q_1 + q_2). \end{array} \right. \quad (2.36)$$

The built-in controller for joint i is supposed to be a PD controller as:

$$\tau_{mi} = P_i(u_i - q_i) - D_i \dot{q}_i, \quad (2.37)$$

where τ_{mi} is the torque applied to the motor i , u_i is the input for joint i , P_i and D_i are the gains.

Denote J_i , B_i , r_i respectively the total inertia for the motor and gear transmission system, the damping coefficient and the gear ratio for joint i , then from (2.8), we get:

$$\left\{ \begin{array}{l} J_1 \ddot{q}_1 + (B_1 + r_1 D_1) \dot{q}_1 + r_1 P_1 q_1 = r_1 P_1 u_1 - r_1^2 \tau_1, \\ J_2 \ddot{q}_2 + (B_2 + r_2 D_2) \dot{q}_2 + r_2 P_2 q_2 = r_2 P_2 u_2 - r_2^2 \tau_2, \end{array} \right. \quad (2.38)$$

where τ_1 and τ_2 are detailed in (2.36).

For simulation, we consider the set-point control problem. The initial joint position and the desired joint position for joint i are respectively denoted as q_{0i} and q_{di} . All the parameters are set as shown in Table 2.1. In addition, a noisy signal with $SNR = 30dB$ is introduced to the position measurement signal.

Table 2.1 Parameters of 2DOF manipulator for simulation

Parameter	Value	Unit
$r_1 = r_2$	0.01	
$I_1 = I_2$	0.5	$kg.m^2$
$m_1 = m_2$	0.5	kg
$L_1 = L_2$	0.1	m
$d_1 = d_2$	0.05	m
$F_{v1} = F_{v2}$	0.25	$N.m.s.rad^{-1}$
$J_1 = J_2$	0.1	$kg.m^2$
$B_1 = B_2$	0.2	$N.m.s.rad^{-1}$
$P_1 = P_2$	2	$N.m.rad^{-1}$
$D_1 = D_2$	0.5	$N.m.s.rad^{-1}$
$q_{01} = q_{02}$	0	rad
$\dot{q}_{01} = \dot{q}_{02}$	0	$rad.s^{-1}$
$q_{d1} = q_{d2}$	0.5	rad
g	9.8	$m.s^{-2}$

With these parameters, from (2.11), the two links share a model of the same form as:

$$\ddot{x} = -2x - 2.5\dot{x} + 2u + \lambda, \quad (2.39)$$

where λ denotes the disturbance.

In what follows in this chapter, we will compare the control performance among built-in controller, auxiliary PID controller and auxiliary adaptive controller, all the simulation are performed in Matlab[®] Simulink.

2.5.2 Constant input

Denote q_{di} as the desired position for joint i , without any auxiliary controller, the input is constant and takes form as

$$u_i = q_{di}.$$

Figure 2.5 presents the control performance of the built-in controller with constant input. From which we can see that position errors are presented for both joints. From (2.10), the lower link has a bigger error due to a bigger gravity torque.

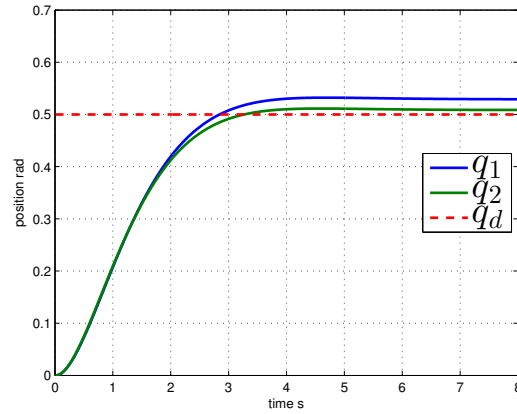


Fig. 2.5 Performance with constant input

2.5.3 Model parameter identification

The model identification is conducted based on the position output from Section 2.5.2. To get the velocity and acceleration estimates, the four derivative observers presented in Section 2.3.3 are tested, for the first link, the result is illustrated in Figure 2.6 and Figure 2.7.

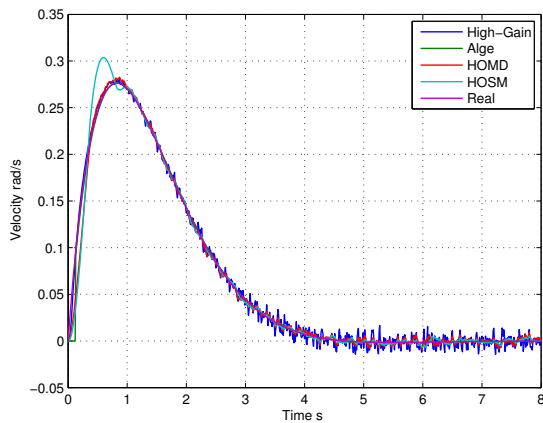


Fig. 2.6 Velocity estimation

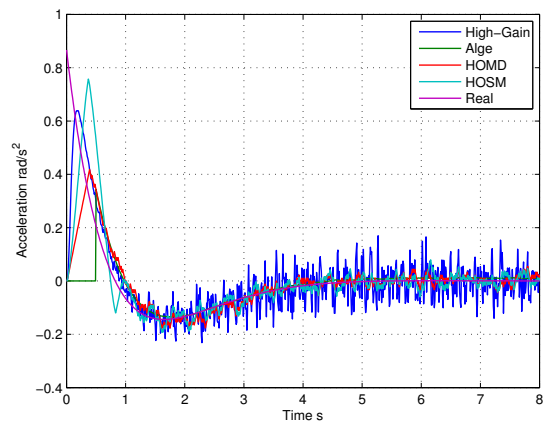


Fig. 2.7 Acceleration estimation

From Figure 2.6, the velocity can be well estimated with all the four differentiators, while the high-gain one is more chattering than the others and the HOSM one presents a lower

convergence speed, the algebraic-based one gives the best result which is quite close to the real velocity. However, for the acceleration estimation in Figure 2.7, only the algebraic-based one gives good results. As a result, we will use the algebraic-based differentiator for the parameter identification.

With the velocity and acceleration estimation results, according to (2.15), we get the nominal model of the first link dynamics as:

$$\ddot{q}_1 = -2.23q_1 - 2.88\dot{q}_1 + 2.32u_1, \quad (2.40)$$

compared to the real model in (2.39), the error rates for the three parameters are respectively 11.5%, 15.2% and 16.0%.

The robustness with respect to noise of the algebraic-based differentiator owns to its integration operation during an interval, however, in real-time computation, this will also leads to delay. For off-time task, the delay can be compensated by shifting the results, as it was done here.

2.5.4 Auxiliary adaptive controller

The auxiliary controller proposed in Section 2.4.1 is simulated for the first link, with the identified model parameters in (2.40). A and B are determined by the identity results, then P is chosen such that $A^T P + PA = -I_2$ where I_2 is the 2×2 identical matrix. γ and κ are taken as 3 and 0.35. The initial value of $\hat{\theta}$ is $(0, 0, 0)$. Figure 2.8a shows the performance of the proposed controller, with which the e_{s1} reduced to $0.0048rad$.

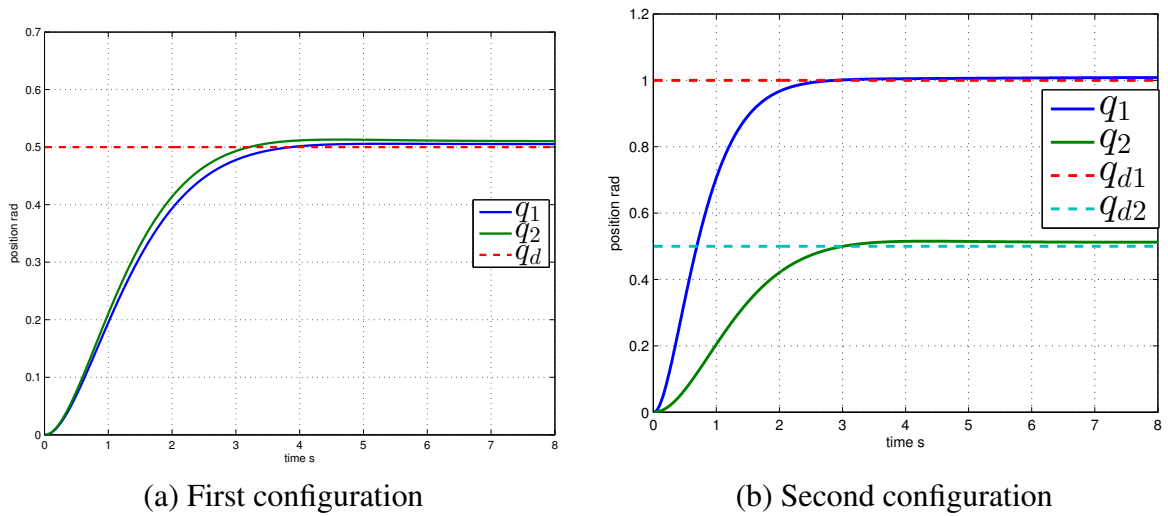


Fig. 2.8 Performance with auxiliary adaptive controller

To test the robustness of the controller with respect to model and configuration changes, now m_1 and I_1 are changed respectively to $1m$ and $1kg.m^2$, while q_{1d} switches to $1 rad$, Figure 2.8b shows the performance of the same adaptive controller after the change.

2.5.5 Auxiliary PID controller

The classic PID controller with constant gains is also considered for the first link as a benchmark. The PID controller is described as:

$$u_i = 3.2(q_{d1} - q_1) - 1.5\dot{q}_1 + 1.15 \int (q_{d1} - q_1). \quad (2.41)$$

The performances of the PID controller under the initial condition and after the model change are respectively illustrated in Figure 2.9a and Figure 2.9b. Compared to the performance of the auxiliary adaptive controller, both of these two are capable of reducing the steady state error to an acceptable range, however, the PID controller with constant gains may work very well only in one case (Figure 2.9a), but the performance may degrade after system model changes, such as prolongation of the convergence time (Figure 2.9b).

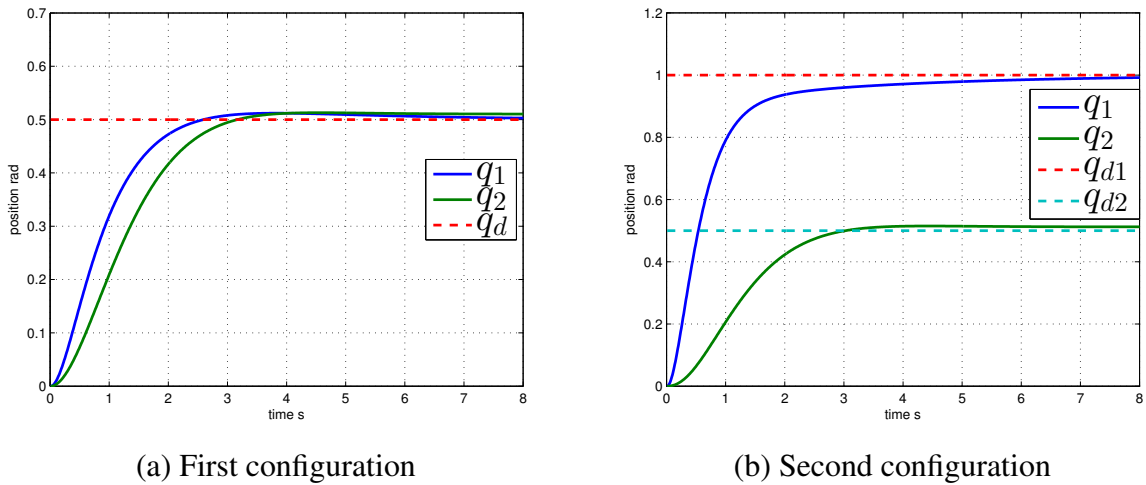


Fig. 2.9 Performance with auxiliary PID controller

2.6 Conclusion

The set-point control problem of low-cost rigid manipulators with “all-in-one” actuators is addressed in this chapter. For the derivation of the dynamics model linking the input with the state variables, the effect of the driven motor and the transmission system is

considered, as a result, a second-order differential equation with constant parameters and highly bounded disturbance is obtained, then identification method of a nominal model is proposed, based on the identified model parameters, a model-based adaptive controller is developed. In simulation, the ability of error reduction is validated, and advantage on performance robustness with respect to model change is observed with comparison to PID controller with constant gains.

Chapter 3

Identification and control of single-link flexible-joint robots using velocity measurement

3.1 Introduction

In some case, limited by the cost and weight, plastic shafts which link the actuator to the link side are adopted, e.g., Dynamixel AX-12A actuators, this leads to the consideration of torsional elasticity of the shaft, especially with a high link load. With the presence of joint-flexibility, the joint position measured by the motor-side encoder matches no more the link position, and oscillation is also evoked.

Based on the model for FJR (flexible-joint robot) proposed by Spong in [82], both the motor position and the link position are used as generalized coordinates. However, most industrial robots are generally only equipped with motor-side encoders [93], accurate estimation of the link position is thus difficult, due to joint flexibility. To obtain information about the link-side part, additional sensors are needed. For example, in addition to motor position sensors, DLR light-weight robot III (Figure 3.1) is equipped with joint torque sensors and link position sensors [35].

However, limited by the cost, these additional sensors seem impossible to be adopted by low-cost robot manufacturers. However, for individual users, mounting of sensors like encoders or strain gauges can be a challenge, since they have to be strictly attached to the link-side shaft, which is generally inside the robots. An alternative solution is to use inertial sensors (e.g., accelerometer, gyroscope, compass, etc.), which are of low cost and small size, and used in various robotic applications, as in [84]. With MEMS (Micro Electro-Mechanical

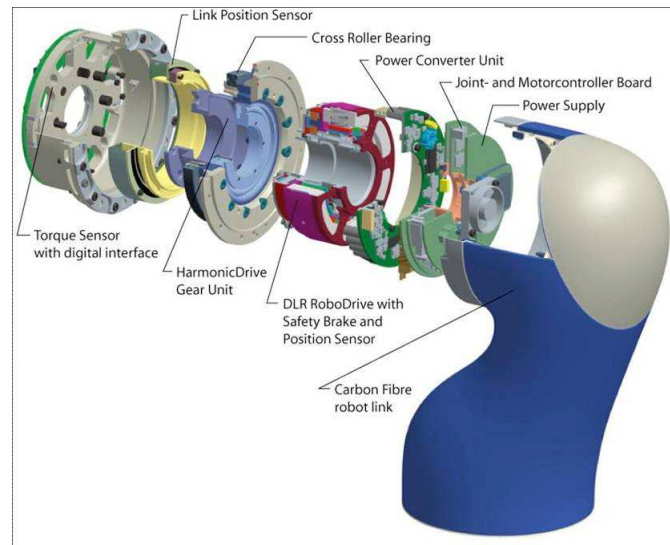


Fig. 3.1 DLR light weight robot III

Systems) technology, an IMU (Inertial Measurement Unit) including a gyroscope and an accelerometer with printed circuit board, can be made into just a coin's size (Fig. 3.2), or even smaller. Besides, due to their inertial property, they just need to be fixed on the surface of the link, and can be easily removed.

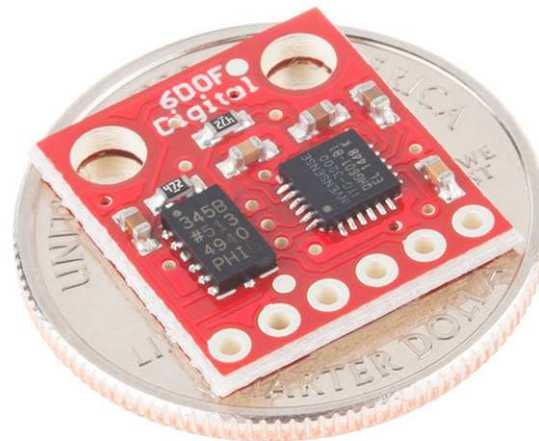


Fig. 3.2 A MEMS IMU

Considerable researches have been conducted on the control of FJR, a recent survey can be found in [70]. Most existing control methods need exact knowledge of the plant model parameters, while to deal with parameter uncertainties, adaptive controllers have been

proposed, like in [53]. From theoretical point of view, these control schemes are complete, however, in practice, most of them are difficult to implement due to: lack of sensors or limited performance of observers, weak robustness on parameter uncertainties, deficiency of computational power of the control unit, difficulties in interpreting and debugging, nonlinearities like torque saturation, etc. As pointed out in [3], even on the latest DLR light-weight robot, the full feedback linearization algorithm cannot be implemented in real time. As a result, the simple PD controller proposed by Tomei in [90], and variations of it, for example [23], are still widely used in industrial robots [88], as this controller uses only motor-side position and velocity.

In Chapter 2, we considered a rigid low-cost manipulator with light weight and small size. In practice, the materials used for such kind of manipulators cannot be absolutely rigid, they can be considered as rigid since for light-weight and small-size robots, the inertial parameters of each link (mass, inertial moment, first moment, etc) is rather small compared to the stiffness of the materials, i.e. the stiffness can be regarded as infinite with respect to those tiny dynamic parameters. However, if the stiffness of the motor shaft or of the gear system is not that dominant (e.g. plastic shaft or harmonic gears) and the link inertial parameters increase (e.g. the link gets longer and/or heavier), then the joint flexibility should be taken into account.

In this chapter, we consider a low-cost single-link manipulator equipped with all-in-one actuators, of which the built-in controller is a P controller, and joint flexibility is presented. The objective is to realize link position control and attenuate oscillation, by using first-order derivative measurement, for set-point regulation.

The remainder of this chapter is organized as follows: first of all, the problem statement is clarified with assumptions. Then the dynamics of single-link FJR is presented and followed by parameter identification method using link velocity measurement. After that, a simple PD controller and a two-stage controller are proposed and the stability is analysed. Finally, the simulation results are given.

3.2 Problem statement

Consider a single-link joint-flexible robot driven by actuator with built-in controller. The built-in controller generates output torque τ_m , based on the input position u and the motor position feedback θ , τ_m works on the motor to drive the motor shaft and the load link, due to the joint flexibility of the shaft, two output are presented: the motor position θ and the link position q , as shown in Figure 3.3. The motor position θ is measured by the motor-side encoder, and it is supposed that the velocity of the link can be measured.

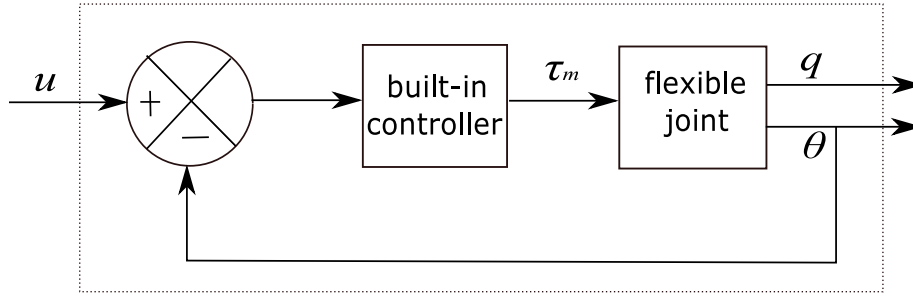


Fig. 3.3 Actuator with built-in controller

Specifically, the following assumptions are made:

Assumption 3.1. *The link is rigid.*

Assumption 3.2. *With the standard assumptions in [82], the joint elasticity is modelled as a linear torsional spring, introduced between the motor and the link, with unknown constant stiffness K , as illustrated in Fig. 3.4. Denote τ as the torque exerted on the link side, then we have*

$$\tau = K(\theta - q). \tag{3.1}$$

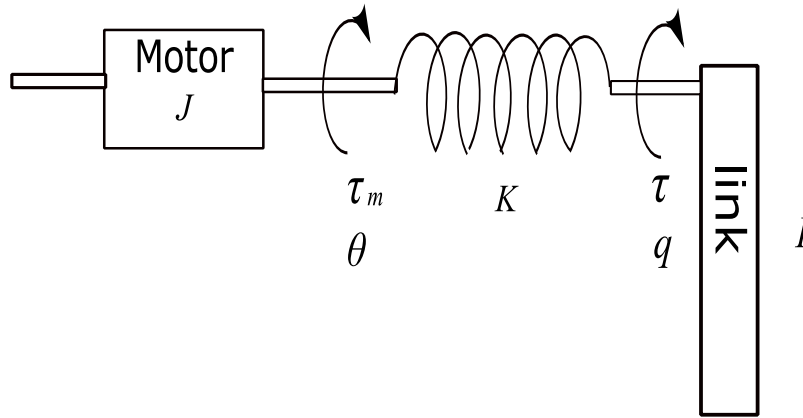


Fig. 3.4 Flexible-joint robot model

Assumption 3.3. *The built-in controller of the actuator is a PD controller with with unknown gains P and D , as described by*

$$\tau_m = P(u - \theta) - D\dot{\theta}. \tag{3.2}$$

Assumption 3.4. *The manipulator is of light weight and of small size.*

Assumption 3.5. *The motor position θ and link angular velocity \dot{q} can be measured. Besides, the manipulator moves in a vertical plan, and the link position at static state can be measured.*

Assumption 3.6. *Inertial parameters of both the motor and the link, i.e., masses, initial moments, first moments, etc, are unknown.*

3.3 System model

Denote I and J as the inertial moment of the link and of the motor, F and H are the viscous friction parameter on the link side and on the motor side, m is the mass of the link, l is the distance between the mass center of the link and the rotational axe, g is the gravitational acceleration, τ_m and τ are the torque exerted on the motor and on the link. Then the dynamic model of the single-link flexible-joint robot is given by

$$\begin{cases} J\ddot{\theta} + H\dot{\theta} + \tau = \tau_m, \\ I\ddot{q} + F\dot{q} - mgl \sin q = \tau. \end{cases} \quad (3.3)$$

Substitute (3.1) and (3.2) into (3.3), and denote $G = mgl$ for simplicity, then we have

$$\begin{cases} J\ddot{\theta} + H\dot{\theta} + K(\theta - q) = P(u - \theta) - D\dot{\theta}, \\ I\ddot{q} + F\dot{q} - G \sin q = K(\theta - q). \end{cases} \quad (3.4)$$

Suppose $P \neq 0$ and $K \neq 0$, then (3.4) can be transformed into

$$\begin{cases} \frac{J}{P}\ddot{\theta} + \frac{H+D}{P}\dot{\theta} + \frac{K}{P}(\theta - q) = u - \theta, \\ \frac{I}{K}\ddot{q} + \frac{F}{K}\dot{q} - \frac{G}{K} \sin q = \theta - q. \end{cases} \quad (3.5a)$$

$$\begin{cases} \frac{I}{K}\ddot{q} + \frac{F}{K}\dot{q} - \frac{G}{K} \sin q = \theta - q. \end{cases} \quad (3.5b)$$

For simplicity, denote $J_p = \frac{J}{P}$, $H_p = \frac{H+D}{P}$, $K_p = \frac{K}{P}$, $I_k = \frac{I}{K}$, $F_k = \frac{F}{K}$, $G_k = \frac{G}{K}$, recall Assumption 3.5, without measurement noise, then the system can be summarized as

$$\begin{cases} J_p\ddot{\theta} + H_p\dot{\theta} + K_p(\theta - q) = u - \theta, \\ I_k\ddot{q} + F_k\dot{q} - G_k \sin q = \theta - q, \\ Y_1 = \theta, \\ Y_2 = \dot{q}, \\ Y_3 = q, \text{ if } \dot{q} = 0, \end{cases} \quad (3.6)$$

where Y_i ($i = 1, 2, 3$) denotes the output measurements.

3.4 Parameter identification using angular velocity measurement

Assumption 3.7. *The static link position can be measured.*

In fact, there are several sensors on the market which can be used for precise angular-position measurements, like accelerometers [72], fibre-optic sensors [42], 3-D silicon hall sensor [11], etc.

For simplicity, assume $t_0 = 0$ and $\dot{q}(t_0) = 0$, denote $q_0 = q(t_0)$, by Assumption 3.7, q_0 can be measured, recall the fact that we have also measurement of \dot{q} , then we have

$$q = q_0 + \int \dot{q} dt, \quad (3.7)$$

then the first equation of (3.6) is equivalent to

$$(\ddot{\theta}, \dot{\theta}, \theta - q)(J_p, H_p, K_p)^T = u - \theta, \quad (3.8)$$

from which J_p, H_p, K_p can be estimated by using least square method as in Section 2.3.2, provided that $\ddot{\theta}$ and $\dot{\theta}$ can be obtained using numerical differentiation. The estimates of J_p, H_p, K_p , are denoted as $\hat{J}_p, \hat{H}_p, \hat{K}_p$.

With (3.7), the second equation of (3.6) is equivalent to

$$(\ddot{q}, \dot{q}, -\sin q)(I_k, F_k, G_k)^T = \theta - q, \quad (3.9)$$

from which I_k, F_k, G_k can then be estimated by using least square method, provided that \ddot{q} can be obtained using numerical differentiation. The estimates of I_k, F_k and G_k are denoted as $\hat{I}_k, \hat{F}_k, \hat{G}_k$.

Remark 3.1. *With the proposed identification method, we cannot identify the real physique parameters, like the inertial moment, the stiffness, friction coefficients or other parameters appearing in (3.4), but we can identify the ratios between the parameters, which essentially determine the dynamics of the system.*

Remark 3.2. *The proposed identification method involves estimation of $\ddot{\theta}$ and $\dot{\theta}$ from θ , and \ddot{q} from \dot{q} , 4 differentiators are presented in Section 2.3.3.*

Remark 3.3. *With the proposed identification method, we can identify directly $\hat{J}_p, \hat{H}_p, \hat{K}_p, \hat{I}_k, \hat{F}_k, \hat{G}_k$, and other ratios can be derived from these results, e.g. $\hat{G}_p = \hat{G}_k \hat{K}_p$.*

3.5 PD controller with gravity compensation

3.5.1 Without parameter uncertainty

To be applicable to our studied case, a modified PD plus gravity compensation controller based on the one proposed in [90] is expressed as

$$\begin{cases} u = -K_1(\theta - \theta_d) - K_2\dot{\theta} - G_p \sin q_d + \theta, & (3.10a) \\ \theta_d = q_d - G_k \sin q_d, & (3.10b) \end{cases}$$

where $G_p = \frac{G}{P} = G_k K_p$ and $G_k = \frac{G}{K}$ as defined previously, q_d is the desired set-point link position, K_1 and K_2 are constant positive gains.

To investigate the stability of the controller (3.10a) and (3.10b), first we give the following preliminary: For a matrix $A \in \mathbb{R}^{n \times n}$ the vector of its eigenvalues is denoted as $\lambda(A)$, $A_{min} = \min \lambda(A)$, and $\|A\| = \sqrt{\max_{i=1, \dots, n} \lambda_i(A^T A)}$ (the induced L_2 matrix norm).

Introduce the matrix

$$C = \begin{bmatrix} K + PK_1 & -K \\ -K & K \end{bmatrix},$$

then the following theorem holds:

Theorem 3.1. *Consider the system (3.4) with the control law (3.10a) and (3.10b), if $C_{min} > G$, then the point $(\theta = \theta_d, q = q_d, \dot{\theta} = 0, \dot{q} = 0)$ is the unique equilibrium point, and this equilibrium point is globally asymptotically stable.*

Proof. The equilibrium points of (3.4) and (3.10a) are the solutions of

$$\begin{cases} K(\theta - q) + PK_1(\theta - \theta_d) + G \sin q_d = 0, \\ K(\theta - q) + G \sin q = 0. \end{cases} \quad (3.11)$$

From (3.10b) we have $K(\theta_d - q_d) + G \sin q_d = 0$, this allows us to subtract $K(\theta_d - q_d) + G \sin q_d$ from the left sides of (3.11), and it yields

$$\begin{cases} (K + PK_1)(\theta - \theta_d) - K(q - q_d) = 0, \\ K(\theta - \theta_d) - K(q - q_d) + G(\sin q - \sin q_d) = 0, \end{cases}$$

which can be rewritten in matrix form as

$$C \begin{bmatrix} \theta - \theta_d \\ q - q_d \end{bmatrix} = \begin{bmatrix} 0 \\ G(\sin q - \sin q_d) \end{bmatrix}. \quad (3.12)$$

Using the theorem assumption, for all $(\theta, q) \neq (\theta_d, q_d)$, we have

$$\begin{aligned} \left\| C \begin{bmatrix} \theta - \theta_d \\ q - q_d \end{bmatrix} \right\| &\geq C_{min} \left\| \begin{bmatrix} \theta - \theta_d \\ q - q_d \end{bmatrix} \right\| \\ &> G \left\| \begin{bmatrix} \theta - \theta_d \\ q - q_d \end{bmatrix} \right\| \\ &\geq G \| q - q_d \| \\ &\geq G \| \sin q - \sin q_d \| \\ &= \left\| \begin{bmatrix} 0 \\ G(\sin q - \sin q_d) \end{bmatrix} \right\|, \end{aligned}$$

hence (θ_d, q_d) is the unique equilibrium point. Now, define a position-dependent energy function

$$H(\theta, q) = \frac{1}{2}K(\theta - q)^2 + \frac{1}{2}PK_1(\theta - \theta_d)^2 + G \cos q + \theta G \sin q_d, \quad (3.13)$$

its gradient can be expressed as

$$\nabla H(\theta, q) = \begin{bmatrix} \frac{\partial H}{\partial \theta} \\ \frac{\partial H}{\partial q} \end{bmatrix}^T = \begin{bmatrix} K(\theta - q) + PK_1(\theta - \theta_d) + G \sin q_d \\ -K(\theta - q) - G \sin q \end{bmatrix}^T.$$

The stationary points of $H(\theta, q)$ such that $\nabla H(\theta, q) = \mathbf{0}$ are given by the solutions of

$$\begin{cases} \frac{\partial H}{\partial \theta} = 0, \\ \frac{\partial H}{\partial q} = 0, \end{cases}$$

which coincides exactly with (3.11), thus (θ_d, q_d) is the unique stationary point of $H(\theta, q)$. Moreover, the second order gradient of $H(\theta, q)$ (Hessian matrix) is

$$\nabla^2 H(\theta, q) = \begin{bmatrix} \frac{\partial^2 H}{\partial \theta^2} & \frac{\partial^2 H}{\partial \theta \partial q} \\ \frac{\partial^2 H}{\partial q \partial \theta} & \frac{\partial^2 H}{\partial q^2} \end{bmatrix} = \begin{bmatrix} K + PK_1 & -K \\ -K & K - G \cos q \end{bmatrix},$$

from which it yields

$$\nabla^2 H(\theta_d, q_d) = C - \begin{bmatrix} 0 & 0 \\ 0 & G \cos q_d \end{bmatrix}.$$

For any vector $x = [x_1, x_2]^T \in \mathbb{R}^2$ and $x \neq \mathbf{0}$, we have

$$\begin{aligned} x \nabla^2 H(\theta_d, q_d) x^T &= x C x^T - x \begin{bmatrix} 0 & 0 \\ 0 & G \cos q_d \end{bmatrix} x^T \\ &\geq C_{\min} x x^T - G x_2^2 \cos q_d \\ &> G(x_1^2 + x_2^2) - G x_2^2 \cos q_d \\ &\geq G x_2^2 (1 - \cos q_d) \\ &\geq 0, \end{aligned}$$

thus $\nabla^2 H(\theta_d, q_d)$ is positive definite, as a result, (θ_d, q_d) is an absolute minimum for $H(\theta, q)$. Now, take a candidate Lyapunov function as

$$V(\theta, q, \dot{\theta}, \dot{q}) = \frac{1}{2} J \dot{\theta}^2 + \frac{1}{2} I \dot{q}^2 + H(\theta, q) - H(\theta_d, q_d),$$

then V is positive definite with respect to $(\theta = \theta_d, q = q_d, \dot{\theta} = 0, \dot{q} = 0)$, the time derivative of V is given by

$$\begin{aligned} \dot{V} &= J \dot{\theta} \ddot{\theta} + I \dot{q} \ddot{q} + \dot{H}(\theta, q) \\ &= \dot{\theta} [-PK_1(\theta - \theta_d) - PK_2 \dot{\theta} - G \sin q_d - D \dot{\theta} - H \dot{\theta} - K(\theta - q)] + \\ &\quad K(\theta - q)(\dot{\theta} - \dot{q}) + PK_1(\theta - \theta_d) \dot{\theta} - G \dot{q} \sin q + G \dot{\theta} \sin q_d + \\ &\quad \dot{q} [K(\theta - q) + G \sin q - F \dot{q}] \\ &= -(PK_2 + D + H) \dot{\theta}^2 - F \dot{q}^2 \\ &\leq 0. \end{aligned}$$

Since $\dot{V} = 0$ implies $\dot{q} = 0$ and $\dot{\theta} = 0$, from the first part of the proof, the unique solution to $\dot{q} = 0$ and $\dot{\theta} = 0$ is $q = q_d$ and $\theta = \theta_d$, then the proof is completed using LaSalle Theorem. \square

3.5.2 With parameter uncertainty

However, in practice, there is no guarantee that the parameters appearing directly in the controller design, here as G_p and G_k , can be known exactly. Using the parameter identification results, we have only access to \hat{G}_p and \hat{G}_k , then the controller becomes

$$\begin{cases} u = -K_1(\theta - \hat{\theta}_d) - K_2\dot{\theta} - \hat{G}_p \sin q_d + \theta, & (3.14a) \\ \hat{\theta}_d = q_d - \hat{G}_k \sin q_d, & (3.14b) \end{cases}$$

where \hat{G}_p and G_k are respectively the estimates of $\frac{G}{P}$ and $\frac{G}{K}$. Then the following theorem holds:

Theorem 3.2. *Consider the system (3.4) with the control law (3.14a) and (3.14b), if $C_{min} > G$, then the system has only one equilibrium point, denoted as $(\theta = \bar{\theta}_d, q = \bar{q}_d, \dot{\theta} = 0, \dot{q} = 0)$. Moreover, this unique equilibrium point is globally asymptotically stable.*

Proof. The equilibrium points of (3.4) and (3.14a) are the solutions of

$$\begin{cases} K(\theta - q) + PK_1(\theta - \hat{\theta}_d) + \hat{G} \sin q_d = 0, & (3.15) \\ K(\theta - q) + G \sin q = 0, \end{cases}$$

where $\hat{G} = P\hat{G}_p$. (3.15) can be rewritten as:

$$\begin{cases} K(\theta - q) + PK_1(\theta - \theta_d) + PK_1(\theta_d - \hat{\theta}_d) + \hat{G} \sin q_d = 0, & (3.16) \\ K(\theta - q) + G \sin q = 0, \end{cases}$$

where θ_d is defined as in (3.10b). Subtracting $K(\theta_d - q_d) + G \sin q_d$ which is null by (3.10b) to the left sides of (3.16), we obtain

$$\begin{cases} (K + PK_1)(\theta - \theta_d) - K(q - q_d) + PK_1(\theta_d - \hat{\theta}_d) + \hat{G} \sin q_d - G \sin q_d = 0, \\ K(\theta - \theta_d) - K(q - q_d) + G \sin q - G \sin q_d = 0, \end{cases}$$

which can be rewritten in matrix form as

$$C \begin{bmatrix} \theta - \theta_d \\ q - q_d \end{bmatrix} = \begin{bmatrix} PK_1(\hat{\theta}_d - \theta_d) + G \sin q_d - \hat{G} \sin q_d \\ G(\sin q - \sin q_d) \end{bmatrix}. \quad (3.17)$$

Now, define a position-dependent energy function

$$H(\theta, q) = \frac{1}{2}K(\theta - q)^2 + \frac{1}{2}PK_1(\theta - \theta_d)^2 + G \cos q + \theta[PK_1(\theta_d - \hat{\theta}_d) + \hat{G} \sin q_d], \quad (3.18)$$

its gradient can be expressed as

$$\nabla H(\theta, q) = \begin{bmatrix} \frac{\partial H}{\partial \theta} \\ \frac{\partial H}{\partial q} \end{bmatrix}^T = \begin{bmatrix} K(\theta - q) + PK_1(\theta - \theta_d) + PK_1(\theta_d - \hat{\theta}_d) + \hat{G} \sin q_d \\ -K(\theta - q) - G \sin q \end{bmatrix}^T,$$

and the second order gradient of $H(\theta, q)$ (Hessian matrix) is

$$\nabla^2 H(\theta, q) = \begin{bmatrix} \frac{\partial^2 H}{\partial \theta^2} & \frac{\partial^2 H}{\partial \theta \partial q} \\ \frac{\partial^2 H}{\partial q \partial \theta} & \frac{\partial^2 H}{\partial q^2} \end{bmatrix} = \begin{bmatrix} K + PK_1 & -K \\ -K & K - G \cos q \end{bmatrix},$$

as shown in the proof of Theorem 3.1, $\nabla^2 H(\theta, q) > 0$, thus $H(\theta, q)$ is a convex function which allows only one absolute minimum. Denote the unique absolute minimum as $(\bar{\theta}_d, \bar{q}_d)$, then $(\bar{\theta}_d, \bar{q}_d)$ is the unique stationary points of $H(\theta, q)$ such that $\nabla H(\theta, q) = \mathbf{0}$, i.e, the solutions of

$$\begin{cases} \frac{\partial H}{\partial \theta} = 0, \\ \frac{\partial H}{\partial q} = 0, \end{cases}$$

which coincides exactly with (3.16), thus we have

$$C \begin{bmatrix} \bar{\theta}_d - \theta_d \\ \bar{q}_d - q_d \end{bmatrix} = \begin{bmatrix} PK_1(\hat{\theta}_d - \theta_d) + G \sin q_d - \hat{G} \sin q_d \\ G(\sin \bar{q}_d - \sin q_d) \end{bmatrix}. \quad (3.19)$$

Subtracting (3.19) from (3.17), we obtain

$$C \begin{bmatrix} \theta - \bar{\theta}_d \\ q - \bar{q}_d \end{bmatrix} = \begin{bmatrix} 0 \\ G(\sin q - \sin q_d) \end{bmatrix}. \quad (3.20)$$

As indicated in the proof of Theorem 3.1, with the assumption of $C_{min} > G$, (3.20) owns the unique solution $(\theta = \bar{\theta}_d, q = \bar{q}_d)$. Now, the first part of this theorem is proved.

The global asymptotic stability of the equilibrium point $(\theta = \bar{\theta}_d, q = \bar{q}_d), \dot{\theta} = 0, \dot{q} = 0$ can be proved by considering the following Lyapunov function:

$$V(\theta, q, \dot{\theta}, \dot{q}) = \frac{1}{2}J\dot{\theta}^2 + \frac{1}{2}I\dot{q}^2 + H(\theta, q) - H(\bar{\theta}_d, \bar{q}_d),$$

and proceeding the same way as in the proof of Theorem 3.1. \square

By comparing (3.12) to (3.19), we can see that if $PK_1(\hat{\theta}_d - \theta_d) + G \sin q_d - \hat{G} \sin q_d \neq 0$, then the actual equilibrium position $(\bar{\theta}_d, \bar{q}_d)$ differs from the desired one (θ_d, q_d) .

From the left-hand side of (3.19), we have

$$\left\| C \begin{bmatrix} \bar{\theta}_d - \theta_d \\ \bar{q}_d - q_d \end{bmatrix} \right\| \geq C_{min} \left\| \begin{bmatrix} \bar{\theta}_d - \theta_d \\ \bar{q}_d - q_d \end{bmatrix} \right\|. \quad (3.21)$$

From the right-hand side of (3.19), we have

$$\begin{aligned} \left\| \begin{bmatrix} PK_1(\hat{\theta}_d - \theta_d) + G \sin q_d - \hat{G} \sin q_d \\ G(\sin \bar{q}_d - \sin q_d) \end{bmatrix} \right\| &\leq \| G(\sin \bar{q}_d - \sin q_d) \| + \\ &\| PK_1(\hat{\theta}_d - \theta_d) + G \sin q_d - \hat{G} \sin q_d \| \\ &\leq G \| \bar{q}_d - q_d \| + \| PK_1(G_k \sin q_d - \hat{G}_k \sin q_d) + \\ &P(G_p \sin q_d - \hat{G}_p \sin q_d) \| \\ &\leq G \left\| \begin{bmatrix} \bar{\theta}_d - \theta_d \\ \bar{q}_d - q_d \end{bmatrix} \right\| + \\ &P \| \sin q_d \| \| K_1(G_k - \hat{G}_k) + G_p - \hat{G}_p \|. \end{aligned} \quad (3.22)$$

Combining (3.21) and (3.22), we obtain

$$C_{min} \left\| \begin{bmatrix} \bar{\theta}_d - \theta_d \\ \bar{q}_d - q_d \end{bmatrix} \right\| \leq G \left\| \begin{bmatrix} \bar{\theta}_d - \theta_d \\ \bar{q}_d - q_d \end{bmatrix} \right\| + P \| \sin q_d \| \| K_1(G_k - \hat{G}_k) + G_p - \hat{G}_p \|,$$

from which we obtain

$$\left\| \begin{bmatrix} \bar{\theta}_d - \theta_d \\ \bar{q}_d - q_d \end{bmatrix} \right\| \leq \frac{P}{C_{min} - G} \|\sin q_d\| \|K_1(G_k - \hat{G}_k) + G_p - \hat{G}_p\|. \quad (3.23)$$

Remark 3.4. From (3.23), we can see that with parameter uncertainties, the error between the actual equilibrium point and the desired one is bounded, and the boundedness is influenced by the precision of the estimates \hat{G}_k and \hat{G}_p . As pointed out in Remark 3.3, \hat{G}_p can not be directly identified, but can be obtained as $\hat{G}_p = \hat{G}_k \hat{K}_p$, thus essentially, the error is affected by the estimates \hat{G}_k and \hat{K}_p . $\hat{G}_k \neq G_k$ or $\hat{K}_p \neq K_p$

Remark 3.5. The estimation of \hat{K}_p by (3.8) includes the estimation of the second-order derivative of θ , of which the precision can hardly be guaranteed in practice.

3.6 Two-stage adaptive controller using inertial sensors

The advantage of the PD controller is that only motor-side information is needed for the implementation, while the control precision is less robust with respect to parameter uncertainties. As commonly acknowledged, the more sensor information is used, a better result should be obtained. Here we propose a two-stage adaptive controller, to proceed we need the following assumption:

Denote $q(t_0)$ the initial static position of the link, which can be measured by the accelerometer, then we have

$$q(t) = q(t_0) + \int_{t_0}^t \dot{q} dt, \quad (3.24)$$

where \dot{q} is measured by the gyroscope. Thus the state variable q and \dot{q} are available.

The single-link flexible-joint robot dynamics can be regarded as two subsystems on cascade, as described by (3.5a) and (3.5b). In this section, we propose a controller based on the two-stage control design method. Firstly, based on the link-side subsystem (3.5b), a motor-side position reference denoted by θ_d is established, which, if well followed, should drive the link to the desired set-point position q_d , within an acceptable error. Secondly, to guarantee that θ_d can be well tracked, an adaptive controller is formulated for the motor-side subsystem (3.5a), considering model parameter uncertainties, with which asymptotic stability can be guaranteed.

3.6.1 Motor position reference design

Introduce θ_d as the desired motor position trajectory, then (3.5b) can be rewritten as

$$I_k \ddot{q} + F_k \dot{q} - G_k \sin q = \theta_d - q + \tilde{\theta}, \quad (3.25)$$

where $\tilde{\theta} = \theta - \theta_d$. (3.25) can be considered as controlled by θ_d with presence of an actuator perturbation $\tilde{\theta}$, which will be coped with in the next subsection by the controller u exerted on the motor-side subsystem. Here, we suppose that $\tilde{\theta}$ is bounded.

Suppose I_k and F_k are positive, based on the identification results, giving θ_d as

$$\theta_d = -\hat{G}_k \sin q + q_d + k_p(q - q_d), \quad (3.26)$$

where q_d is the desired link position and K_p is a dumping factor with $K_p \leq 1$. Substitute (3.26) into (3.25), we can obtain

$$\ddot{q} = -\frac{1-k_p}{I_k}(q - q_d) - \frac{F_k}{I_k}\dot{q} + \frac{(G_k - \hat{G}_k) \sin q + \tilde{\theta}}{I_k}.$$

Note $e_q = q - q_d$, $E_q = \begin{bmatrix} e_q \\ \dot{e}_q \end{bmatrix}$, $M = \begin{bmatrix} 0 & 1 \\ -\frac{1-k_p}{I_k} & -\frac{F_k}{I_k} \end{bmatrix}$, $N = \begin{bmatrix} 0 \\ 1 \end{bmatrix}$ and $d = \frac{(G_k - \hat{G}_k) \sin q + \tilde{\theta}}{I_k}$, M is Hurwitz. For a set-point regulation problem, it yields

$$\dot{E}_q = ME_q + Nd. \quad (3.27)$$

Choose the Lyapunov function as:

$$V_q = E_q^T P_q E_q,$$

where P_q is symmetric and $P_q > 0$. The time derivative of V equals:

$$\dot{V}_q = -E_q^T Q_q E_q + 2E_q^T P_q N d, \quad (3.28)$$

where $Q_q > 0$ and satisfies $Q_q = -(P_q M + M^T P_q)$. By Young's inequality, we have

$$\begin{aligned} 2E_q^T P_q N d &= 2E_q^T \frac{Q_q^{0.5}}{\sqrt{2}} * \sqrt{2} Q_q^{-0.5} P_q N d \\ &\leq \frac{1}{2} E_q^T Q_q E_q + 2d^T N^T P_q^T Q_q^{-1} P_q N d. \end{aligned} \quad (3.29)$$

Denote $\lambda_{\min}(Q_q)$, $\lambda_{\max}(P_q)$ and δ the minimal eigenvalue of Q_q , the maximal eigenvalue of P_q and the maximal eigenvalue of $N^T P_q^T Q_q^{-1} P_q N$ respectively, since P_q and Q_q are positive definite, $\lambda_{\min}(Q_q) > 0$ and $\lambda_{\max}(P_q) > 0$, then we have

$$-E_q^T Q_q E_q \leq -\lambda_{\min}(Q_q) |E_q|^2 \leq -\frac{\lambda_{\min}(Q_q)}{\lambda_{\max}(P_q)} E_q^T P_q E_q, \quad (3.30)$$

and

$$2d^T N^T P_q^T Q_q^{-1} P_q N d \leq 2\delta |d|^2. \quad (3.31)$$

With (3.29), (3.30) and (3.31), we get

$$\dot{V}_q \leq -\frac{\lambda_{\min}(Q_q)}{2\lambda_{\max}(P_q)} E_q^T P_q E_q + 2|\delta| |d|^2. \quad (3.32)$$

By the definition of d , since $\tilde{\theta}$ is bounded, $|(G_k - \hat{G}_k) \sin q| \leq |G_k - \hat{G}_k|$ is also bounded, thus d is bounded, then it exists $d_{sup} > 0$ such that

$$|d| \leq d_{sup}.$$

Define $\beta = 2|\delta| d_{sup}^2$ and $\alpha = \frac{\lambda_{\min}(Q)}{2\lambda_{\max}(P)}$, it is obvious that $\alpha > 0$ and $\beta > 0$, then we have

$$\dot{V}_q \leq -\alpha V + \beta.$$

As time tends to infinity, $V_{qt \rightarrow \infty}$ will be bounded by $\frac{\beta}{\alpha}$, then we derive

$$\lambda_{\min}(P_q) |E_{qt \rightarrow \infty}|^2 \leq E_{qt \rightarrow \infty}^T P_q E_{qt \rightarrow \infty} = V_{qt \rightarrow \infty} \leq \frac{\beta}{\alpha},$$

where $\lambda_{\min}(P)$ is the minimal eigenvalue of P_q . This gives

$$|E_{qt \rightarrow \infty}| \leq \sqrt{\frac{\beta}{\alpha \lambda_{\min}(P_q)}}. \quad (3.33)$$

So, finally $E_{qt \rightarrow \infty}$ will be bounded.

Remark 3.6. The boundedness depends on the precision of \hat{G}_k , and the disturbance $\tilde{\theta}$. If $G_k = \hat{G}_k$ and $\tilde{\theta} = 0$, then $d = 0$ and asymptotic stability can be guaranteed.

3.6.2 Adaptive input design

It is proved in the previous subsection that, if the desired motor position trajectory θ_d can be well tracked, then the regulation task can be achieved with certain boundedness. Now, we need to propose a control input u for the motor-side subsystem, which will guarantee the convergence of the motor position to θ_d .

Equation (3.5a) is equivalent to

$$\ddot{\theta} = -\frac{K+P}{J}\theta - \frac{H+D}{J}\dot{\theta} + \frac{P}{J}u + \frac{K}{J}q.$$

Denote $a_0 = \frac{K+P}{J}$, $a_1 = \frac{H+D}{J}$, $b = \frac{P}{J}$ and $c = \frac{K}{J}$, then we have

$$\ddot{\theta} = -a_0\theta - a_1\dot{\theta} + bu + cq.$$

The estimates of a_0, a_1, b, c , denoted respectively as $\bar{a}_0, \bar{a}_1, \bar{b}, \bar{c}$ can all be derived from the previous parameter estimates (e.g. $\bar{a}_0 = \frac{\hat{K}_p + 1}{\hat{J}_p}$). Then we get

$$\ddot{\theta} = -\bar{a}_0\theta - \bar{a}_1\dot{\theta} + \bar{b}(u + \frac{\bar{c}}{\bar{b}}q + \varphi^T \omega),$$

with

$$\varphi = \begin{bmatrix} \theta \\ \dot{\theta} \\ u \\ q \end{bmatrix}, \omega = \begin{bmatrix} (\bar{a}_0 - a_0)/\bar{b} \\ (\bar{a}_1 - a_1)/\bar{b} \\ (b - \bar{b})/\bar{b} \\ (c - \bar{c})/\bar{b} \end{bmatrix},$$

where ω stands for the constant parameter uncertainties.

Recall the reference θ_d defined in (3.26) and denote $e = \theta - \theta_d$, then it yields

$$\ddot{e} = -\bar{a}_0e - \bar{a}_1\dot{e} + \bar{b}(u + v + \varphi^T \omega), \quad (3.34)$$

with

$$v = -\frac{\bar{a}_0}{\bar{b}}\theta_d - \frac{\bar{a}_1}{\bar{b}}\dot{\theta}_d - \frac{1}{\bar{b}}\ddot{\theta}_d + \frac{\bar{c}}{\bar{b}}q. \quad (3.35)$$

Denote $E = \begin{bmatrix} e \\ \dot{e} \end{bmatrix}$, $A = \begin{bmatrix} 0 & 1 \\ -\bar{a}_0 & -\bar{a}_1 \end{bmatrix}$ and $B = \begin{bmatrix} 0 \\ \bar{b} \end{bmatrix}$, \bar{a}_1 is chosen such that A is Hurwitz. Then (3.34) can be rewritten as

$$\dot{E} = AE + B(u + v + \varphi^T \omega). \quad (3.36)$$

From [7], the *control law* is given by

$$u = -v - \varphi^T \hat{\omega}, \quad (3.37)$$

where $\hat{\omega}$ denotes the estimate of ω and will be derived hereafter. Note $\tilde{\omega} = \omega - \hat{\omega}$, then (3.36) becomes

$$\dot{E} = AE + B\varphi^T \tilde{\omega}.$$

Choosing the following Lyapunov function candidate as:

$$V = E^T P E + \tilde{\omega}^T \tilde{\omega},$$

where P is a positive definite symmetric matrix, so V is positive definite. The time derivative of V equals:

$$\dot{V} = E^T (PA + A^T P) E + 2(E^T P B \varphi^T + \dot{\tilde{\omega}}^T) \tilde{\omega}. \quad (3.38)$$

Defining a positive-definite, symmetric matrix Q that satisfies equation

$$Q = -(PA + A^T P),$$

and taking

$$\dot{\tilde{\omega}} = -\varphi B^T P E,$$

then (3.38) becomes:

$$\dot{V} = -E^T Q E \leq 0.$$

From this last expression of \dot{V} , we can conclude that V is lower bounded by zero in the time interval $[0, +\infty)$ and $\dot{V}(t)$ is uniformly continuous, and non positive. Therefore, by Barbalat's lemma, we have

$$\lim_{t \rightarrow +\infty} \dot{V} = 0,$$

which means that by the Rayleigh-Ritz Theorem

$$\lim_{t \rightarrow +\infty} \lambda_{\min}\{Q\} \|E\|^2 = 0,$$

where $\lambda_{\min}\{Q\}$ is the minimal eigenvalue of Q . As $\lambda_{\min}\{Q\} > 0$, it is clear that

$$\lim_{t \rightarrow +\infty} E = 0. \quad (3.39)$$

Finally, by recalling that the parameter uncertainty ω is constant, i.e., $\dot{\omega} = 0$, we obtain the *adaptive update rule* for $\hat{\omega}$ as

$$\dot{\hat{\omega}} = -\dot{\tilde{\omega}} = \varphi B^T P E. \quad (3.40)$$

Remark 3.7. Equation (3.26), (3.37) and (3.40) form the controller for the whole system, from which it can be found that $\ddot{\theta}$ is avoided for the controller.

Remark 3.8. The proposed adaptive input design guarantees asymptotic stability despite of parameter uncertainties, i.e, $\lim_{t \rightarrow +\infty} \tilde{\theta} = 0$, then by Remark 3.6, the final error of q will only depend on the precision of \hat{G}_k , which is an advantage over the PD controller.

3.7 Simulation

3.7.1 Model specification

For a light-weight and small-size single-link flexible-joint robot, select:

$$J_p = 0.0020, H_p = 0.0370, K_p = 3.667, I_k = 0.0010, F_k = 0.0190, G_k = 0.0870, \\ \theta_0 = 0, \dot{\theta}_0 = 0, q_0 = 0, \dot{q}_0 = 0.$$

Besides, uniformly distributed pseudorandom noise of magnitude bounded by 0.001 exerts on both the motor position θ and link velocity \dot{q} measurements.

For the off-line identification, the algebraic-based estimator (2.18) is used to estimate $\dot{\theta}$ and $\ddot{\theta}$ from θ , and \dot{q} from q . While for the control implementation, $\ddot{\theta}$ and \ddot{q} are no more needed, thus homogeneous differentiator (2.19) is adopted to estimate $\dot{\theta}$ in real time.

3.7.2 Identification results

For the identification, adopt the input

$$u(t) = 0.1 \sin(5t) + 0.1 \cos t - 0.1 \sin \frac{t}{3}.$$

The output θ and q during the first 3 seconds, and the estimation performance are illustrated in Figure 3.5, from which we can see that θ and q differ from each other due to joint elasticity, and the first-order derivative estimates $\hat{\dot{\theta}}$ and $\hat{\dot{q}}$ have higher precision than the second-order derivative estimate $\hat{\ddot{\theta}}$.

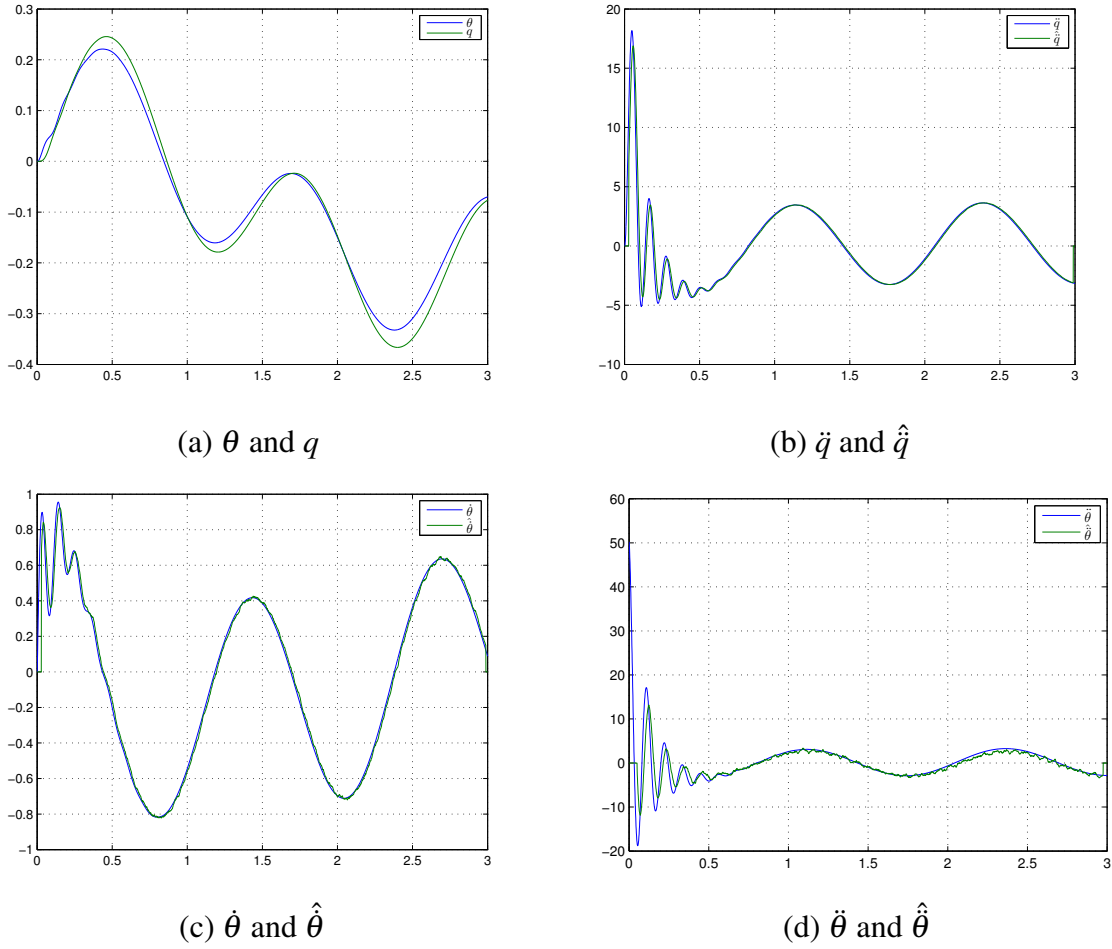


Fig. 3.5 Derivative estimates for identification

Based on (3.8) and (3.9), the identification results are presented in Table 3.1, from which it can be concluded that second-order derivative estimates bring lower precision.

Table 3.1 Identification result with velocity measurement

	J_p	H_p	K_p	I_k	F_k	G_k
Real	0.0020	0.0370	3.6670	0.0010	0.0190	0.0870
Estimated	0.0015	0.3154	4.3263	0.0009	0.0185	0.0855

3.7.3 Controller performance

Using the identified parameters, the performance of the PD controller and the two-stage adaptive controller are illustrated respectively in Figure 3.6 and Figure 3.7, the initial static

link position is supposed to be known due to measurement. For the PD controller, since two parameter estimates (\hat{K}_p and \hat{G}_k) are involved in the controller, we can see that θ_d is not well tracked and position error on q is evident. While for the adaptive controller, θ_d is well tracked and q is of good precision, as \hat{G}_k is the only parameter concerned, and \hat{G}_k is of relatively high precision.

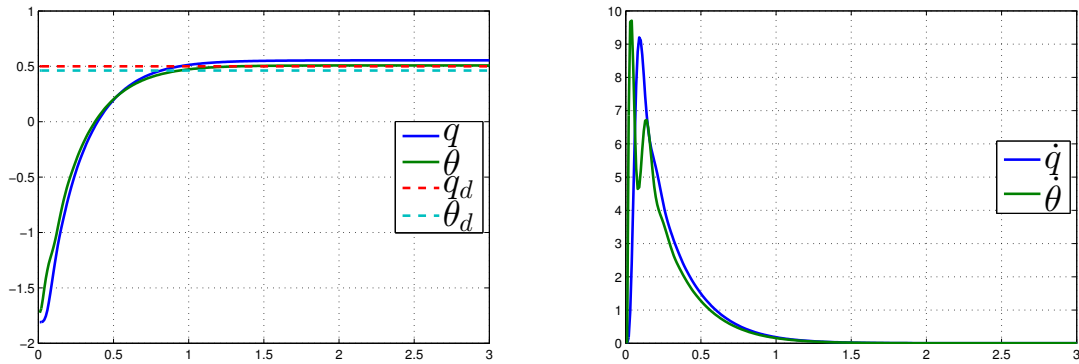


Fig. 3.6 PD controller

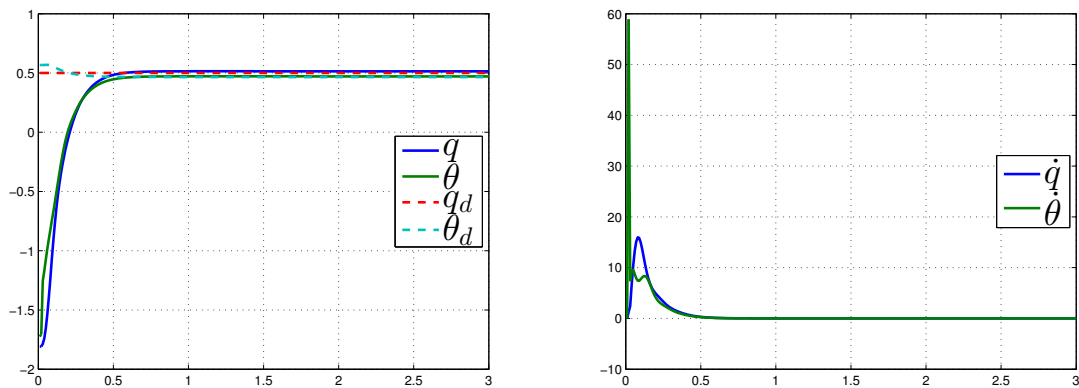


Fig. 3.7 Two-stage adaptive controller

3.8 Conclusion

This chapter considers point-to-point control of single-link position-controlled robot with joint flexibility, to obtain link side information, link angular velocity measurement is assumed to be provided. An identification scheme of the model parameters is presented, based on the classic model of flexible-joint robots, and with the measurement of initial link angles. As a benchmark, a modified simple PD plus gravity compensation controller is considered, of which the regulation error depends on two parameter estimates. To improve the robustness

with respect to parameter uncertainties, a two-stage adaptive controller is proposed, with which the final position error depends on the precision of only one parameter estimate, provided that the initial static link position can be measured. Simulation results illustrate that, the proposed two-stage controller is more robust than the PD one.

Chapter 4

Identification and control using measurements of higher order derivatives

4.1 Introduction

In Chapter 3, we proposed identification and control methods using angular velocity and tilt measurements, for single-link flexible-joint robots, in this chapter, we introduce identification and control methods using angular acceleration and tilt measurements.

The idea of using second order derivative measurement can also be generalised to any high order derivative measurement, for the identification, estimation and control problems of linear systems, with the presence of measurement noise.

The outline of this chapter is as follows. The identification and control for single-link flexible-joint robots using angular acceleration measurement is addressed in Section 4.2, and simulation result is also included. In Section 4.3, we discuss the identification, estimation and control problems for linear systems, with high order derivative measurement. Two controller, adaptive controller and robust controller have been proposed, and simulation result is given.

4.2 Identification and control for single-link flexible-joint robots with acceleration measurement

Consider the same problem in Chapter 3, but we will use angular acceleration measurement instead of angular velocity measurement, then the system can be expressed as

$$\begin{cases} J_p \ddot{\theta} + H_p \dot{\theta} + K_p(\theta - q) = u - \theta, \\ I_k \ddot{q} + F_k \dot{q} - G_k \sin q = \theta - q, \\ Y_1 = \theta, \\ Y_2 = \ddot{q}, \\ Y_3 = q, \text{ if } \dot{q} = 0, \end{cases} \quad (4.1)$$

where Y_i ($i = 1, 2, 3$) denotes the output measurements without noise.

4.2.1 Identification

Define variables for $t_0 \geq 0$:

$$\begin{aligned} \psi_1(t) &= \int_{t_0}^t \ddot{q}(s) ds, \\ \psi_2(t) &= \int_{t_0}^t \psi_1(s) ds, \end{aligned}$$

then we have

$$\begin{cases} \dot{q}(t) = \psi_1(t) + \dot{q}(t_0), \\ q(t) = \psi_2(t) + \dot{q}(t_0)(t - t_0) + q(t_0). \end{cases} \quad (4.2)$$

To proceed, the following assumption is made:

Assumption 4.1. $\dot{q}(t_0) = 0$ and $q(t_0)$ can thus be measured.

For simplicity, assume $t_0 = 0$, denote $q_0 = q(t_0)$, by Assumption 4.1, (4.2) can be rewritten as

$$\begin{cases} \dot{q} = \psi_1, \\ q = \psi_2 + q_0. \end{cases} \quad (4.3)$$

From (4.2.2), the first equation of (4.1) can be rewritten as

$$J_p \ddot{\theta} + H_p \dot{\theta} + K_p(\theta - \psi_2 - q_0) = u - \theta,$$

which is equivalent to

$$(\ddot{\theta}, \dot{\theta}, \theta - \psi_2 - q_0)(J_p, H_p, K_p)^T = u - \theta, \quad (4.4)$$

from which J_p , H_p , K_p can be estimated by using least square method as in Section 2.3.2, provided that $\ddot{\theta}$ and $\dot{\theta}$ can be obtained using numerical differentiation. The estimates of J_p , H_p , K_p are denoted as \hat{J}_p , \hat{H}_p , \hat{K}_p .

In the same way, the second equation of (4.1) becomes

$$I_k \ddot{q} + F_k \psi_1 - G_k \sin(\psi_2 + q_0) = \theta - \psi_2 - q_0,$$

which is equivalent to

$$(\ddot{q}, \psi_1, -\sin(\psi_2 + q_0))(I_k, F_k, G_k)^T = \theta - \psi_2 - q_0, \quad (4.5)$$

from which I_k , F_k , G_k can then be estimated, the estimates of I_k , F_k , G_k are denoted as \hat{I}_k , \hat{F}_k , \hat{G}_k .

4.2.2 Two-stage adaptive controller using accelerometer

Under Assumption 4.1, the same controller proposed in Section 3.6 can be performed, with only modification as

$$\begin{cases} \dot{q} = \psi_1, \\ q = \psi_2 + q_0. \end{cases}$$

4.2.3 Simulations for single-link flexible-joint robots

Here we use the same model and initial condition as in Section 3.7. On the measurement of θ , uniformly distributed pseudorandom noise with limited magnitude of 0.001 is performed, while on the measurement of \ddot{q} , a sinusoidal noise denoted by n_{acc} is expressed as

$$n_{acc} = 0.02 \sin(3t).$$

Identification

For the identification task, the same input as in Section 3.7 is adopted and the same algebraic-based estimator is used, thus we get the same plots as in figures 3.5a, 3.5c and 3.5d, while the estimation performances of \dot{q} and q are illustrated in Figure 4.1. We can see that \hat{q} by integration is of high precision, while for \hat{q} by twice integration, the drift accumulates with time.

Based on (4.4) and (4.5), the identification results are presented in Table 4.1, from which it can be concluded that second-order derivative estimates bring lower precision.

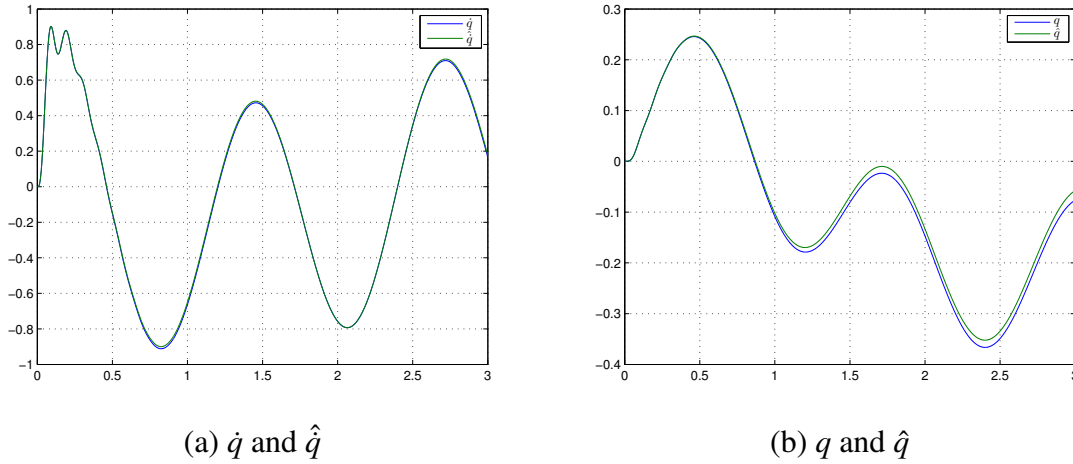


Fig. 4.1 Velocity and position estimates by integration

Table 4.1 Identification result with acceleration measurement

	J_p	H_p	K_p	I_k	F_k	G_k
Real	0.0020	0.0370	3.6670	0.0010	0.0190	0.0870
Estimated	0.0026	0.0268	3.6059	0.0009	0.0218	0.0917

Control performance

Using the identified parameters, the performance of the two-stage adaptive controller using accelerometer is illustrated in Figure 4.2. Since the same controller is used, the performance is similar to the performance shown in Figure 3.7.

4.3 Generalisation to linear system with high-order derivative measurement

4.3.1 Preliminaries

The real numbers are denoted by \mathbb{R} , $\mathbb{R}_+ = \{\tau \in \mathbb{R} : \tau \geq 0\}$. Euclidean norm for a vector $x \in \mathbb{R}^n$ will be denoted as $|x|$, and for a measurable and locally essentially bounded input $u : \mathbb{R}_+ \rightarrow \mathbb{R}$ the symbol $\|u\|_{[t_0, t_1]}$ denotes its L_∞ norm:

$$\|u\|_{[t_0, t_1]} = \text{ess sup}_{t \in [t_0, t_1]} |u(t)|,$$

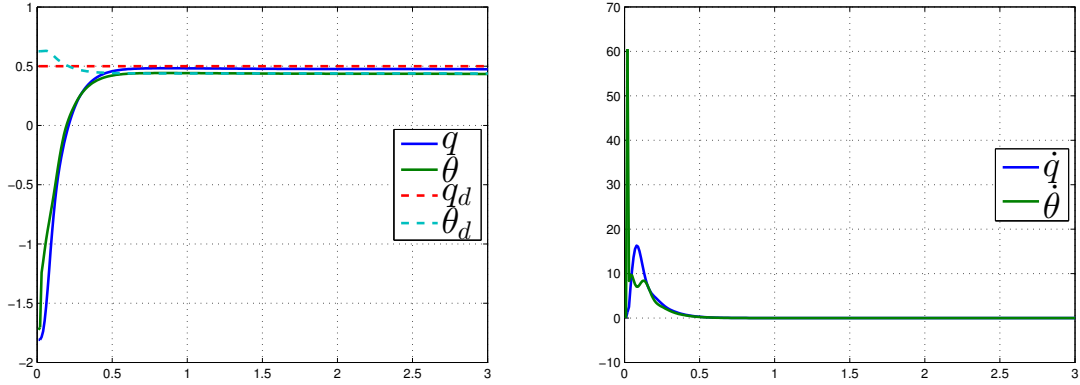


Fig. 4.2 Two-stage adaptive controller using accelerometer

if $t_1 = +\infty$ then we will simply write $\|u\|_\infty$. We will denote as \mathcal{L}_∞ the set of all inputs u with the property $\|u\|_\infty < \infty$. The symbols I_n , $E_{n \times m}$ and E_p denote the identity matrix with dimension $n \times n$, the matrix with all elements equal 1 with dimensions $n \times m$ and $p \times 1$, respectively. For a matrix $A \in \mathbb{R}^{n \times n}$ the vector of its eigenvalues is denoted as $\lambda(A)$, $\lambda_{\min}(A) = \min \lambda(A)$, and $\|A\|_2 = \sqrt{\max_{i=1, \dots, n} \lambda_i(A^T A)}$ (the induced L_2 matrix norm). The conventional results and definitions on L_2/L_∞ stability for linear systems can be found in [40].

4.3.2 Problem statement

Let us consider a SISO linear uncertain system of the form:

$$y^{(n)}(t) = \sum_{i=0}^{n-1} a_i y^{(i)}(t) + b_0 [u(t) + \varpi(t)], \quad (4.6)$$

where $y(t) \in \mathbb{R}$ is the system “position”, $y^{(i)}(t)$ for $i = 1, \dots, n$ are derivatives of $y(t) = y^{(0)}(t)$, the vector $x = [y, \dot{y}, \dots, y^{(n-1)}]$ represents the state of (4.6); $u(t) \in \mathbb{R}$ is the system control input and $\varpi \in \mathcal{L}_\infty$ is the input disturbance. It is assumed that the coefficients a_i , $i = 0, \dots, n-1$ and b_0 are unknown constants, $b_0 \neq 0$.

In this work we will assume the signal as

$$\psi(t) = y^{(n)}(t) + v(t), \quad (4.7)$$

which is available for measurements, where $v \in \mathcal{L}_\infty$ is the measurement noise. For the case of a mechanical system, when $y(t)$ is a position of some component of a robot, usually $n = 2$ and $\psi(t)$ is the measured acceleration signal with some noise $v(t)$.

Assumption 4.2. *The case $y^{(n)}(t) = \sum_{i=0}^{n-1} a_i y^{(i)}(t) + \sum_{j=0}^m b_j u^{(j)}(t) + \varpi(t)$ for some $1 \leq m \leq n$ can be also treated by the proposed below approach. However, for brevity of presentation only the case of (4.6) is considered.*

It is required to stabilize the system (4.6), (4.7) at the origin for the case $\varpi(t) = v(t) = 0$ for all $t \geq 0$, and ensure boundedness of all trajectories for bounded disturbances and noises.

To solve this problem it is necessary to design identification, estimation and control algorithms for (4.6), (4.7), that is done in the next section.

To proceed we need the following assumptions.

Assumption 4.3. *For all $i = 1, \dots, n$, consider the signals*

$$v_i(t, t_0) = \int_{t_0}^t v_{i-1}(s, t_0) ds,$$

where $v_0(t, t_0) = v(t)$ are essentially bounded for all $t \geq t_0 \geq 0$.

In this work for dependence in the second argument we will use the convention $v_i(t) = v_i(t, 0)$.

Assumption 4.4. *There is a known constant $V_\infty > 0$ such that $\max\{\|\varpi\|_\infty, \|v_0\|_\infty, \dots, \|v_n\|_\infty\} \leq V_\infty$.*

Note that integration of a high frequency noise $v(t)$ (usual for inertial sensors) leads to amplitude decreasing for $v_i(t)$ with $i \geq 1$, *i.e.* integration acts as a filter in this case.

4.3.3 Identification

Define variables for $t_0 \geq 0$:

$$\begin{aligned} \psi_0(t, t_0) &= \psi(t), \\ \psi_i(t, t_0) &= \int_{t_0}^t \psi_{i-1}(s, t_0) ds \quad \forall i = 1, \dots, n, \end{aligned}$$

then by recursive integration for all $i = 1, \dots, n$ we obtain that

$$y^{(i)}(t) = \psi_{n-i}(t, t_0) + \sum_{j=1}^{n-i} y^{(n-j)}(t_0) \frac{(t-t_0)^{n-i-j}}{(n-i-j)!} - v_{n-i}(t, t_0). \quad (4.8)$$

Substituting the obtained expressions for the derivatives $y^{(i)}(t)$ in (4.6) we get:

$$\psi_0(t, t_0) = \sum_{i=0}^{n-1} a_i \left(\Psi_{n-i}(t, t_0) + \sum_{j=1}^{n-i} y_{t_0}^{(n-j)} \frac{(t-t_0)^{n-i-j}}{(n-i-j)!} \right) + b_0[u(t) + d(t)],$$

where $y_{t_0}^{(i)} = y^{(i)}(t_0)$ and

$$d(t) = \bar{\omega}(t) + b_0^{-1} [v_0(t, t_0) - \sum_{i=0}^{n-1} a_i v_{n-i}(t, t_0)],$$

is a new essentially bounded disturbance by Assumption 4.3, and $\|d\|_\infty \leq (1 + |b_0^{-1}| [1 + \sum_{i=0}^{n-1} |a_i|]) V_\infty$ according to Assumption 4.4. Performing a direct expansion we can observe that

$$\sum_{i=0}^{n-1} a_i \sum_{j=1}^{n-i} y_{t_0}^{(n-j)} \frac{(t-t_0)^{n-i-j}}{(n-i-j)!} = \sum_{i=0}^{n-1} \frac{(t-t_0)^i}{i!} \sum_{j=1}^{n-i} a_{n-i-j} y_{t_0}^{(n-j)},$$

then

$$\begin{aligned} \psi_0(t, t_0) &= \sum_{i=0}^{n-1} a_i \Psi_{n-i}(t, t_0) + \sum_{i=0}^{n-1} \frac{(t-t_0)^i}{i!} \sum_{j=1}^{n-i} a_{n-i-j} y_{t_0}^{(n-j)} + b_0[u(t) + d(t)] \\ &= \omega(t, t_0) \theta + b_0 d(t), \end{aligned} \quad (4.9)$$

where the regressor vector

$$\omega(t, t_0) = [\Psi_n(t, t_0), \dots, \Psi_1(t, t_0), \frac{(t-t_0)^{n-1}}{(n-1)!}, \frac{(t-t_0)^{n-2}}{(n-2)!}, \dots, t-t_0, 1, u(t)],$$

is composed by known signals (integrals of the measurable output $\psi_0(t, t_0)$, functions of time t and $u(t)$), and the vector

$$\begin{aligned} \theta &= [a_0, \dots, a_{n-1}, \\ & a_0 y_{t_0}^{(n-1)}, a_1 y_{t_0}^{(n-1)} + a_0 y_{t_0}^{(n-2)}, \dots, \sum_{j=1}^{n-1} a_{n-j-1} y_{t_0}^{(n-j)}, \sum_{j=1}^n a_{n-j} y_{t_0}^{(n-j)}, b_0]^T, \end{aligned}$$

contains all unknown parameters of the regression model (4.9), which is an equivalent representation of (4.6).

There exist many methods to solve the equation (4.9) with respect to θ minimizing the noise influence [48]. The simplest one consists in multiplication of both sides in (4.9) by $\omega^T(t, t_0)$,

$$\omega^T(t, t_0) \psi_0(t, t_0) = \omega^T(t, t_0) \omega(t, t_0) \theta + \omega^T(t, t_0) b_0 d(t),$$

and integration till the instant that the matrix $M(t, t_0) = \int_{t_0}^t \omega^T(s, t_0)\omega(s, t_0)ds$ becomes nonsingular, then

$$\hat{\theta}(t, t_0) = M^{-1}(t, t_0) \int_{t_0}^t \omega^T(s, t_0)\psi_0(s, t_0)ds, \quad (4.10)$$

is an estimate of θ with the estimation error:

$$|\theta - \hat{\theta}(t, t_0)| \leq |b_0| \lambda_{\min}^{-1}(M(t, t_0)) \|\omega^T(\cdot, t_0)\|_{[t_0, t]} \|d\|_{\infty}.$$

The non-singularity of $M(t, t_0)$ is related with the property of persistence of excitation in (4.9) [64], which we have to impose.

Assumption 4.5. For any $t \geq 0$ there exist $T > 0$ and $\mu > 0$ such that $\lambda_{\min}(M(t+T, t)) \geq \mu$.

Note that the norm $\|\omega(\cdot, t_0)\|_{[t_0, t]}$ is growing with time, thus a minimal imposition of T is desirable by a selection of $u(t)$.

Remark 4.1. In order to minimize the estimation error $|\theta - \hat{\theta}(t, t_0)|$ one can filter the both sides of (4.9) in order to minimize the influence of the disturbance $d(t)$, then we obtain:

$$\tilde{\psi}_0 = \tilde{\omega}^T \theta + b_0 \tilde{d},$$

where $\tilde{\psi}_0 = W_f(s)\psi_0$, $\tilde{\omega} = W_f(s)\omega$, $\tilde{d} = W_f(s)d$ and $W_f(s)$ is transfer function of a filter. It is well-known [64] that linear filters do not destroy persistence of excitation condition (Assumption 4.5 stays true for $\tilde{\omega}$ for some $\tilde{T} > 0$ and $\tilde{\mu} > 0$), while the amplitude of the noise \tilde{d} can be much reduced with respect to d by W_f . In order to keep the notation compact this step is omitted.

Proposition 4.1. Let Assumptions 4.3, 4.4, 4.5 be satisfied and there exist $\mathbb{T} > 0$ such that $\|x\|_{[0, \mathbb{T}]} + \|u\|_{[0, \mathbb{T}]} < +\infty$. Then there exists $\Theta > 0$ such that in (4.10),

$$|\theta - \hat{\theta}(kT, (k-1)T)| \leq \Theta, \quad \forall 1 \leq k \leq \frac{\mathbb{T}}{T}.$$

Proof. By construction and imposed assumptions $|\theta - \hat{\theta}(kT, (k-1)T)| \leq |b_0| \mu^{-1} \|\omega(\cdot, (k-1)T)\|_{[(k-1)T, kT]} \|d\|_{\infty}$. By assumptions 4.3 and 4.4, $\|d\|_{\infty} < +\infty$, and μ is a real by Assumption 4.5, the same is $b_0 \neq 0$. It is necessary to evaluate $\|\omega(\cdot, (k-1)T)\|_{[(k-1)T, kT]}$, but all components dependent explicitly on time are bounded on the interval $[(k-1)T, kT]$, u is bounded by conditions of the proposition, and ψ_i are bounded by construction and due to boundedness of x . Therefore, $\|\omega(\cdot, (k-1)T)\|_{[(k-1)T, kT]} < +\infty$ while $\|x\|_{[(k-1)T, kT]} + \|u\|_{[(k-1)T, kT]} < +\infty$, that was necessary to prove. \square

Consequently, according to Proposition 4.1 on any finite time interval (4.6) is a linear system, thus no finite-time escape is possible and for any finite $\mathbb{T} > 0$ the property $\|x\|_{[0,\mathbb{T}]} + \|u\|_{[0,\mathbb{T}]} < +\infty$ is satisfied) the identification algorithm (4.10) provides a solution with a bounded error. The crucial step in (4.10) is resetting of all integrators after T period of time, in order to avoid integration drift and unboundedness of the regressor ω .

Assume that for $t_0 \geq 0$ in the conditions of Proposition 4.1 (Assumptions 4.3, 4.4, 4.5 are satisfied) the estimate $\hat{\theta}(t_0 + T, t_0)$ is obtained and $|\theta - \hat{\theta}(t_0 + T, t_0)| \leq \Theta$ for some $\Theta > 0$, then from the definition of θ it is easy to check that the estimate $\hat{\eta}(t_0 + T, t_0)$ of the constant vector

$$\eta = [a_0, \dots, a_{n-1}, y_{t_0}^{(0)}, \dots, y_{t_0}^{(n-1)}, b_0],$$

can be calculated with the property

$$|\eta - \hat{\eta}(t_0 + T, t_0)| \leq \Theta',$$

for some $\Theta' > 0$ related with Θ . Indeed, a_0, \dots, a_{n-1} and b_0 are the first and the last elements of θ , respectively, next $y_{t_0}^{(n-1)}$ can be found from the value of $n+1$ element of θ , and next recursively all $y_{t_0}^{(i)}$. Denote

$$\hat{\eta} = [\hat{a}_0, \dots, \hat{a}_{n-1}, \hat{y}_{t_0}^{(0)}, \dots, \hat{y}_{t_0}^{(n-1)}, \hat{b}_0],$$

then for all $i = 0, \dots, n-1$

$$\hat{y}^{(i)}(t) = \psi_{n-i}(t, t_0) + \sum_{j=1}^{n-i} \hat{y}_{t_0}^{(n-j)} \frac{(t-t_0)^{n-i-j}}{(n-i-j)!},$$

and defining the state estimation error $e_i(t) = y^{(i)}(t) - \hat{y}^{(i)}(t)$ we obtain that

$$e_i(t) = \sum_{j=1}^{n-i} (y_{t_0}^{(n-j)} - \hat{y}_{t_0}^{(n-j)}) \frac{(t-t_0)^{n-i-j}}{(n-i-j)!} - v_{n-i}(t, t_0). \quad (4.11)$$

Denote $\hat{x} = [\hat{y}^{(0)}, \hat{y}^{(1)}, \dots, \hat{y}^{(n-1)}]$ and $e = [e_0, \dots, e_{n-1}]$. Finally, from (4.6) the estimate of $\varpi(t)$ can be derived as follows:

$$\hat{\varpi}(t) = \hat{b}_0^{-1} [\psi_0(t, t_0) - \sum_{i=0}^{n-1} \hat{a}_i \hat{y}^{(i)}(t)] - u(t).$$

4.3.4 State space representation for control design

To simplify forthcoming analysis we will suppose that the control gain is given (or the value of \hat{b}_0 after identification has been obtained correctly).

Assumption 4.6. *The value $b_0 \neq 0$ is known.*

In such a case the discrepancy $|b_0 - \hat{b}_0|$ can be used for the constant Θ' evaluation.

In the state space form the system (4.6) can be written as follows:

$$\begin{cases} \dot{x} = Ax + B(u + \varpi), \\ Y = \hat{y}^{(n-1)} = y^{(n-1)} + \delta = Cx + \delta, \end{cases} \quad (4.12)$$

where $x = [y, y^{(1)}, \dots, y^{(n-1)}]^T$ is the state vector, $Y \in \mathbb{R}$ is the estimate of $y^{(n-1)}$, served as a new measured output with new measurement noise δ , and

$$A = \begin{bmatrix} 0 & & & & \\ \vdots & & & & \\ 0 & & I_{n-1} & & \\ a_0 & a_1 & \dots & a_{n-1} & \end{bmatrix}, \quad B = \begin{bmatrix} 0 \\ \vdots \\ 0 \\ b_0 \end{bmatrix},$$

$$C = [0, \dots, 0, 1].$$

Specifically, we have

$$\begin{aligned} \delta &= \hat{y}^{(n-1)} - y^{(n-1)} \\ &= \psi_1(t, t_0) + \hat{y}_{t_0}^{(n-1)} - (\psi_1(t, t_0) + y_{t_0}^{(n-1)} - v_1(t, t_0)) \\ &= \hat{y}_{t_0}^{(n-1)} - y_{t_0}^{(n-1)} + v_1(t, t_0), \end{aligned}$$

thus, despite the estimates \hat{x} for the complete vector x are available (if (4.10) has been used in advance) and can be considered as measurable, only the last component $y^{(n-1)}$ is selected since it is estimated with a bounded estimation error. In fact, from 4.11, we have

$$\delta = -e_{n-1} = \sum_{j=1}^{n-i} (\hat{y}_{t_0}^{(n-j)} - y_{t_0}^{(n-j)}) \frac{(t - t_0)^{n-i-j}}{(n-i-j)!} + v_{n-i}(t, t_0),$$

so for $0 \leq i \leq n-2$, δ depends on powers of t .

4.3.5 Adaptive control

There exists an unknown vector $k = [k_1, k_2, \dots, k_n]^T \in \mathbb{R}^n$ such that $D = A - Bk^T$ is a given matrix in the canonical controllability form with desired eigenvalues, then (4.12) becomes:

$$\dot{x} = Dx + B(u + k^T x + \bar{\omega}). \quad (4.13)$$

By the definition of k and x , and from 4.8, we have

$$\begin{aligned} k^T x &= \sum_{i=0}^{n-1} k_{i+1} y^{(i)} \\ &= \sum_{i=0}^{n-1} k_{i+1} \left(\psi_{n-i}(t, t_0) + \sum_{j=1}^{n-i} y^{(n-j)}(t_0) \frac{(t-t_0)^{n-i-j}}{(n-i-j)!} - v_{n-i}(t, t_0) \right) \\ &= \sum_{i=0}^{n-1} k_{i+1} \psi_{n-i}(t, t_0) + \sum_{i=0}^{n-1} k_{i+1} \left(\sum_{j=1}^{n-i} y^{(n-j)}(t_0) \frac{(t-t_0)^{n-i-j}}{(n-i-j)!} \right) - \\ &\quad \sum_{i=0}^{n-1} k_{i+1} v_{n-i}(t, t_0). \end{aligned}$$

Introduce $m = i + j$, then we have

$$\begin{aligned} \sum_{i=0}^{n-1} k_{i+1} \left(\sum_{j=1}^{n-i} y^{(n-j)}(t_0) \frac{(t-t_0)^{n-i-j}}{(n-i-j)!} \right) &= \sum_{i=0}^{n-1} \sum_{j=1}^{n-i} \left(k_{i+1} y^{(n-j)}(t_0) \frac{(t-t_0)^{n-i-j}}{(n-i-j)!} \right) \\ &= \sum_{m=1}^n \sum_{j=1}^m \left(k_{m-j+1} y^{(n-j)}(t_0) \frac{(t-t_0)^{n-m}}{(n-m)!} \right) \\ &= \sum_{m=1}^n \frac{(t-t_0)^{n-m}}{(n-m)!} \left(\sum_{j=1}^m k_{m-j+1} y^{(n-j)}(t_0) \right). \end{aligned}$$

Then it yields

$$k^T x + \sum_{i=0}^{n-1} k_{i+1} v_{n-i}(t, t_0) = \sum_{i=0}^{n-1} k_{i+1} \psi_{n-i}(t, t_0) + \sum_{m=1}^n \frac{(t-t_0)^{n-m}}{(n-m)!} \left(\sum_{j=1}^m k_{m-j+1} y^{(n-j)}(t_0) \right). \quad (4.14)$$

Denote $\bar{\omega}^T(t, t_0)$ as

$$\bar{\omega}^T(t, t_0) = [\psi_n(t, t_0), \psi_{n-1}(t, t_0), \dots, \psi_1(t, t_0), \frac{(t-t_0)^{n-1}}{(n-1)!}, \frac{(t-t_0)^{n-2}}{(n-2)!}, \dots, t-t_0, 1], \quad (4.15)$$

and $\bar{\theta}$ as

$$\bar{\theta} = [k_1, k_2, \dots, k_n, k_1 y^{n-1}(t_0), \sum_{j=1}^2 k_{3-j} y^{(n-j)}(t_0), \dots, \sum_{j=1}^n k_{n-j+1} y^{(n-j)}(t_0)]^T, \quad (4.16)$$

where $\bar{\omega}^T(t, t_0)$ is the new regressor vector and $\bar{\theta} \in \mathbb{R}^{2n}$ is the vector of unknown constant parameters, then from (4.14) we have

$$k^T x + \sum_{i=0}^{n-1} k_{i+1} v_{n-i}(t, t_0) = \bar{\omega}^T(t, t_0) \bar{\theta}. \quad (4.17)$$

Define a new perturbation signal $\phi(t) = \bar{\omega}(t) - \sum_{i=0}^{n-1} k_{i+1} v_{n-i}(t, t_0)$ and substitute (4.17) into (4.13), we obtain

$$\dot{x} = Dx + B(u + \bar{\omega}^T(t, t_0) \bar{\theta} + \phi(t)). \quad (4.18)$$

Choose the control law in the form

$$u(t) = -\bar{\omega}^T(t, t_0) \hat{\theta}(t), \quad (4.19)$$

where $\hat{\theta} \in \mathbb{R}^{2n}$ is an estimate of $\bar{\theta}$ to be calculated, then the system (4.12) with the control (4.19) takes the form:

$$\dot{x}(t) = Dx(t) + B \left[\bar{\omega}^T(t, t_0) [\bar{\theta} - \hat{\theta}(t)] + \phi(t) \right].$$

There are many ways to derive $\hat{\theta}$ using direct or indirect adaptive control theory [24], for example, by designing an adaptive observer [45, 99] (the only difficulty is to select a solution providing a better robustness with respect to v_i and $\bar{\omega}$):

$$\begin{aligned} \dot{z}(t) &= Dz(t) - B \bar{\omega}^T(t, t_0) \hat{\theta}(t), \\ \dot{\Omega}(t) &= D\Omega(t) - B \bar{\omega}^T(t, t_0), \\ \dot{\hat{\theta}}(t) &= -\gamma \Omega^T(t) C^T [Y(t) - Cz(t) + C\Omega(t) \hat{\theta}(t)], \end{aligned} \quad (4.20)$$

where $\gamma > 0$ is a tuning parameter, $z \in \mathbb{R}^n$ and $\Omega \in \mathbb{R}^{n \times 2n}$ are two auxiliary variables. For (4.12), (4.19) with the adaptive observer (4.20) for an error $\varepsilon = x - z + \Omega \bar{\theta}$ we obtain

$$\dot{\varepsilon}(t) = D\varepsilon(t) + B\phi(t),$$

which explains the structure of the used adaptation law:

$$\dot{\hat{\theta}}(t) = -\gamma \Omega^T(t) C^T [C \varepsilon(t) + \delta(t) + C \Omega(t) \{\hat{\theta}(t) - \bar{\theta}\}].$$

Since D is a Hurwitz matrix and $\phi \in \mathcal{L}_\infty$ by Assumption 4.4, then also $\varepsilon \in \mathcal{L}_\infty$ with the norm asymptotically proportional to $\|\phi\|_\infty$, and the discrepancy $\bar{\theta} - \hat{\theta}(t)$ possesses the same property [25] provided that the variable $\Omega^T(t) C^T$ is persistently excited.

Assumption 4.7. For any $t \geq 0$ there exist $T' > 0$ and $\nu > 0$ such that

$$\int_t^{t+T'} \Omega^T(s) C^T C \Omega(s) ds \geq \nu I_{2n}.$$

In general Assumptions 4.5 and 4.7 are related, but we prefer to state them separately, one for identification and one for control phase, respectively.

The following result has been proven.

Theorem 4.1. Let Assumptions 4.3, 4.4, 4.6 and 4.7 be satisfied. Then in the system (4.6), (4.7) with the control (4.19) and the adaptive observer (4.20) for any $t_0 \geq 0$ and $\mathbb{T} > 0$, the variables x , z , Ω , $\hat{\theta}$ stay bounded on the interval $[t_0, t_0 + \mathbb{T}]$.

Proof. Note that on any finite time interval $[t_0, t_0 + \mathbb{T}]$ the regressor $\bar{\omega}$ is bounded (consequently, Ω has the same property since D is Hurwitz) and using Lemma 1 of [25] and Assumption 4.7 we obtain boundedness of the discrepancy $\bar{\theta} - \hat{\theta}(t)$. Boundedness of the variables x and z follows Hurwitz property of D and boundedness of all external signals in the right-hand side of the differential equations describing dynamics of these variables. \square

Note that in the considered case it is hard to state an asymptotic result, or consider the system on unbounded interval $[0, +\infty]$, since the regressor $\bar{\omega}$ depends on powers of t for $n \geq 2$ and it is asymptotically unbounded.

Remark 4.2. If the identification algorithm (4.10) has been applied, then the value for $\hat{\theta}(t_0)$ can be properly selected (minimizing the initial error) and the measurement noise bias $y_{t_0}^{(n-1)} - \hat{y}_{t_0}^{(n-1)}$ can be decreased.

Remark 4.3. The identification algorithm (4.10) can also be used in parallel with the adaptive control algorithm (4.19), (4.20), providing an independent update on values of all parameters. In addition, due to integration applied for calculation of the variables ψ_i , it is necessary to perform a persistent resetting of that integrators using corresponding estimates obtained by (4.10).

4.3.6 Robust control

If the identification algorithm (4.10) is applied periodically at instants t_m , $m = 0, 1, \dots$, then a simple static feedback can be applied:

$$u = -\kappa^T \hat{x}, \quad (4.21)$$

where the vector of coefficients $\kappa \in \mathbb{R}^n$ is selected in a way to ensure that the matrix $H = A - B\kappa^T$ is Hurwitz. For example, if it is possible to evaluate the value of Θ' , then taking into account uncertainty on the values of a_0, \dots, a_{n-1}, b_0 given by Θ' , the choice of κ is simple.

Theorem 4.2. *Let Assumptions 4.3 and 4.4 be satisfied. Then in the system (4.6), (4.7) with the control (4.21) for any $t_0 \geq 0$ and $\mathbb{T} > 0$, the variable x stays bounded on the interval $[t_0, t_0 + \mathbb{T}]$.*

Proof. Substituting the control (4.21) in (4.12) (an equivalent representation of (4.6), (4.7)) we obtain:

$$\begin{aligned} \dot{x} &= Ax + B(-\kappa^T \hat{x} + \varpi) \\ &= Hx + B(\kappa^T e + \varpi). \end{aligned}$$

On any finite time interval the error e is bounded, the same property has the signal ϖ , while the matrix H is Hurwitz, thus the state variable is bounded. \square

In this case the identification algorithm (4.10) can also be used in parallel providing a persistent resetting of integrators for ψ_i .

Both results, for the adaptive control in Theorem 4.1 and for the robust control in Theorem 4.2, guarantee just boundedness of the state for the system (4.6), (4.7). Their efficiency comparison is given in the next section using computer numerical experiments.

4.3.7 Simulations for linear system

Model specification

In robotic applications, accelerometers are largely used to measure the linear acceleration, as the second-order derivative of the position. Thus we select $n = 2$, $t_0 = 0$ and the model is

specified as:

$$\begin{aligned} a_0 &= 2, a_1 = -4, b_0 = 2, \\ v(t) &= 0.0025 \sin(25t), \bar{w}(t) = 0.002 \sin(t), \\ x(0) &= [0.5 \ 5]^T. \end{aligned}$$

In state space representation, we have

$$\begin{aligned} A &= \begin{bmatrix} 0 & 1 \\ 2 & -4 \end{bmatrix}, B = \begin{bmatrix} 0 \\ 2 \end{bmatrix}, \\ C &= [0, 1], \end{aligned}$$

then the system is unstable.

Identification

During the identification phase, choosing the control as

$$u(t) = -\cos(8t) + \sin\left(\frac{1}{4}t\right) - \cos(5t).$$

The step time is set to be 1ms, after 1000 samples (1 second), based on (4.10), we obtain the estimates as:

$$\begin{aligned} \hat{a}_0 &= 2.015, \hat{a}_1 = -3.997, \hat{b}_0 = 2.000, \\ y_0^{(0)} &= 0.468, y_0^{(1)} = 4.991. \end{aligned}$$

This result is very close to the model parameters and initial state variables. According to (4.11), the state estimation error can be expressed as

$$\begin{aligned} e(t) = y(t) - \hat{y}(t) &= (y_0^{(1)} - \hat{y}_0^{(1)})t + y_0^{(0)} - \hat{y}_0^{(0)} - v_2(t) \\ &= 0.009t + 0.032 - v_2(t), \\ \dot{e}(t) = \dot{y}(t) - \dot{\hat{y}}(t) &= y_0^{(1)} - \hat{y}_0^{(1)} - v_1(t) \\ &= 0.009 - v_1(t). \end{aligned}$$

Adaptive controller

Giving D such that $D = A - Bk^T$ where $k = [k_1 \ k_2]^T$, then from 4.15 and 4.16, we have

$$\bar{\omega}^T(t, t_0) = [\psi_2(t, t_0), \psi_1(t, t_0), t - t_0, 1],$$

and

$$\bar{\theta} = [k_1, k_2, k_1 y^{(1)}(t_0), k_2 y^{(1)}(t_0) + k_1 y^{(0)}(t_0)]^T.$$

For the proposed adaptive control scheme, taking

$$D = \begin{bmatrix} 0 & 1 \\ -4 & -4 \end{bmatrix}, \gamma = 0.4,$$

as parameters of the adaptive control algorithm (4.19), (4.20).

To minimize the initial error of the adaptive error, $\hat{\theta}(t_0)$ can be estimated using the identification results, to do this, define $\hat{k} = [\hat{k}_1 \ \hat{k}_2]^T$ the estimate of the unknown vector k , then by the definition of D , \hat{k} is given as

$$\hat{k} = (\hat{B}^T \hat{B})^{-1} \hat{B}^T (\hat{A} - D), \quad (4.22)$$

where

$$\hat{A} = \begin{bmatrix} 0 & 1 \\ \hat{a}_0 & \hat{a}_1 \end{bmatrix}, \hat{B} = \begin{bmatrix} 0 \\ \hat{b}_0 \end{bmatrix}.$$

Then we have

$$\hat{\theta} = [\hat{k}_1, \hat{k}_2, \hat{k}_1 \hat{y}_0^{(1)}, \hat{k}_2 \hat{y}_0^{(1)} + \hat{k}_1 \hat{y}_0^{(0)}]^T.$$

The results of application of the adaptive controller during the 9 seconds after the identification process are shown in Figure 4.3. We observed that the error $e(t)$ increased with time while $\dot{e}(t)$ stays always quite close to zero.

Robust controller

We take the same desired matrix, i.e. $H = D$, and then $\kappa = \hat{k}$ as the gains of the robust control (4.21), while \hat{k} is determined by (4.22), the results of the robust controller are shown in figure 4.4. Compared to the performance of the adaptive controller, as we can conclude, the robust control converges more quickly than the adaptive one, and it is easier to implement.

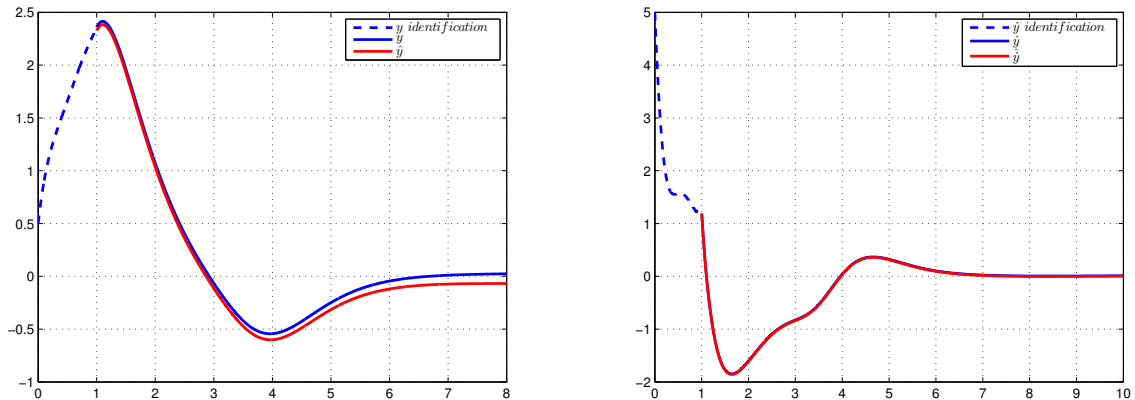


Fig. 4.3 The simulation result for adaptive controller

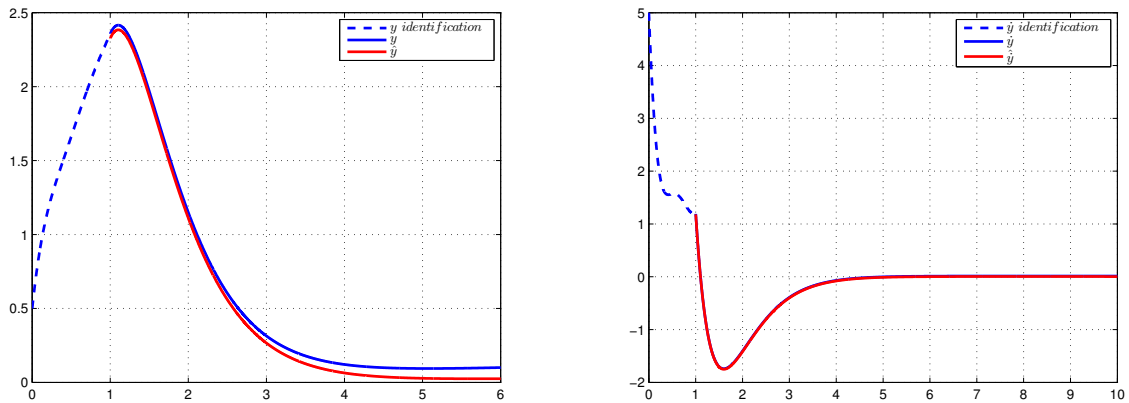


Fig. 4.4 The simulation result for robust controller

4.4 Conclusion

In this chapter, firstly, the control problem of single-link flexible-joint robots using link angular acceleration has been studied. With also tilt angle measurement, identification algorithm based on linear square method and the same two-stage adaptive controller are proposed, simulation result showed similar performance as using angular velocity measurement in Chapter 3. Secondly, the problem of model identification and output control has been discussed for linear time-invariant SISO system with completely unknown parameters, external disturbances, and output measurement noise. It is shown that by introducing recursive integrals and using a simple identification algorithm, some estimates on vector of unknown parameters and states can be obtained. Next, these information can be used in control, adaptive or robust, to provide boundedness of the state vector of the system. Due to integration drift all results are obtained

on final intervals of time. Efficacy of the proposed identification and control algorithms is demonstrated in simulations.

Chapter 5

Experiment results

5.1 Introduction

In this chapter, for experiment validation, a 5-DOF low-cost manipulator with light weight and small size, is used as test platform. Each joint of the manipulator is driven by an all-in-one actuator, of which the built-in controller is a programmable P like controller, but the proportional gain is unknown, besides, the shaft inside the actuator which couples the joint part to the link part is of some kind of plastic, thus the stiffness is limited. As a 5-DOF manipulator, the inertial parameters of each link (mass, inertial moment, first moment, etc) is rather small compared to the stiffness of the shaft, i.e. the stiffness can be considered as infinite with respect to other dynamic parameters, thus the manipulator can be regarded as rigid. Under this configuration, the controller proposed in Chapter 2 for rigid manipulators is implemented, and no additional sensors are demanded.

However, when the last three links and the end-effector are constrained as one link, the whole manipulator becomes a single-link manipulator driven by the first actuator, and the inertial parameters for this single link are several times of those for each link in the 5-DOF manipulator (the mass becomes 4 times and inertial moment becomes 64 times if all the links are identical), in this case, the shaft stiffness can no longer be considered as infinite with comparison to the inertial parameters, and the manipulator should be treated as joint-flexible. Under this configuration, the controllers proposed in Chapter 3 and Chapter 4 for single-link flexible-joint manipulator are concerned.

In Chapter 3, to proceed the proposed identification and two-stage adaptive controller, angular velocity and static angle measurements are demanded, this can be satisfied by using gyroscope and accelerometer, the former is used to measure the angular velocity and the later measures static angle position [72].

In Chapter 4, the proposed identification and adaptive controller need angular acceleration and static angle measurements. For the moment, there is no low-cost and MEMS device which can measure angular acceleration directly. Although the angular acceleration can be measured indirectly using either a rotating angle sensor or a velocity sensor, the noise-amplification problem related to the differentiation process limits the precision. Direct measuring of linear acceleration is in wide use, which can be converted to angular acceleration provided that the projection of the gravitational acceleration on the measurement axis is known, i.e. the link angular position need to be known, thus this task cannot be performed with only accelerometer, and addition of more additional sensors complicate the problem. As a result, the methods proposed in Chapter 4 is not implemented.

5.2 Introduction of the experiment plate-form

5.2.1 Description of the robot arm

The test robot arm is of 5 degrees of freedom, as shown in Figure 5.1. All links and the end-effector are driven by AX-12A Dynamixel Actuators, all the actuators are connected to an Arduino printed circuit board by a daisy chain bus. The PCB is connected to PC via a FTDI programming cable.

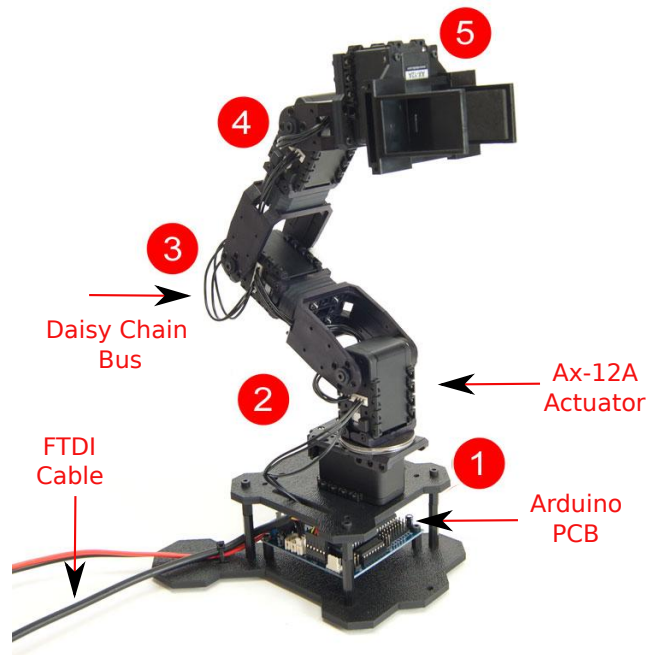


Fig. 5.1 Test manipulator

The robot is a light-weight and small-size robot arm, the physical specifications are shown in Table 5.2.

Table 5.1 Specifications of the robot arm

Weight	550 G
Vertical Reach	35 CM
Horizontal Reach	31 CM

5.2.2 All-in-one actuator

The Dynamixel AX-12A robot actuator (Figure 5.2) is a smart, modular actuator that incorporates a gear reducer, a precision DC motor and a control circuitry with networking functionality, all in a single package. Despite its compact size, it can produce high torque and is made with high quality materials to provide the necessary strength and structural resilience to withstand large external forces. Position, temperature and input voltage are provided as feedback with reliable precision. It also has the ability to detect and act upon internal conditions such as changes in internal temperature or supply voltage.



Fig. 5.2 AX-12A all-in-one actuators

5.2.3 Built-in controller

According to the manual of the AX-12A actuator, the compliance of the built-in controller is defined by setting the compliance Margin, Slope and Punch. This feature can be utilized for absorbing shocks at the output shaft. The following graph shows how each compliance value (length of *A*, *B*, *C*, *D* and *E*) is defined by the Position Error and applied torque, as illustrated in Figure 5.3, where:

τ_{max} is the maximal output torque the actuator can produce,

Table 5.2 Specifications of AX-12A actuator

Weight (g)	54.6	
Gear Reduction Ratio	1/254	
Input Voltage (V)	7 ~10	
Final Max Holding Torque (kgf.cm)	12 (7V)	16.5 (10V)
No-load Speed (sec/60°)	0.269 (7V)	0.196 (10V)
Resolution (degree)	0.29	
Operating Angle (degree)	300	
Command Signal	Digital Packet	
Communication Speed (bps)	7343 ~1M	
Material	Engineering Plastic	

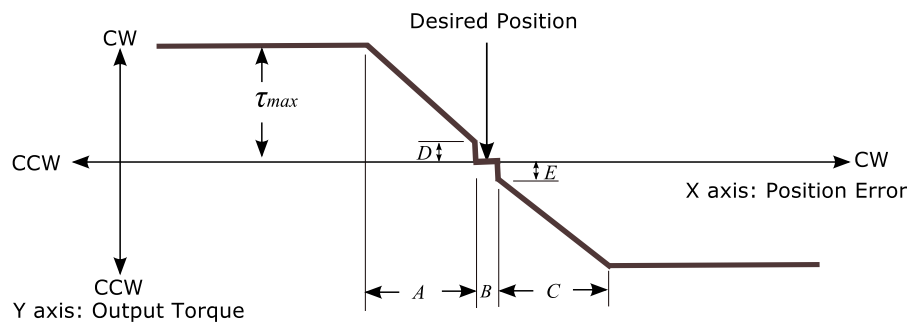


Fig. 5.3 Built-in controller

D and E are the output torque corresponding to the minimum current supplied to the motor during operation,

B is the compliance margin, means the acceptable error between goal position and present position,

A and C are the compliance slope which set the changing rate of output torque with respect to the position error.

A , B , C , D and E are programmable, can be set by the user. For modelling and analysis simplicity, by setting B , D and E close to zero and $A = C \geq 0$ ($A \in 0.29^\circ \times \{2, 4, 8, 16, 32, 64, 128\}$), then the built-in controller becomes a P controller with output torque saturation, as shown in Figure 5.4.

For this controller, denote u the desired angular position, serves as the input of the system. x denotes the current joint position and serves as the feedback, then the output torque τ can be expressed as

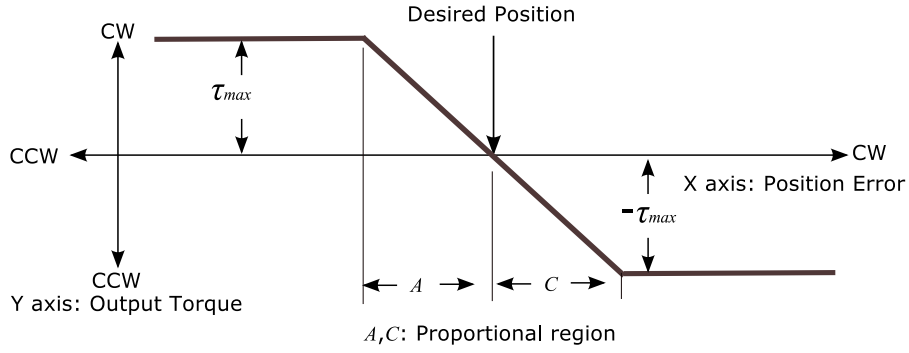


Fig. 5.4 P controller with saturation

$$\tau = \begin{cases} \tau_{max}, & \text{if } x - u \leq -A, \\ \frac{\tau_{max}}{A}(u - x) = P(u - x), & \text{if } |x - u| \leq A, \\ -\tau_{max}, & \text{if } x - u \geq A. \end{cases} \quad (5.1)$$

where P is the proportional gain.

5.2.4 Propositions and physical constraints

To test our algorithms proposed in the previous chapters, several propositions are introduced:

Proposition 5.1. *The motor shaft is considered as rigid with small-size and light-weight link, and should be regarded as flexible when the link inertial parameters become large.*

Proposition 5.2. *The non-saturated part of the built-in controller is a P controller, as illustrated in Figure 5.4.*

Due to the hardware and software limitations, following constraints are imposed:

Constraint 5.1. *The inertial parameters of the actuators and the links are unknown.*

Constraint 5.2. *The maximal output torque τ_{max} the actuator can produce is unknown, thus the proportional gain P in (5.1) is unknown.*

Constraint 5.3. *The built-in controller is saturated by unknown value, and the proportional part range is quite limited ($A \leq 37.12^\circ$).*

Constraint 5.4. *The angular velocity is bounded and the boundedness is unknown.*

Constraint 5.5. *Only motor position feedback is of interest and reliable, and the sampling frequency is limited to 143Hz.*

5.3 Rigid case

If each link is driven by a corresponding actuator, then the robot can be regarded as rigid, due to the small size and light weight of each link, which makes the inertial parameters ignorable compared to the plastic motor shaft elasticity.

5.3.1 Built-in controller performance

Since the built-in controller works as a P controller within the compliance slope region, at steady state, the final position error is mainly caused by the gravity load torque. As the first link rotates around a vertical axis on which the projection of the gravity load torque is zero, there will be no steady state error. Thus we focus on the middle 3 joints without considering the open and close of the grasper.

The performance of the built-in controller under constant input for the middle 3 revolute joints is shown in Figure 5.5, two departure-destination configurations are considered, and for each configuration, without and with an additional load of 18g on the grasper are tested.

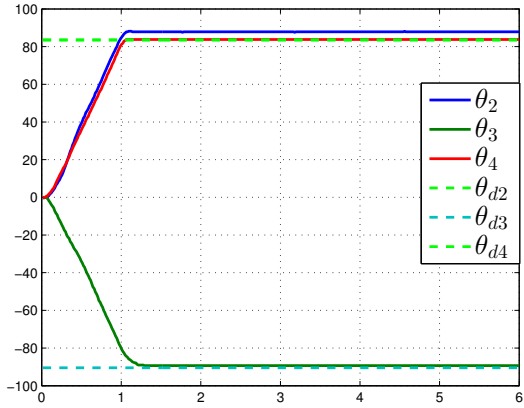
It can be observed that, evident steady state errors are presented for the second and the third joints, and the second one has a bigger error than the third one due to a greater gravity load torque, while the error on the fourth joint is ignorable for all case due to a minor gravity load torque. Besides, a somehow uniform-velocity motion is presented due to the output torque saturation beyond the short compliance slope region. As a result, we focus on the second and the third joints for the auxiliary controller implementation.

5.3.2 Model identification

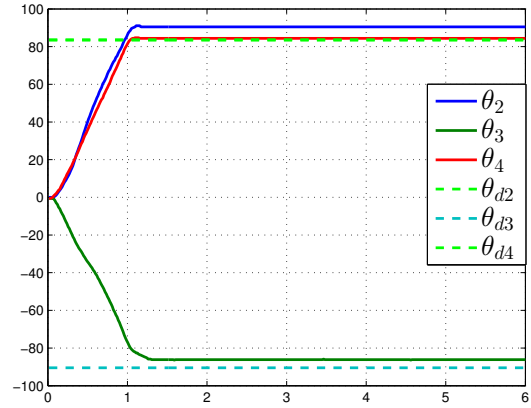
Observer performance

All the four observer candidates are tested for a measured trajectory (Figure 5.6(a)). For algebraic-based observer, the result is shifted with half of the window size to compensate for the delay. The performance of the observers for velocity and acceleration estimation are illustrated respectively in Figure 5.6(b) and Figure 5.6(c).

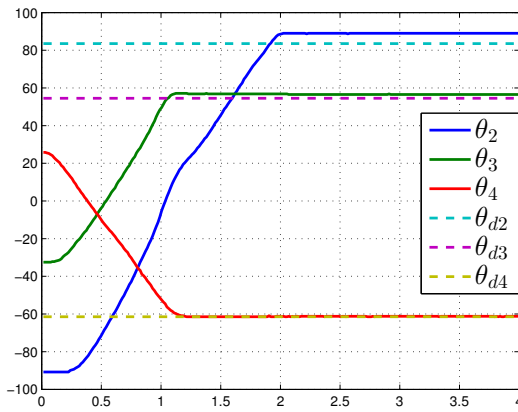
Algebraic-based observer gives smoother results than the others, however, for real-time estimation, the delay cannot be compensated, thus we use it to do off-line identification. For velocity estimation, all the results are close to each other, while for acceleration estimation, the results differ and get chattering for HOMD, HOSM and High-gain differentiators. Fortunately, the proposed auxiliary controller needs only the velocity estimates, HOMD is chosen for its quicker convergence.



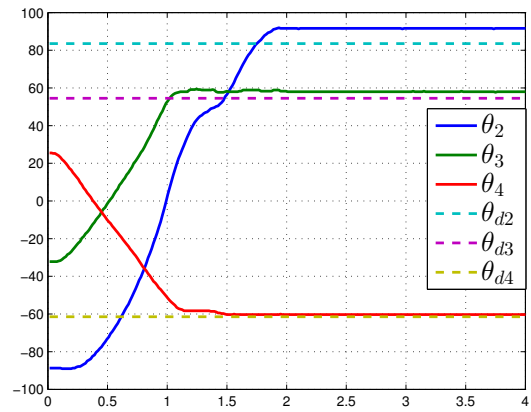
(a) Configuration 1 without additional load



(b) Configuration 1 with additional load



(c) Configuration 2 without additional load



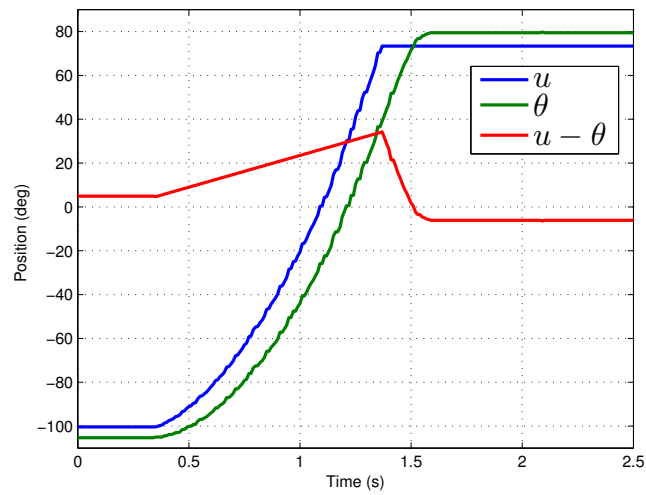
(d) Configuration 2 with additional load

Fig. 5.5 Built-in controller performance

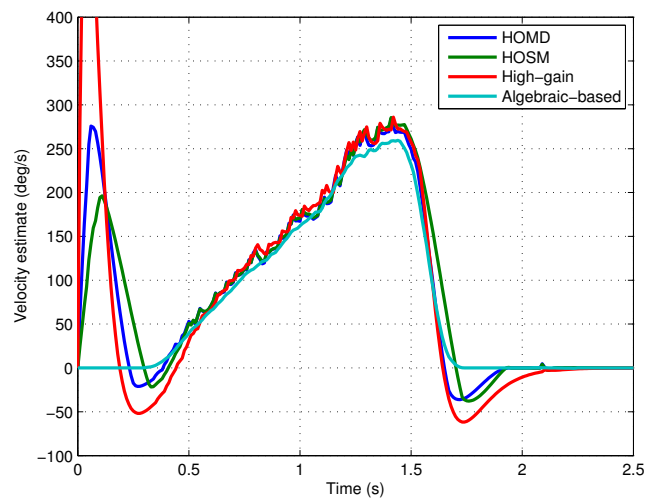
Identification result

To identify the nominal model of each joint, excite the system with an increasing sequence of the input signal u in proportional range. (5.2) is obtained for the nominal model for the second and the third joint.

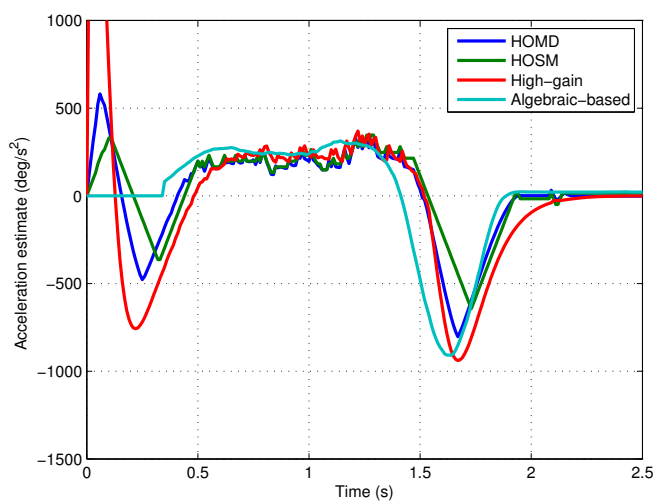
$$\begin{cases} \ddot{x}_2 = -32.52x_2 - 3.07\dot{x}_2 + 33.13u_2, \\ \ddot{x}_3 = -34.86x_3 - 4.42\dot{x}_3 + 34.26u_3. \end{cases} \quad (5.2)$$



(a) Measured trajectory position



(b) First-order derivative estimates



(c) Second-order derivative estimates

Fig. 5.6 Observer performance

5.3.3 Control strategy

The performance degrades under closed-loop control with saturation. Since the proportional region of the built-in controller is known, so we design a switching control strategy as described in Figure 5.7.

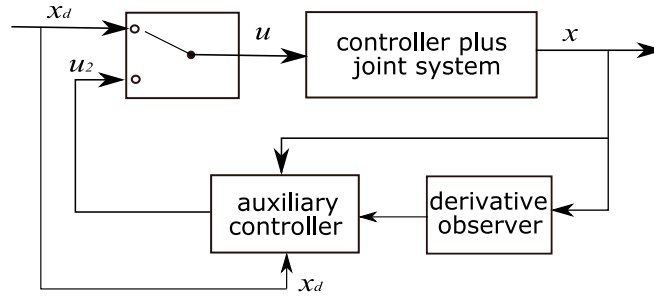


Fig. 5.7 Switched control strategy

For this, let us firstly define a neighbourhood Ω around the desired position x_d :

$$\Omega = \{x : |x - x_d| \leq \omega\},$$

where ω is a pre-defined distance, chosen by us. Outside of this region, i.e. $x \notin \Omega$, we use only the built-in controller, since trajectory tracking is not considered, the advantage of this switching strategy is the rapidity, as either the torque or the velocity is saturated at an early stage. Within this region, we activate this auxiliary controller which generates desired position u_2 . This switching method can be summarized as below:

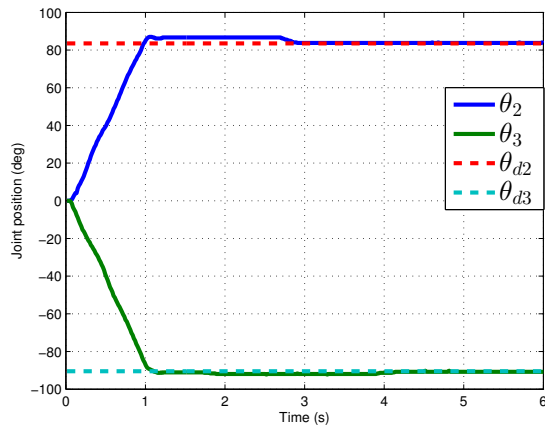
$$u = \begin{cases} x_d, & \text{if } x \notin \Omega, \\ u_2, & \text{if } x \in \Omega. \end{cases} \quad (5.3)$$

5.3.4 Performance with auxiliary controller

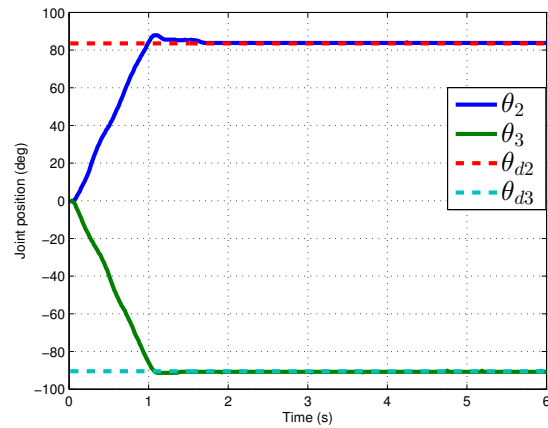
With the control strategy described in (5.3), the activated range for the auxiliary controller is very limited, thus for the implementation of the PID controller, we will only consider an integral term for simplicity. Both the integral controller and the adaptive controller are tested in the same case as the built-in controller is, the performance with auxiliary controllers for the two configurations is illustrated in Figure 5.8 and 5.9. A video recording the performance with auxiliary controller is available at https://youtu.be/UQwLV0V_VZ4.

Both the adaptive and integral auxiliary controller can finally eliminate the steady state error, however, since the gain for integral controller is constant, the performance degrades

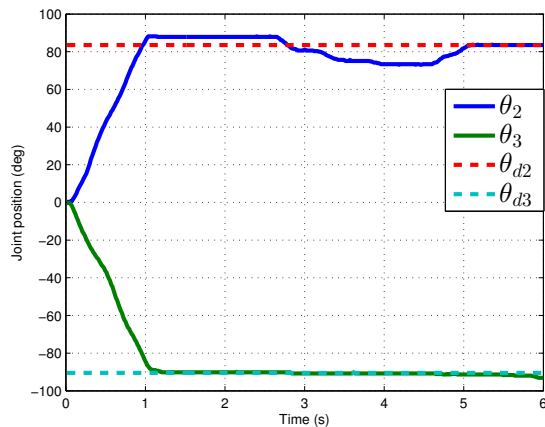
when operational condition changes, obvious overshoot and prolonged convergence time are observed. While for the proposed adaptive controller, the good performance persists even operational condition changes.



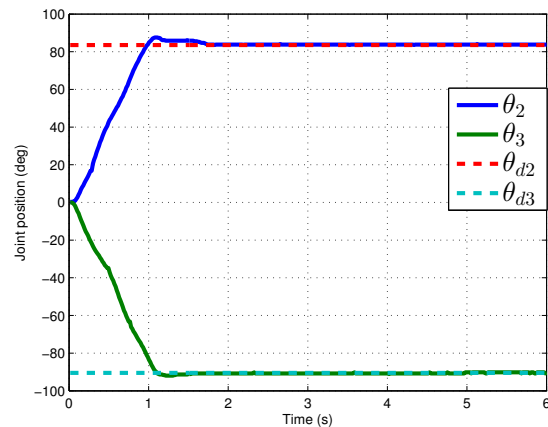
(a) Integral controller



(b) Adaptive controller



(c) Integral controller with additional load



(d) Adaptive controller with additional load

Fig. 5.8 Auxiliary controller for Configuration 1

5.4 Flexible-joint case

With larger and heavier link, the elasticity of the plastic motor shaft can no longer be ignored. To get link-side information, a MEMS IMU (Inertial Measurement Unit) composed of an accelerometer and a gyroscope is mounted on the link side, the accelerometer is used to measure static link angular position and gyroscope gives link angular velocity measurement. The sensor information communication and controller computation are performed under

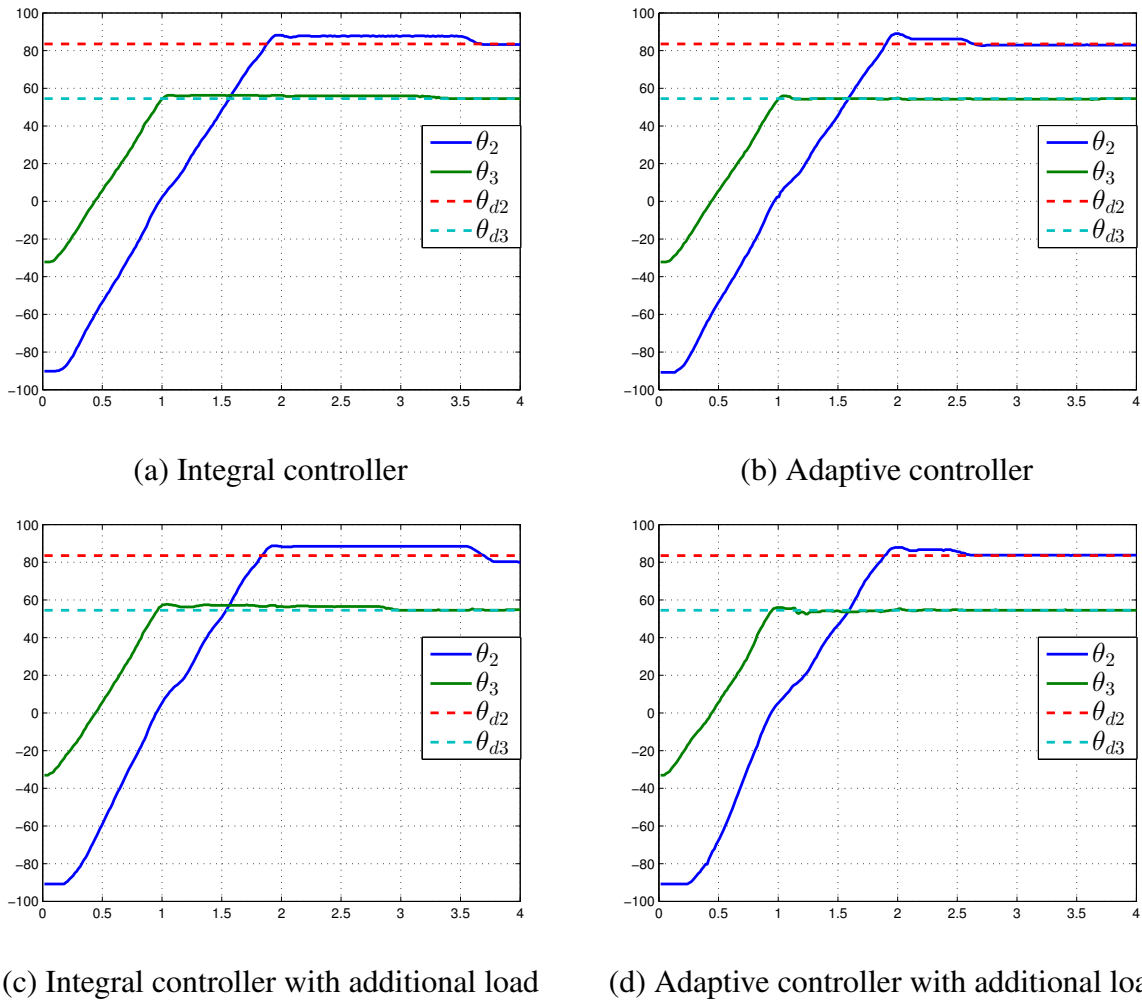


Fig. 5.9 Auxiliary controller for Configuration 2

ROS (Robot Operating System) framework. As discussed previously in this chapter, the identification and control methods proposed in Chapter 3 are implemented. For the experiment, the sampling frequency of the motor encoder and the gyroscope are set to 100Hz.

5.4.1 Inertial sensors

A simple breakout (Figure 5.10) for the ADXL345 MEMS accelerometer and the ITG-3200 MEMS gyroscope is adopted, for its tiny size and ease to mount. The sensors communicate with the PC through I2C interface.

The ITG-3200 Gyroscope from InvenSense features three 16-bit analog-to-digital converters (ADCs) for digitizing the gyro outputs, a user-selectable internal low-pass filter bandwidth, and a Fast-Mode I²C (400kHz) interface. Additional features include an embed-

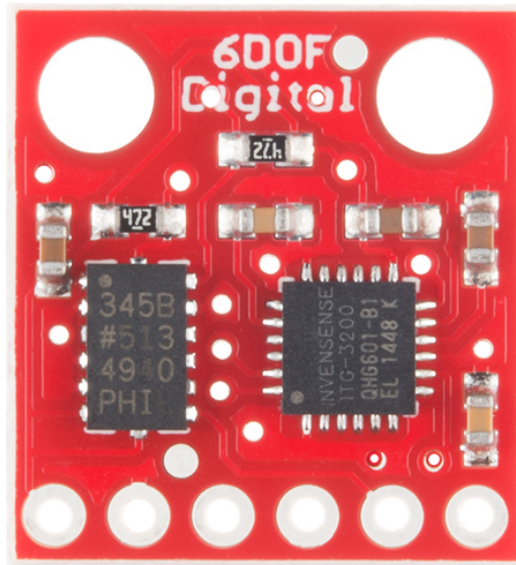


Fig. 5.10 6 DOF IMU Digital Combo Board

ded temperature sensor and a 2% accurate internal oscillator. This breakthrough in gyroscope technology provides a dramatic 67% package size reduction, delivers a 50% power reduction, and has inherent cost advantages compared to competing multi-chip gyro solutions.

The ADXL345 accelerometer from ANALOG DEVICES is a small, thin, low power, 3-axis accelerometer with high resolution (13-bit) measurement at up to $\pm 16g$. Digital output data is formatted as 16-bit twos complement and is accessible through either a SPI or I²C digital interface. The ADXL345 is well suited for mobile device applications. It measures the static acceleration of gravity in tilt-sensing applications, as well as dynamic acceleration resulting from motion or shock. Its high resolution (4 mg/LSB) enables measurement of inclination changes less than 1.0° .

5.4.2 Built-in controller performance

For a point-to-point link position control problem, denote q_d the desired position of the link, with the built-in controller, the input is by default

$$u = q_d, \quad (5.4)$$

and the performance is illustrated in Figure 5.11, in which θ is the joint motor position, q_0 is the initial static position and q_f the final static position of the link, both measured by the accelerometer, \dot{q} is the angular velocity of the link captured by the gyroscope, the real time link position q is considered as the sum of the initial position and the integration of the angular velocity ($q_0 + \int \dot{q}$). To avoid output torque saturation, q_d (input u) is set to be within the proportional range of the built-in P-like controller.

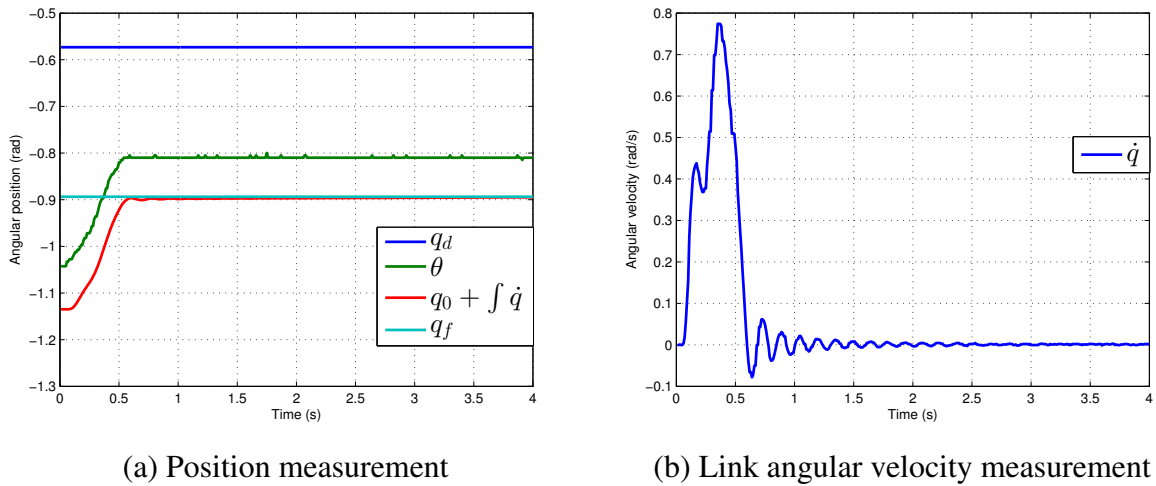


Fig. 5.11 Performance of built-in controller for single-link flexible-joint robot

(5.4) intends to control the position of the motor, the steady state error between q_d and θ is due to the P controller, as in the rigid case, and the error magnitude depends on the link gravity torque. The error between θ and q justifies the joint flexibility. In Figure 5.11(a), the convergence of q to q_f confirms the reliability of the measurement (after filtering) of the gyroscope and accelerometer, at least during the experiment duration, while integration drift may occur for a longer duration. In Figure 5.11(b), oscillation of the link is observed, as a common consequence of the joint flexibility.

5.4.3 Model identification

To avoid the output torque saturation, the input is designed such that the error between the input and the current motor feedback position stays always in the proportional zone, as shown in Figure 5.12(a), where the error is set to be constant for most of the time. The initial link position q_0 is measured by the accelerometer, and then q is given as $q_0 + \int \dot{q}$, algebraic-based differentiator is used to get the estimates \ddot{q} , $\dot{\theta}$ and $\ddot{\theta}$ from \dot{q} and θ . The measurements and the estimation performance are illustrated in Figure 5.12(b), 5.12(c) and 5.12(d).

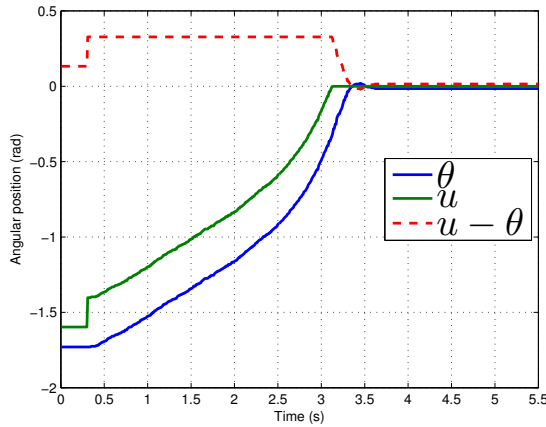
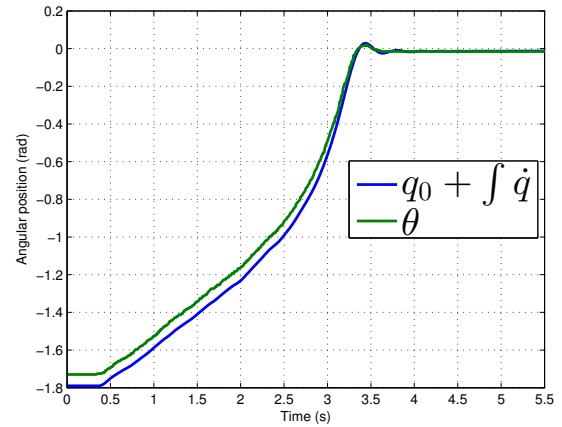
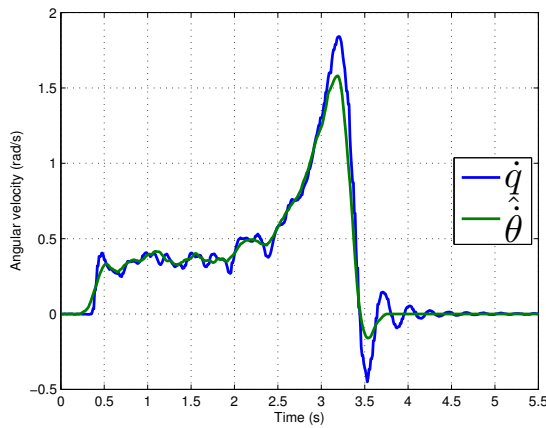
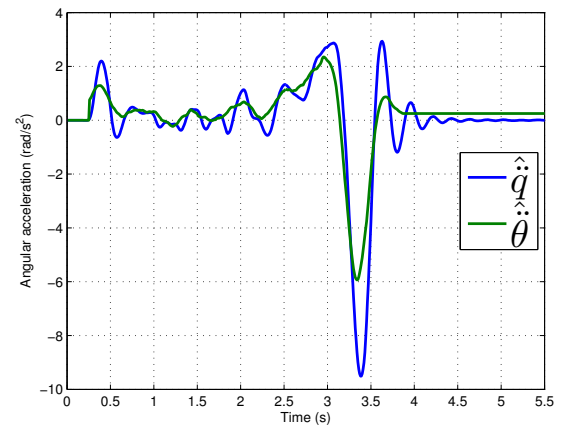
(a) Input u and θ (b) q and θ (c) \dot{q} and $\hat{\theta}$ (d) \ddot{q} and $\hat{\hat{\theta}}$

Fig. 5.12 Identification for single-link flexible-joint robot

Based on the data obtained, (3.8) and (3.9) are used to identify the parameters, several scenarios are tested and the average is taken as the final result, as shown in Table 5.3.

Model validation

Based on the estimated parameters in Table 5.3, we simulate the behaviour of the system under the same input and the same initial conditions, the behaviour of the system is given in Figure 5.13, which shows large conformity with the real behaviour of the robot.

5.4.4 Controller performance

Based on the parameters estimated shown in Table 5.3, the PD controller (3.14a) and (3.14b) can be designed, and the performance is shown in Figure 5.14(a) and 5.14(b).

Table 5.3 Identification results for flexible-joint robot

	J_p	H_p	K_p	I_k	F_k	G_k
Estimates	0.0020	0.0370	3.6670	0.0010	0.0190	0.0870

The proposed two-stage adaptive controller described as (3.26), (3.37) and (3.40) is also implemented, for which the performance is illustrated in Figure 5.14(c) and 5.14(d). For both two controllers, homogeneous finite-time differentiator (HOMD) is used to estimate the derivatives. A video recording the performance with auxiliary controller is available at <https://youtu.be/l7lW7F0pJpI>.

Compared to the built-in controller, both controllers reduce the link position error and the oscillation of the link is somehow attenuated. Further more, the two-stage adaptive controller gives a better control precision, corresponds to the fact that the two-stage controller is more robust with respect to parameter uncertainties.

5.5 Conclusion

In this chapter, a low-cost, small-size and light-weight test robot arm is introduced, for which the plastic motor shaft brings in torsional elasticity, and the built-in controller is a P-like controller with output saturation. Firstly, with each joint driven independently by the attached actuator, the stiffness of the motor shaft can be considered as infinite compared to those tiny inertial parameters of each link, and thus the robot is regarded as rigid, the performance of the mere built-in controller is investigated and evident steady state error is presented, to reduce the position error, the controllers proposed in Chapter 2 are implemented and compared, the result shows that the position error can be effectively reduced for both integral and adaptive controller, besides, the later preserves quick convergence while the former is more subject to configuration changes. Secondly, if only the second joint is driven, the attached rest part can be considered as a whole link, for which the inertial parameters multiply and thus the shaft elasticity must be taken into account for controller design. The identification and control methods proposed in Chapter 3 can be implemented using gyroscope and accelerometer, the identification result is given and the model parameters are validated. Both the PD controller and the two-stage adaptive controllers are implemented and the later gives better regulation precision. As a pity, the similar methods presented in Chapter 4 have not been implemented due to the difficulty to obtain the angular acceleration.

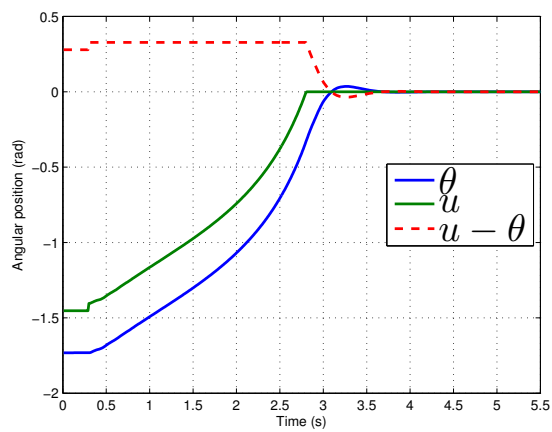
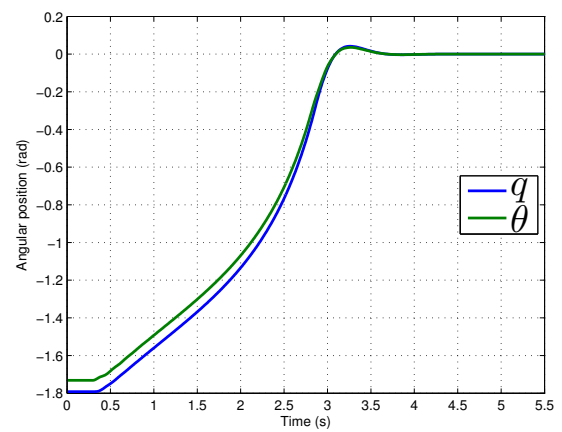
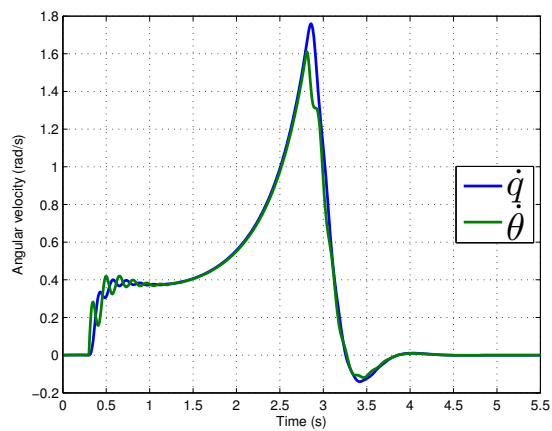
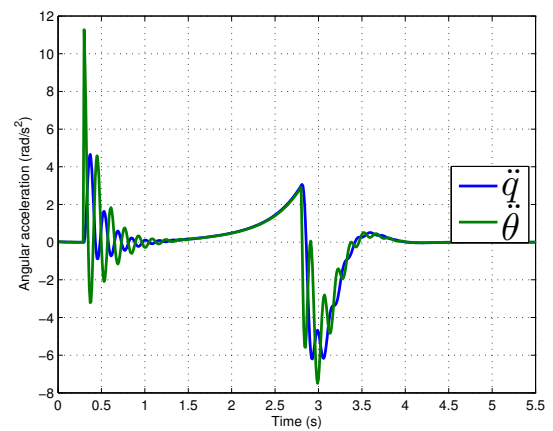
(a) Input u and θ (b) q and θ (c) \dot{q} and $\hat{\theta}$ (d) \ddot{q} and $\hat{\theta}$

Fig. 5.13 Simulation of the model based on the identification result

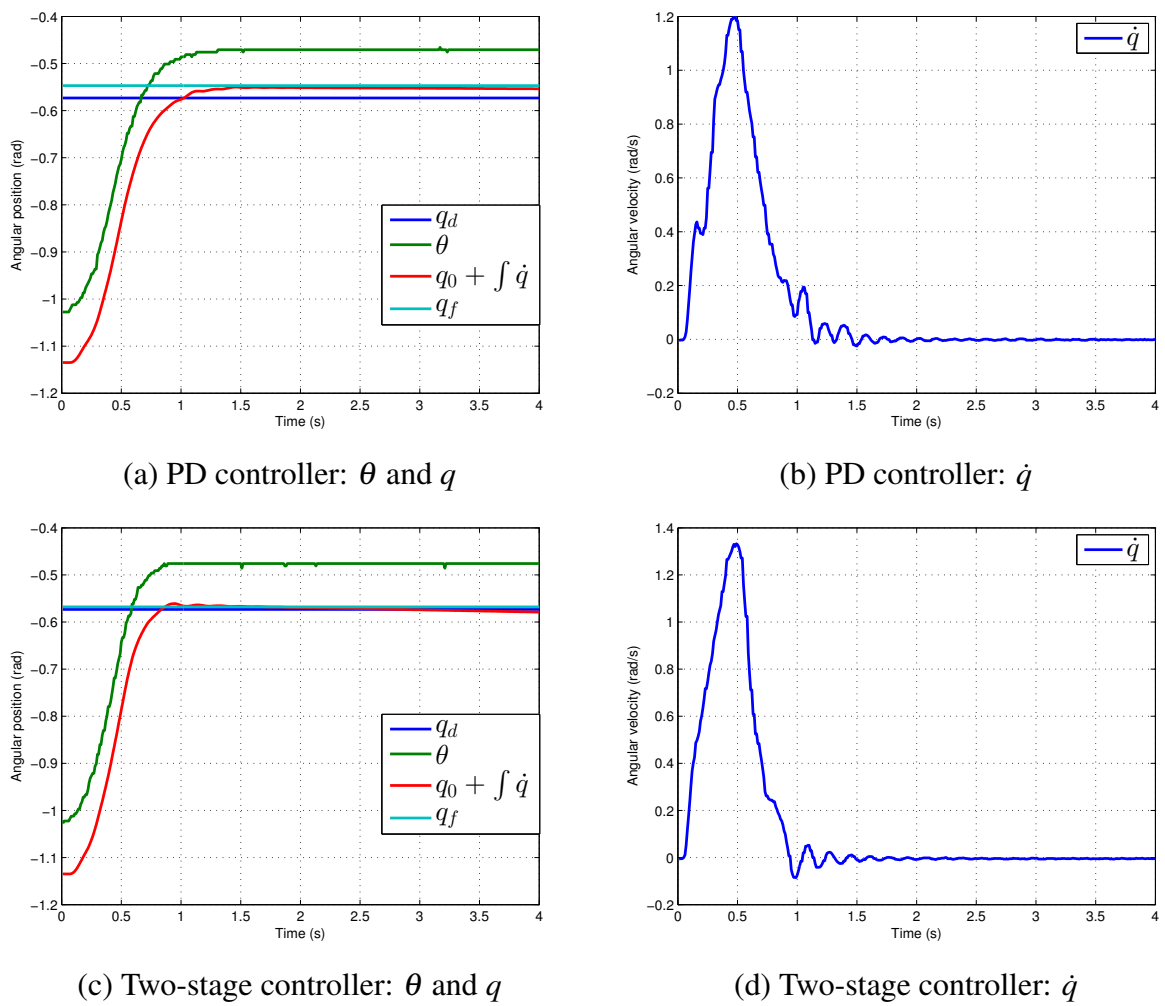


Fig. 5.14 Performances of PD controller and two-stage controller

Conclusions and Perspectives

The purpose of this chapter is to summarize the contributions presented in the thesis and propose some perspectives for future work.

Conclusions

This thesis investigates the control problem of low-cost light-weight position-controlled robot arms.

In Chapter 1, the background and the motivation of this thesis is introduced, then a survey of the previous work concerning the control of both rigid and flexible-joint robot arms is given.

In Chapter 2, we focus on the rigid case. The set-point control problem of low-cost rigid manipulators with “all-in-one” actuators is addressed in this chapter. For the derivation of the dynamics model linking the input with the state variables, the effect of the driven motor and the transmission system is considered, as a result, a second-order differential equation with constant parameters and highly bounded disturbance is obtained, then identification method of a nominal model is proposed, based on the identified model parameters, a model-based adaptive controller is developed. In simulation, the ability of error reduction is validated, and advantage on performance robustness with respect to model change is observed with comparison to PID controller with constant gains.

In Chapter 3, we consider point-to-point control of single-link position-controlled robot with joint flexibility, to obtain link side information, link angular velocity measurement is assumed to be provided. An identification scheme of the model parameters is presented, based on the classic model of flexible-joint robots, and with the measurement of initial link angles. As a benchmark, a modified simple PD plus gravity compensation controller is considered, of which the regulation error depends on two parameter estimates. To improve the robustness with respect to parameter uncertainties, a two-stage adaptive controller is proposed, with which the final position error depends on the precision of only one parameter

estimate, provided that the initial static link position can be measured. Simulation results illustrate that, the proposed two-stage controller is more robust than the PD one.

In Chapter 4, firstly, the control problem of single-link flexible-joint robots using link angular acceleration has been studied. With also tilt angle measurement, identification algorithm based on linear square method and the same two-stage adaptive controller are proposed, simulation result showed similar performance as using angular velocity measurement in Chapter 3. Secondly, the problem of model identification and output control has been discussed for linear time-invariant SISO system with completely unknown parameters, external disturbances, and output measurement noise. It is shown that by introducing recursive integrals and using a simple identification algorithm, some estimates on vector of unknown parameters and states can be obtained. Next, these information can be used in control, adaptive or robust, to provide boundedness of the state vector of the system. Due to integration drift all results are obtained on final intervals of time. Efficacy of the proposed identification and control algorithms is demonstrated in simulations.

In Chapter 5, a low-cost, small-size and light-weight test robot arm is introduced, for which the plastic motor shaft brings in torsional elasticity, and the built-in controller is a P-like controller with output saturation. Firstly, with each joint driven independently by the attached actuator, the stiffness of the motor shaft can be considered as infinite compared to those tiny inertial parameters of each link, and thus the robot is regarded as rigid, the performance of the mere built-in controller is investigated and evident steady state error is presented, to reduce the position error, the controllers proposed in Chapter 2 are implemented and compared, the result shows that the position error can be effectively reduced for both integral and adaptive controller, besides, the later preserves quick convergence while the former is more subject to configuration changes. Secondly, if only the second joint is driven, the attached rest part can be considered as a whole link, for which the inertial parameters multiply and thus the shaft elasticity must be taken into account for controller design. The identification and control methods proposed in Chapter 3 can be implemented using gyroscope and accelerometer, the identification result is given and the model parameters are validated. Both the PD controller and the two-stage adaptive controllers are implemented and the later gives better regulation precision. As a pity, the similar methods presented in Chapter 4 have not been implemented due to the difficulty to obtain the angular acceleration.

Perspectives

At the end of this thesis, some issues remain unresolved, and some other methods can be developed. The theoretical concepts introduced in this thesis can lead to several extensions and future applications.

In Chapter 2, for the rigid case, only the point-to-point regulation problem is addressed, it is also worthy to investigate the tracking problem and its implementation. Besides, control in task space (end-effector) instead of joint space can also be considered.

In Chapter 3 and Chapter 4, for flexible-joint case, firstly, the proposed identification and control methods limited to single-link configuration, some work can be done to extend them to n -DOF flexible-joint robot arms. Secondly, controller design for trajectory tracking remains unconsidered.

In Chapter 5, the identification and control for single-link flexible-joint manipulators has not been implemented, for the difficulty of direct or indirect angular acceleration measurement, this may be realisable for the future work.

References

- [1] Abdallah, C. T., Dawson, D., Dorato, P., and Jamshidi, M. (1991). Survey of robust control for rigid robots.
- [2] Abouelsoud, A. (1998). Robust regulator for flexible-joint robots using integrator backstepping. *Journal of Intelligent and Robotic Systems*, 22(1):23–38.
- [3] Albu-Schäffer, A. and Hirzinger, G. (2000). State feedback controller for flexible joint robots: a globally stable approach implemented on dlr's light-weight robots. In *IROS*, pages 1087–1093.
- [4] An, C. H., Atkeson, C. G., and Hollerbach, J. M. (1988). *Model-based control of a robot manipulator*, volume 214. MIT press Cambridge, MA.
- [5] Arimoto, S. (1984). Stability and robustness of pid feedback control for robot manipulators of sensory capability. *Robotics Research*, pages 783–799.
- [6] Asada, H. and Slotine, J.-J. (1986). *Robot analysis and control*. John Wiley & Sons.
- [7] Åström, K. J. and Wittenmark, B. (2013). *Adaptive control*. Courier Corporation.
- [8] Brogliato, B., Ortega, R., and Lozano, R. (1995). Global tracking controllers for flexible-joint manipulators: a comparative study. *Automatica*, 31(7):941–956.
- [9] Brogliato, B. and Rey, D. (1998). Further experimental results on nonlinear control of flexible joint manipulators. In *American Control Conference, 1998. Proceedings of the 1998*, volume 4, pages 2209–2211. IEEE.
- [10] Brogliato, B., Rey, D., Pastore, A., and Barnier, J. (1998). Experimental comparison of nonlinear controllers for flexible joint manipulators. *The International Journal of Robotics Research*, 17(3):260–281.
- [11] Burger, F., Besse, P.-A., and Popovic, R. (1998). New fully integrated 3-d silicon hall sensor for precise angular-position measurements. *Sensors and Actuators A: Physical*, 67(1):72–76.
- [12] Craig, J. (2005a). Introduction to robotics: mechanics and control.
- [13] Craig, J. J. (2005b). *Introduction to robotics: mechanics and control*, volume 3. Pearson Prentice Hall Upper Saddle River.
- [14] Craig, J. J., Hsu, P., and Sastry, S. S. (1987). Adaptive control of mechanical manipulators. *The International Journal of Robotics Research*, 6(2):16–28.

- [15] Dabroom, A. and Khalil, H. K. (1997). Numerical differentiation using high-gain observers. In *Decision and Control, 1997., Proceedings of the 36th IEEE Conference on*, volume 5, pages 4790–4795. IEEE.
- [16] Dabroom, A. M. and Khalil, H. K. (1999). Discrete-time implementation of high-gain observers for numerical differentiation. *International Journal of Control*, 72(17):1523–1537.
- [17] Datta, A. and Ho, M.-T. (1993). Computed torque adaptive control of rigid robots with improved transient performance. In *American Control Conference, 1993*, pages 1418–1422. IEEE.
- [18] Dawson, D., Qu, Z., Bridges, M., and Carroll, J. (1991). Robust tracking of rigid-link flexible-joint electrically-driven robots. In *Decision and Control, 1991., Proceedings of the 30th IEEE Conference on*, pages 1409–1412. IEEE.
- [19] De Luca, A. (1996). Decoupling and feedback linearization of robots with mixed rigid/elastic joints. In *Robotics and Automation, 1996. Proceedings., 1996 IEEE International Conference on*, volume 1, pages 816–821. IEEE.
- [20] De Luca, A. (2000). Feedforward/feedback laws for the control of flexible robots. In *Robotics and Automation, 2000. Proceedings. ICRA'00. IEEE International Conference on*, volume 1, pages 233–240. IEEE.
- [21] De Luca, A., Isidori, A., and Nicolo, F. (1985). Control of robot arm with elastic joints via nonlinear dynamic feedback. In *Decision and Control, 1985 24th IEEE Conference on*, pages 1671–1679. IEEE.
- [22] De Luca, A. and Lucibello, P. (1998). A general algorithm for dynamic feedback linearization of robots with elastic joints. In *Robotics and Automation, 1998. Proceedings. 1998 IEEE International Conference on*, volume 1, pages 504–510. IEEE.
- [23] De Luca, A., Siciliano, B., and Zollo, L. (2005). Pd control with on-line gravity compensation for robots with elastic joints: Theory and experiments. *Automatica*, 41(10):1809–1819.
- [24] Efimov, D. (2005). *Robust and adaptive control of nonlinear oscillations*. Nauka, St. Petersburg.
- [25] Efimov, D. and Fradkov, A. (2015). Design of impulsive adaptive observers for improvement of persistency of excitation. *Int. J. Adaptive Control and Signal Processing*, 29(6):765–782.
- [26] Efimov, D. V. and Fridman, L. (2011). A hybrid robust non-homogeneous finite-time differentiator. *sign*, 1(1.5):1–5.
- [27] Fliess, M., Join, C., and Sira-Ramirez, H. (2008). Non-linear estimation is easy. *International Journal of Modelling, Identification and Control*, 4(1):12–27.
- [28] Fu, S. H.-S. and Cheng, C.-C. (2005). Robust direct adaptive control of nonlinear uncertain systems with unknown disturbances. In *American Control Conference, 2005. Proceedings of the 2005*, pages 3731–3736. IEEE.

- [29] Ge, S. S., Sun, Z., and Lee, T. H. (2001). Nonregular feedback linearization for a class of second-order nonlinear systems. *Automatica*, 37(11):1819–1824.
- [30] Gilbert, E. G. and Ha, I. J. (1984). An approach to nonlinear feedback control with applications to robotics. *Systems, Man and Cybernetics, IEEE Transactions on*, (6):879–884.
- [31] Goldfarb, M. and Sirithanapipat, T. (1999). The effect of actuator saturation on the performance of pd-controlled servo systems. *Mechatronics*, 9(5):497–511.
- [32] Gorez, R. (1997). Sliding mode as a rational approach to robot controller design. In *Add. to Proc. Workshop on Modelling and Control of Mechanical Systems, Imperial College Press, London, UK*, pages 1–15.
- [33] Hashimoto, M., Kiyosawa, Y., and Paul, R. P. (1993). A torque sensing technique for robots with harmonic drives. *Robotics and Automation, IEEE Transactions on*, 9(1):108–116.
- [34] Hirose, S. and Yoneda, K. (1990). Development of optical six-axial force sensor and its signal calibration considering nonlinear interference. In *Robotics and Automation, 1990. Proceedings., 1990 IEEE International Conference on*, pages 46–53. IEEE.
- [35] Hirzinger, G., Albu-Schaffer, A., Hahnle, M., Schaefer, I., and Sporer, N. (2001). On a new generation of torque controlled light-weight robots. In *Robotics and Automation, 2001. Proceedings 2001 ICRA. IEEE International Conference on*, volume 4, pages 3356–3363. IEEE.
- [36] Hsia, T. S. (1989). A new technique for robust control of servo systems. *Industrial Electronics, IEEE Transactions on*, 36(1):1–7.
- [37] Jain, S. and Khorrami, F. (1998). Robust adaptive control of flexible joint manipulators. *Automatica*, 34(5):609–615.
- [38] Kawasaki, H., Bito, T., and Kanzaki, K. (1996). An efficient algorithm for the model-based adaptive control of robotic manipulators. *Robotics and Automation, IEEE Transactions on*, 12(3):496–501.
- [39] Kelly, R. (1990). Adaptive computed torque plus compensation control for robot manipulators. *Mechanism and machine theory*, 25(2):161–165.
- [40] Khalil, H. K. (2002). *Nonlinear Systems*. Prentice Hall PTR, 3rd edition.
- [41] Khatib, O., Thaulad, P., Yoshikawa, T., and Park, J. (2008). Torque-position transformer for task control of position controlled robots. In *Robotics and Automation, 2008. ICRA 2008. IEEE International Conference on*, pages 1729–1734. IEEE.
- [42] Khiat, A., Lamarque, F., Prelle, C., Bencheikh, N., and Dupont, E. (2010). High-resolution fibre-optic sensor for angular displacement measurements. *Measurement Science and Technology*, 21(2):025306.
- [43] Khorasani, K. (1990). Nonlinear feedback control of flexible joint manipulators: A single link case study. *Automatic Control, IEEE Transactions on*, 35(10):1145–1149.

- [44] Kim, M. S. and Lee, J. S. (2004). Adaptive tracking control of flexible-joint manipulators without overparametrization. *Journal of Robotic Systems*, 21(7):369–379.
- [45] Kreisselmeier, G. (1977). Adaptive observers with exponential rate of convergence. *IEEE Trans. Automat. Contr.*, 22:2–8.
- [46] Kuntze, H.-B., Jacobasch, A., Richalet, J., and Arber, C. (1986). On the predictive functional control of an elastic industrial robot. In *Decision and Control, 1986 25th IEEE Conference on*, pages 1877–1881. IEEE.
- [47] Kutner, M. H., Nachtsheim, C., and Neter, J. (2004a). *Applied linear regression models*. McGraw-Hill/Irwin.
- [48] Kutner, M. H., Nachtsheim, C. J., and Neter, J. (2004b). *Applied Linear Regression Models*. McGraw-Hill/Irwin, Boston, 4th edition.
- [49] Landau, I. D., Lozano, R., M'Saad, M., and Karimi, A. (2011). *Adaptive control: algorithms, analysis and applications*. Springer Science & Business Media.
- [50] Leahy Jr, M. B., Valavanis, K. P., and Saridis, G. (1989). Evaluation of dynamic models for puma robot control. *Robotics and Automation, IEEE Transactions on*, 5(2):242–245.
- [51] Levant, A. (2003). Higher-order sliding modes, differentiation and output-feedback control. *International journal of Control*, 76(9-10):924–941.
- [52] Lewis, F. L., Abdallah, C. T., and Dawson, D. M. (1993). *Control of robot manipulators*, volume 236. Macmillan New York.
- [53] Liu, C., Cheah, C. C., and Slotine, J.-J. E. (2008a). Adaptive task-space regulation of rigid-link flexible-joint robots with uncertain kinematics. *Automatica*, 44(7):1806–1814.
- [54] Liu, G., Abdul, S., and Goldenberg, A. A. (2008b). Distributed control of modular and reconfigurable robot with torque sensing. *Robotica*, 26(01):75–84.
- [55] Lozano, R., Valera, A., Albertos, P., Arimoto, S., and Nakayama, T. (1999). Pd control of robot manipulators with joint flexibility, actuators dynamics and friction. *Automatica*, 35(10):1697–1700.
- [56] Luca, A. D. (1988). Dynamic control of robots with joint elasticity. In *Robotics and Automation, 1988. Proceedings., 1988 IEEE International Conference on*, pages 152–158. IEEE.
- [57] Luh, J. (1983). Conventional controller design for industrial robots—a tutorial. *IEEE Transactions on Systems Man and Cybernetics*, 13:298–316.
- [58] Macnab, C. J., D'Eleuterio, G. M., and Meng, M. (2004). Cmac adaptive control of flexible-joint robots using backstepping with tuning functions. In *Robotics and Automation, 2004. Proceedings. ICRA'04. 2004 IEEE International Conference on*, volume 3, pages 2679–2686. IEEE.
- [59] Maliotis, G. (1991). A hybrid model reference adaptive control/computed torque control scheme for robotic manipulators. *Proceedings of the Institution of Mechanical Engineers, Part I: Journal of Systems and Control Engineering*, 205(3):215–221.

- [60] Marino, R. and Spong, M. (1986). Nonlinear control techniques for flexible joint manipulators: a single link case study. In *Robotics and Automation. Proceedings. 1986 IEEE International Conference on*, volume 3, pages 1030–1036. IEEE.
- [61] Mboup, M., Join, C., and Fliess, M. (2007). A revised look at numerical differentiation with an application to nonlinear feedback control. In *The 15th Mediterrean Conference on Control and Automation-MED'2007*.
- [62] Mrad, F. and Ahmad, S. (1990). Adaptive control of flexible joint robots with stability in the sense of Iyapunov. In *Decision and Control, 1990., Proceedings of the 29th IEEE Conference on*, pages 2667–2672. IEEE.
- [63] Murray, R. M., Li, Z., Sastry, S. S., and Sastry, S. S. (1994). *A mathematical introduction to robotic manipulation*. CRC press.
- [64] Narendra, K. and Annaswamy, A. (1989). *Stable adaptive systems*. Prentice Hall.
- [65] Nicosia, S. and Tomei, P. (1988). On the feedback linearization of robots with elastic joints. In *Decision and Control, 1988., Proceedings of the 27th IEEE Conference on*, pages 180–185. IEEE.
- [66] Nicosia, S. and Tomei, P. (1991). A new approach to control elastic joint robots with application to adaptive control. In *Decision and Control, 1991., Proceedings of the 30th IEEE Conference on*, pages 343–347. IEEE.
- [67] Nicosia, S. and Tomei, P. (1993). Design of global tracking controllers for flexible-joint robots. *Journal of robotic systems*, 10(6):835–846.
- [68] Ortega, R. (1997). Passivity-based control of euler-lagrange systems: applications to robots, ac motors and power converters. In *Proceedings of the Workshop*, volume 17, page 20. World Scientific.
- [69] Ortega, R. and Spong, M. W. (1989). Adaptive motion control of rigid robots: A tutorial. *Automatica*, 25(6):877–888.
- [70] Ozgoli, S. and Taghirad, H. (2006). A survey on the control of flexible joint robots. *Asian Journal of Control*, 8(4):332–344.
- [71] Paul, R. P. (1981). *Robot manipulators: mathematics, programming, and control: the computer control of robot manipulators*. Richard Paul.
- [72] Pedley, M. (2013). Tilt sensing using a three-axis accelerometer. *Freescale Semiconductor Application Note*.
- [73] Perruquetti, W. and Floquet, T. (2007). Homogeneous finite time observer for nonlinear systems with linearizable error dynamics. In *IEEE Conference on Decision and Control*.
- [74] Perruquetti, W., Floquet, T., and Moulay, E. (2008). Finite-time observers: application to secure communication. *Automatic Control, IEEE Transactions on*, 53(1):356–360.
- [75] Rocco, P. (1996). Stability of pid control for industrial robot arms. *Robotics and Automation, IEEE Transactions on*, 12(4):606–614.

- [76] Sadegh, N. and Horowitz, R. (1990). An exponentially stable adaptive control law for robot manipulators. *Robotics and Automation, IEEE Transactions on*, 6(4):491–496.
- [77] Schilling, R. et al. (2013). Fundamentals of robotics.
- [78] Sciavicco, L. and Siciliano, B. (2012). *Modelling and control of robot manipulators*. Springer Science & Business Media.
- [79] Slotine, J.-J. E. (1988). Putting physics in control—the example of robotics. *Control Systems Magazine, IEEE*, 8(6):12–18.
- [80] Slotine, J.-J. E. and Li, W. (1987). On the adaptive control of robot manipulators. *The international journal of robotics research*, 6(3):49–59.
- [81] Slotine, J.-J. E. and Li, W. (1989). Composite adaptive control of robot manipulators. *Automatica*, 25(4):509–519.
- [82] Spong, M. W. (1987). Modeling and control of elastic joint robots. *Journal of dynamic systems, measurement, and control*, 109(4):310–318.
- [83] Spong, M. W. (1996). Control of robots and manipulators. *The control handbook*, pages 1339–1351.
- [84] Staufer, P. and Gattringer, H. (2012). State estimation on flexible robots using accelerometers and angular rate sensors. *Mechatronics*, 22(8):1043–1049.
- [85] Sweet, L. M. and Good, M. (1984). Re-definition of the robot motion control problem: Effects of plant dynamics, drive system constraints, and user requirements. In *Decision and Control, 1984. The 23rd IEEE Conference on*, pages 724–732. IEEE.
- [86] Sweet, L. M. and Good, M. C. (1985). Redefinition of the robot motion-control problem. *Control Systems Magazine, IEEE*, 5(3):18–25.
- [87] Taghirad, H. and Rahimi, H. (2005). Composite qft controller design for flexible joint robots. In *Control Applications, 2005. CCA 2005. Proceedings of 2005 IEEE Conference on*, pages 583–588. IEEE.
- [88] Thümmel, M., Otter, M., and Bals, J. (2001). Control of robots with elastic joints based on automatic generation of inverse dynamics models. In *Intelligent Robots and Systems, 2001. Proceedings. 2001 IEEE/RSJ International Conference on*, volume 2, pages 925–930. IEEE.
- [89] Tomei, P. (1991a). Adaptive pd controller for robot manipulators. *Robotics and Automation, IEEE Transactions on*, 7(4):565–570.
- [90] Tomei, P. (1991b). A simple pd controller for robots with elastic joints. *Automatic Control, IEEE Transactions on*, 36(10):1208–1213.
- [91] Tomei, P. (1994). Tracking control of flexible joint robots with uncertain parameters and disturbances. *IEEE transactions on automatic control*, 39(5):1067–1072.

- [92] Tomei, P., Nicosia, S., and Ficola, A. (1986). An approach to the adaptive control of elastic at joints robots. In *Robotics and Automation. Proceedings. 1986 IEEE International Conference on*, volume 3, pages 552–558. IEEE.
- [93] Wang, C., Chen, W., and Tomizuka, M. (2012). Robot end-effector sensing with position sensitive detector and inertial sensors. In *Robotics and Automation (ICRA), 2012 IEEE International Conference on*, pages 5252–5257. IEEE.
- [94] Yeon, J. S. and Park, J. H. (2008). Practical robust control for flexible joint robot manipulators. In *Robotics and Automation, 2008. ICRA 2008. IEEE International Conference on*, pages 3377–3382. IEEE.
- [95] Yim, J.-G., Yeon, J. S., Lee, J., Park, J. H., Lee, S.-H., and Hur, J.-S. (2006). Robust control of flexible robot manipulators. In *SICE-ICASE, 2006. International Joint Conference*, pages 3963–3968. IEEE.
- [96] Yim, J.-G., Yeon, J. S., Park, J. H., Lee, S.-H., and Hur, J.-S. (2007). Robust control using recursive design method for flexible joint robot manipulator. In *Robotics and Automation, 2007 IEEE International Conference on*, pages 3805–3810. IEEE.
- [97] Yim, W. (2001). Adaptive control of a flexible joint manipulator. In *Robotics and Automation, 2001. Proceedings 2001 ICRA. IEEE International Conference on*, volume 4, pages 3441–3446. IEEE.
- [98] Yuan, J. and Stepanenko, Y. (1994). Adaptive control of flexible joint robots with arbitrary stiffness. *Contr. Eng. Pract*, 2(5):903–906.
- [99] Zhang, Q. (2002). Adaptive observer for MIMO linear time varying systems. *IEEE Trans. Autom. Control*, 47(3):525–529.
- [100] Zhu, W.-H. and Lamarche, T. (2007). Modular robot manipulators based on virtual decomposition control. In *Robotics and Automation, 2007 IEEE International Conference on*, pages 2235–2240. IEEE.

Appendix A

Dynamic of a 2DOF Rigid Robot Manipulator

Consider the 2DOF manipulator in Figure 2.4, denote (x_1, y_1) as the position of the CoM of the first link and (x_2, y_2) the position of the second link, then we have:

$$\begin{cases} x_1 = d_1 \sin q_1, \\ y_1 = d_1 \cos q_1, \\ x_2 = L_1 \sin q_1 + d_2 \sin(q_1 + q_2), \\ y_2 = L_1 \cos q_1 + d_2 \cos(q_1 + q_2), \end{cases}$$

which gives

$$\begin{cases} \dot{x}_1 = d_1 \dot{q}_1 \cos q_1, \\ \dot{y}_1 = -d_1 \dot{q}_1 \sin q_1, \\ \dot{x}_2 = L_1 \dot{q}_1 \cos q_1 + d_2 (\dot{q}_1 + \dot{q}_2) \cos(q_1 + q_2), \\ \dot{y}_2 = -L_1 \dot{q}_1 \sin q_1 - d_2 (\dot{q}_1 + \dot{q}_2) \sin(q_1 + q_2). \end{cases}$$

The **Kinetic Energy** K_1 and K_2 could be formed as

$$\begin{cases} K_1 = \frac{1}{2} m_1 (\dot{x}_1^2 + \dot{y}_1^2) + \frac{1}{2} I_1 \dot{q}_1^2 = \frac{1}{2} m_1 d_1^2 \dot{q}_1^2 + \frac{1}{2} I_1 \dot{q}_1^2, \\ K_2 = \frac{1}{2} m_2 (\dot{x}_2^2 + \dot{y}_2^2) + \frac{1}{2} I_2 (\dot{q}_1 + \dot{q}_2)^2 \\ = \frac{1}{2} m_2 L_1^2 \dot{q}_1^2 + \frac{1}{2} m_2 d_2^2 (\dot{q}_1 + \dot{q}_2)^2 + m_2 L_1 d_2 \dot{q}_1 (\dot{q}_1 + \dot{q}_2) \cos q_2 + \frac{1}{2} I_2 (\dot{q}_1 + \dot{q}_2)^2. \end{cases}$$

The **Potential Energy** P_1 and P_2 are:

$$\begin{cases} P_1 = m_1 g d_1 \cos q_1, \\ P_2 = m_2 g L_1 \cos q_1 + m_2 g d_2 \cos(q_1 + q_2). \end{cases}$$

The Lagrangian is taken as $L = K - P = K_1 + K_2 - P_1 - P_2$. Consider the viscous friction as $F_i = F_{vi}\dot{q}_i$, then by the Lagrangian formulation

$$\tau_i = \frac{d}{dt} \left(\frac{\partial L}{\partial \dot{q}_i} \right) - \frac{\partial L}{\partial q_i} + F_{vi}\dot{q}_i,$$

we get finally

$$\begin{cases} \tau_1 = (m_1 d_1^2 + m_2 L_1^2 + m_2 d_2^2 + 2m_2 L_1 d_2 \cos q_2 + I_1 + I_2)\ddot{q}_1 + (m_2 d_2^2 + m_2 L_1 d_2 \cos q_2 + I_2)\ddot{q}_2 \\ \quad - m_2 L_1 d_2 (2\dot{q}_1 + \dot{q}_2)\dot{q}_2 \sin q_2 + F_{v1}\dot{q}_1 - (m_1 d_1 + m_2 L_1)g \sin q_1 - m_2 d_2 g \sin(q_1 + q_2), \\ \tau_2 = (m_2 d_2^2 + m_2 L_1 d_2 \cos q_2 + I_2)\ddot{q}_1 + (m_2 d_2^2 + I_2)\ddot{q}_2 + m_2 L_1 d_2 \dot{q}_1^2 \sin q_2 + F_{v2}\dot{q}_2 \\ \quad - m_2 d_2 g \sin(q_1 + q_2). \end{cases}$$

Résumé étendu en français

Motivation de la recherche

Aujourd'hui, la plupart des robots manipulateurs industriels sont totalement intégrés, la structure mécanique, composants électroniques, actionneurs, capteurs et systèmes d'exploitation sont pré-intégrés avant la livraison. Grâce à des actionneurs à haute précision et des composants modernes, ces manipulateurs fournissent une performance opérationnelle efficace pour des tâches déterminées, mais sont moins flexibles pour d'autres tâches. En outre, en raison de leur grande taille, prix élevé, entretien et réparation coûteuse, nous ne pouvons trouver ces manipulateurs que dans des usines, des laboratoires, pour des missions spécifiques. De plus, pour éviter des accidents lors de l'interaction homme-machine, ces machines ne peuvent être opérés que par des techniciens qui ont suivi certaines formations. Par conséquent, ces manipulateurs sont beaucoup moins accessibles pour les particuliers. Ceci est exactement la même situation pour les ordinateurs avant 1970, où ils étaient énormes, coûteux et utilisés uniquement à des fins militaires ou de recherche.

De l'avis de l'auteur, contrairement aux manipulateurs aujourd'hui industriels, manipulateurs personnels de l'avenir devrait être de coût bas, de petite taille, de poids léger, mais avec un rapport élevé de charge-poids, utilisateur-reconfigurable, conviviale, flexible et sécuritaire pendant l'intervention humaine, facile à entretenir et à réparer ... Ce genre de manipulateurs peut être appliqué pour la recherche, le divertissement, l'assistance aux personnes, l'éducation ..., où les manipulateurs industriels ne sont pas adaptés, par exemple, quelqu'un peut être effrayé en face d'un robot d'alimentation qui est d'un manipulateur industriel.

En fait, il y a déjà des manipulateurs à prix-bas commercialisés dans le marché. Ils sont de faible coût, de petite taille et de poids léger. Une comparaison entre un manipulateur comme ça (PhantomX Pincher Robot Arm from Trossen Robotics©, Figure 5.1) et le récent KUKA light-weight manipulateur (Figure 5.2) est illustrée dans Table 5.1.

Cependant, ce n'est pas faisable d'exiger d'un manipulateur une performance aussi puissante qu'en un autre conçu et fabriqué avec un budget 20 fois de plus. Les faiblesses des manipulateurs à bas prix comprennent erreur de position dans l'espace des joints, dans



Fig. 5.1 A low-cost manipulator



Fig. 5.2 A Kuka light-weight robot

Table 5.1 comparaison entre manipulateur low-cost et manipulateur industriel

	Manipulateur low-cost	Kuka light-weight robot
Prix	378\$	+20 000€
Poids	550g	48kg
Portée Maximale	31cm	70.7cm

l'espace des liens et oscillation. Ces défauts peuvent être à l'origine des matériaux, des composants et / ou des logiciels.

Cette thèse est motivée par des manipulateurs à bas prix qui adoptent actionneurs “tout-en-un”. Ces actionneurs sont équipés de moteurs, capteurs, systèmes de transmission, unités de contrôle et réseaux de communication, fournissent un rapport charge-poids élevé, et exemptent les praticiens de la conception et de la mise en œuvre des systèmes de transmission et de contrôle. Cependant, parmi ces actionneurs, il y en a certains assez bon-marchés avec contrôleur simple (par exemple, régulateur PD ou P), dans ces cas, les erreurs de positions sont provoquées. En outre, si le matériau qui forme le rotor du moteur est en plastique, alors le rotor n'est pas assez rigide et la flexibilité des joints est présente, par conséquent, oscillation des liens et inadéquation entre la position de lien et celle de joint sont observés.

Cette thèse se concentre sur des manipulateurs à bas prix équipés des actionneurs “tout-en-un”. L'objectif comprend l'élimination de l'erreur de position en cas de joints rigides et aussi en cas de joints flexibles, et l'atténuation d'oscillation en cas de joints flexibles.

Conception de commande pour manipulateurs rigides à bas prix équipés d'actionneurs "tout-en-un"

Le problème de contrôle des manipulateurs rigides à bas prix équipés d'actionneurs "tout-en-un" est abordé. Un modèle classique de manipulateurs avec système d'entraînement est considéré, donc le contrôleur embarqué est de type PD. Pour la dérivation du modèle dynamique reliant l'entrée avec des variables d'état, l'effet de l'entraînement par un moteur et le système de transmission est considéré, par conséquent, une équation différentielle d'ordre 2 avec des paramètres constants et une perturbation bornée est obtenue, puis une méthode d'identification des paramètres nominaux est proposée, basé sur des paramètres identifiés, une commande adaptative est développée. Dans la simulation, la capacité de la réduction d'erreur de la commande proposée est validée, et une robustesse plus forte sur le changement des paramètres de modèle est observée, en comparaison avec le régulateur PID avec des gains constants.

Identification et contrôle des robots avec joints flexibles en utilisant mesures de vitesse de lien

Ici, nous examinons le problème de régulation pour un robot manipulateur de 1DOF, avec lequel la flexibilité des joints est présente. Si seulement un joint est considéré, le modèle du système est composé de deux équation différentielle d'ordre deux avec paramètres constants. Afin d'obtenir des informations du côté de lien, la mesure de vitesse angulaire de lien est supposée être fournie. Avec hypothèse que la position statique puisse aussi être mesurée, une méthode d'identification des paramètres du modèle est présentée. Premièrement, une variation de commande PD classique est considérée avec laquelle l'erreur de régulation dépend de la précision de deux estimations de paramètres. Pour améliorer la robustesse par rapport aux incertitudes de paramètre, une commande adaptative deux-étapes est proposée, avec laquelle l'erreur de position finale dépend seulement de la précision d'une paramètre estimé. Les résultats de simulation est présentés et comparés, qui montrent que la commande adaptative deux-étapes proposée est plus robuste que la commande PD.

Estimation et contrôle en utilisant mesures de dérivées d'ordre élevé

Avec la même hypothèse que positions statiques de lien sont également mesurées, de la même façon, une méthode d'identification basée sur feed-back d'accélération angulaire de lien et une commande adaptative deux-étapes sont proposées, résultats de la simulation montrent des performances similaires par rapport aux résultats obtenus en utilisant des mesures de vitesse angulaire de lien. Ensuite, l'idée d'identification et de contrôle en utilisant des mesures de dérivée d'ordre élevée est généralisée pour un système linéaire, donc des paramètres sont constants mais complètement inconnus, des perturbations externes et le bruit de mesure sont également considérés. Il est démontré que par l'introduction d'intégration récursive et en utilisant un algorithme d'identification simple, des paramètres inconnus et des variables d'états peuvent être estimés. ces résultats d'estimation peuvent être utilisés dans la conception de commande, des commandes adaptatives et des commandes robustes sont proposées. L'efficacité des algorithmes d'identification et de commandes proposées est démontrés par simulation.

Résultats expérimentaux

Dans cette partie, comme la plate-forme expérimentale, un robot manipulateur à bas prix (Figure 5.3), de petite taille et de poids léger est introduit. Chaque lien du robot est entraîné par l'actionneur Ax-12A (Figure 5.4), qui est de type "tout-en-un", pour lequel le rotor du moteur est en plastique qui apporte l'élasticité de torsion, et la commande intégrée est proportionnelle avec saturation de sortie.



Fig. 5.3 Manipulateur low-cost



Fig. 5.4 Actionneur AX-12

Tout d'abord, parce que le robot expérimental est de petite taille et de poids léger, chaque lien est tellement petit et léger que les paramètres inertiels de chaque lien est de magnitude

très petit, même si le rotor du moteur est de matériel plastique, sa rigidité peut être considérée comme infinie par rapport à ces petits paramètres inertiels, par conséquent, si chaque lien est entraîné individuellement, le robot peut être considéré comme rigide. La performance de régulation sous le contrôleur intégré est étudiée qui présente une erreur statique évidente, pour réduire cette erreur de position, la commande adaptative proposée et une commande intégrale sont mises en œuvre et les performances sont comparées entre eux, les résultats montrent que l'erreur de position peut être réduite pour tous les deux, en outre, le temps de convergence pour la commande intégrale varie avec la configuration et avec le modèle de système, qui peut être très long dans certains cas, par contre, le temps de convergence pour la commande adaptative est beaucoup plus robuste.

Les méthodes d'identification et de contrôle proposées en utilisant mesures de vitesse angulaire de lien peuvent être mises en œuvre en utilisant un gyroscope et un accéléromètre (Figure 5.5), le résultat d'identification est donné et validé par un modèle construits par les paramètres estimés. La commande PD et la commande adaptative deux-étapes sont réalisées basé sur les paramètres estimés, les résultats montrent que la dernière donne une meilleure précision de régulation. Comme dommage, les méthodes similaires proposées en utilisant des mesures d'accélération angulaire de lien n'ont pas pu être mises en œuvre en raison de la difficulté d'obtenir l'accélération angulaire.



Fig. 5.5 Capteur IMU

Contributions et perspectives

Contributions

D'abord, pour des robots manipulateurs rigides, la modélisation dynamique en lien avec le système d'actualisation est établie, qui forme une équation différentielle avec paramètres constants et perturbation. Une méthode d'identification des paramètres en utilisant des observateurs et une commande adaptative sont proposées, et des résultats de simulation et

d'expérimentation sont donnés. Ensuite, pour le cas d'articulation flexibles, pour simplifier, le modèle 1DOF est pris en compte. Premièrement, avec la mesure de la vitesse de lien, une méthode d'identification et une loi deux-étages adaptative sont proposées à condition que la position statique de lien puisse également être mesurée, des résultats de simulation sont donnés. Deuxièmement, en utilisant des mesures d'accélération de lien, une méthode d'identification et la même loi deux-étages adaptative sont proposées, cette idée est généralisée à l'identification et au contrôle de systèmes linéaires avec mesures de dérivées d'ordre élevé, des résultats de simulation sont présentés. Pour la mise en œuvre, des capteurs inertiels (gyroscopes et accéléromètres) sont utilisés et des résultats expérimentaux sont présentés.

Perspectives

Dans le cas de robot rigide, nous ne considérons que le problème de régulation point-à-point, il est aussi intéressant d'étudier le problème de suivi de trajectoire et sa mise en œuvre. En outre, le contrôle dans l'espace de tâche (effecteur) à la place de l'espace de joint peut également être étudié. Dans le cas de joints flexibles, premièrement, des méthodes d'identification et de contrôle proposées se limitent à la configuration de lien seul, une généralisation vers un robot de joints flexibles avec n -DOF est attendue. Deuxièmement, comme dans le cas rigide, le problème de suivi de trajectoire n'est pas considéré. Pour l'expérimentation, les méthodes d'identification et de contrôle pour manipulateurs à joints flexibles en utilisant mesure d'accélération n'ont pas été mises en œuvre, par la difficulté de la mesure d'accélération angulaire directe ou indirecte.

List of publications

Accepted conference papers

1. **Shao Z, Zheng G, Efimov D, et al. Modelling and control for position-controlled modular robot manipulators**[C]//Intelligent Robots and Systems (IROS), 2015 IEEE/RSJ International Conference on. IEEE, 2015: 3290-3295.
2. **Shao Z, Zheng G, Efimov D, et al. Modelling and control of actuators with built-in position controller**[C]//IFAC conference on Modelling, Identification and Control of NONlinear systems (MICNON) 2015.
3. **Shao Z, Zheng G, Efimov D, and Perruquetti, W. Robust and adaptive control using measurements of higher order derivatives.** Accepted by *European Control Conference (ECC) 2016*.

Submitted journal papers

1. **Shao Z, Zheng G, Efimov D, and Perruquetti, W. Auxiliary controller design for low-cost manipulators with built-in controller.** Submitted to *Journal of Intelligent and Robotic Systems*.
2. **Shao Z, Zheng G, Efimov D, and Perruquetti, W. Identification, estimation and control for linear systems using measurements of higher order derivatives.** Submitted to *European Journal of Control*.

Title: Identification and control of low-cost position-controlled robot manipulators

Abstract: Unlike industrial robot manipulators which are huge in size and of high price, many low-cost robot manipulators have already entered the market, with small size and light weight, this type of robots are more accessible to the public. However, limited by the cost, the components adopted (materials, actuators, controllers, etc.) are also limited, this often leads to less robust control performance. This thesis focuses on the controller design to improve the performance for such kind low-cost robot manipulators. To start with, for rigid case, dynamic modeling considering the actuator system is established, which forms a differential equation with constant parameters and disturbance, a method to identify the model parameters using observers and then an adaptive controller are proposed, simulation and experimental results are given. Then, in case of flexible joints, for simplicity, a single-link case model is considered. Firstly, link velocity measurement is assumed to provide link information, and an identification method and a two-stage adaptive control law are proposed provided that the static link position can also be measured, simulation result is given. Secondly, by using link acceleration measurement, an identification method and the same two-stage adaptive control law are proposed, this idea is generalized to identification and control of linear system using high-order derivative measurements, simulation result is presented. For implementation, inertial sensors (gyro and accelerometer) are used and experimental result is presented.

Keywords: Low-cost robot manipulators; Modeling; Parameter identification; Flexible joint; Adaptive control; State estimation

Titre: Identification et commande des robots manipulateurs à bas prix

Résumé: Contrairement aux robots manipulateurs industriels qui sont de taille énorme et de prix élevé, beaucoup de robots manipulateurs à bas prix sont déjà entrés dans le marché, avec une petite taille, un poids léger, ce type de robots est plus accessible pour les particuliers. Cependant, limité par le coût de revient, des accessoires (matériaux, actionneurs, contrôleurs, etc) adoptés sont aussi limités, cela conduit souvent à la performance moins robuste au niveau de contrôle. Cette thèse se concentre sur la conception de contrôleur pour améliorer la performance des robots manipulateurs à bas prix. D'abord, pour des robots manipulateurs rigides, la modélisation dynamique en lien avec le système d'actualisation est établie, qui forme une équation différentielle avec paramètres constants et perturbation. Une méthode d'identification des paramètres en utilisant des observateurs et une commande adaptative sont proposées, et des résultats de simulation et d'expérimentation sont donnés. Ensuite, pour le cas de joints flexibles, pour simplifier, le modèle 1DOF est pris en compte. Premièrement, avec la mesure de la vitesse de lien, une méthode d'identification et une loi deux-étages adaptative sont proposées à condition que la position statique de lien puisse également être mesurée, des résultats de simulation sont donnés. Deuxièmement, en utilisant des mesures d'accélération de lien, une méthode d'identification et la même loi deux-étages adaptative sont proposées, cette idée est généralisée à l'identification et au contrôle de systèmes linéaires avec mesures de dérivées d'ordre élevé, des résultats de simulation sont présentés. Pour la mise en œuvre, des capteurs inertiels (gyroscopes et accéléromètres) sont utilisés et des résultats expérimentaux sont présentés.

Mots-clefs: Robots manipulateurs à bas prix; Modélisation; Identification des paramètres; Joints flexibles; Commande adaptative; Estimation d'état